The effect of land use on land surface temperature in the Netherlands

Soheila Youneszadeh Jalili

April, 2013

The effect of land use on land surface temperature in the Netherlands

by

Soheila Youneszadeh Jalili

Thesis submitted to the department of Physical Geography and Ecosystem Science, Lund University, in partial fulfilment of the requirements for the degree of Master of Science in Geo-information Science and Earth Observation for Environmental Modelling and Management

Thesis Assessment Board

First supervisor: Prof. Dr. Petter Pilesjö (Lund University)
Co-supervisors: Dr Anton Vrieling and Dr Janneke Ettema (University of Twente, ITC)

Exam committee:
Dr. Ulrik Mårtensson
Dr. Harry Lankreijer

Lund University GEM thesis series nr 1

Disclaimer

This document describes work undertaken as part of a programme of study at the department of Physical Geography and Ecosystem Science, Lund University. All views and opinions expressed therein remain the sole responsibility of the author, and do not necessarily represent those of the institute.

Abstract

The Netherlands has experienced a rapid rate of land use change from 2000 to 2008. Land use change is especially urban expansion and open agriculture reduction which is due to enhanced economic growth. This thesis reports an investigation into the application of remote sensing, geographic information systems (GIS) and statistical methods to provide quantitative information on the effect of land use on land surface temperature. Remote sensing techniques were used to retrieve the land surface temperature by using MODIS Terra (MOD11A2) product. As land use change alters the thermal environment, LST could be a proper change indicator to show thermal changes in relation to land use changes. GIS was further applied to extract the coverage ratio of each land use in the context of LST pixels. Using correlation and linear regression this interrelationship was then quantified. Night land surface temperature correlates positively with the coverage percentage of open agriculture, forest and greenhouse farming. This association is negative for buildup are and inland water and offshore land use types. The results also show that inland water and offshore area has the highest night LST and the lowest day LST. Build up is the warmest land use during the days and the second warm land use during the night time. The result of this research will be helpful for urban planners and environmental scientists.

Keywords: land use, land surface temperature, LST, skin temperature, UHI

Acknowledgements

I offer my sincerest gratitude to my first supervisor Prof. Dr. Petter Pillesjö for his great knowledge, support, patience and helpful comments. I thank my co-supervisors Dr. Janneke Ettema and Dr. Anton Vrieling for their great help to build the research structure.

I would like to thank my parents: Reza Jalili and Rafat Abravesh, who always support me with their infinite love.

Table of Contents

List of figures

List of tables

Chapter 1

1.1. Introduction

Earth system is a complicated cycle with a lot of interconnected components like The Earth's surface and it's interior. The earth surface is naturally covered by different land cover types which are mainly distributed based on climate patterns. Adding increasing human population and his needs to this balanced system, we will find lots of disturbances stem from the concept of how we change the use of the land to face our needs and regardless to its capacity or environmental impacts.

Land use is defined as "the arrangements, activities and inputs people undertake in a certain land cover type to produce, change or maintain it" (FAO/UNEP, 1999). Land use should be matched with land capability and at the same time it should respect the environment, and global climate systems (FAO/UNEP, 1996). Land use is converting over time and the most important driving force of land use changes is the human need. Human population is increasing and it causes transformation of natural ecosystems into human landscapes. Human settlements and especially, large urban and industrial areas significantly modify their environment. Changing from permeable and moist land uses to impermeable and dry one with paving and building material can sharply affect energy budget and land surface temperature (Guo et al., 2012) as well as many other surface properties like the amount of evaporation, surface infiltration, runoff rate, drainage system, etc. It is therefore critical to have detailed information of temporal and spatial land use changes and its rate.

Land surface temperature (LST) is temperature of the skin surface of land which can be derived from satellite information or direct measurements. LST provides an accurate measure for indicating energy exchange balance between the Earth and the atmosphere (Zhengming et al., 1989). LST shows a high spatial heterogeneity. The degree of LST is affected by land surface attributes, which are significantly influenced by elevation, slope and aspect which exert a direct control on the incoming solar radiation (Dubayah, 1990). Besides, topography is one of the factors that control the soil moisture distribution, thus exerting an additional influence on land surface temperature. Variation in LST also may be subject to seasonality, time of day, sea breeze, surface air temperature, humidity, wind speed, and land use (Wang et al., 2008; Keramitsoglou et al., 2011).

In the remote-sensing terminology LST is the surface radiometric temperature emitted by the land surfaces and observed by sensor at instant viewing angles (Prata et al., 1995). LST is derived from different platforms e.g. Terra/Aqua-MODIS, Terra-ASTER, NOAA-AVHRR and Meteosat-MVIRI. In this study Terra -MODIS is selected. MODIS LST products are particularly suitable for the land surface temperature product due their easy availability, relatively high spatial resolution, global coverage, and high calibration accuracy in multiple thermal bands; furthermore validation of version-3 standard products from Terra MODIS data shows that their accuracy is better than 1 C° in the range from -10 to +50 C° (Wan et al., 2004). The version 4 data quality is higher than previous versions, especially because of changes in the processing of inland water pixels (Wan, 2003). There are also lots of refinements implemented in the V5 daily LST Products including removing cloud-contaminated LSTs from M*D11A1 and M*D11B1 products or combining use of Terra and Aqua data in the day/night algorithm (Wan, 2007). Comparisons between V5 LSTs and in-situ values in 47 clear-sky cases showed that the accuracy of the MODIS LST product is better than 1 Celsius in most cases (39 out of 47) (Wan, 2008)

In case of urbanization as a major land use change, land surface temperature has dominantly been studied as the so-called urban heat island phenomenon (Brandsma et al., 2012; Kantzioura et al., 2012). Urban surfaces absorb and reradiate solar radiation and cause higher temperature; anthropogenic is another important heat sources in urban environment (Rizwan et al., 2008).

The Netherlands is chosen as the focus for this study, because it has a high economic activity and a moderate increase of population accompanied by a large expansion of urban areas (European Environment Agency (EEA), 2006). In 2000, 76.80 % percent of the total population in the Netherlands lived in urban areas, while in 2008 this increased to 81.82 % (Statista, 2012). Land use is well-documented in the Netherlands. Since 2000 every two to three years Statistics Netherlands makes an updated detailed national land use map through visual analysis of aerial photography, called “Bestand Bodemgebruik” (BBG). The Netherlands has an almost uniform flat topography, so it can be a proper case to separate the effect of topographic factors from land use properties on LST behavior. Furthermore large part of the Netherlands is located below sea level and water levels in canals are kept at a high level; the Netherlands is well-known for cities with high density of canals which may influence the spatial pattern of the LST (Steeneveld et al., 2011). Finally, the effect of land use change on LST in the Netherlands has not previously been studied for the whole country.

1.1.1. Related studies

- **Analysis of the impact of Land use/Land cover change on Land Surface Temperature with Remote Sensing**

Jiang et al., (2010) examined the effect of land use/land cover change on LST for Beijing city in China. This city is surrounded by mountains in 3 sides and plain in the other side. Three Landsat images of Beijing with clear weather condition acquired on April 9, 1995 and April 30, 2000 were selected to this research. The land surface temperature (LST) and land use and land cover (LULC) classes were retrieved. To find the pure effect of LULC change on LST and reduce the effect of seasonal variation, images were selected in the same season. To this end temperature/vegetation index (TVX) approach were used. TVX space is a plot of normalized NDVI and LST. The cross point of LST and NDVI was indicated For some LULC type pixels in 1995 and for correspond pixels which was converted to urban in 2000.The pixel trajectory was performed to relate cross points shifts with LST temporal behavior. One of the results which is useful for the current research is that the land use change (urbanization) led to the migration of pixels from cool to hot surface condition.

- **Land surface temperature in response to land use/cover change based on remote sensing data in Sangong River**

Cao et al. (2008) analyzed Land surface temperature changes in response to land use/cover change in Sangong River basin in China. The study area is oasis located in the edge of desert. To achieve their objective, they selected two images of Landsat TM/ETM+ which belong to 1990 and 1999 respectively and analyzed them for retrieving Land Use/Cover Change (LUCC) and land surface temperature (LST) data. They used mono-window algorithm to get LST values. Then changes of LST from 1990 to 1999 were got from the LST of 1990 and 1999 by Using Arc/Info 9.0 (ESRI, ArcGIS Desktop: Release 9. Redlands, CA: Environmental Systems Research Institute). Besides, using Matrix in ArcGIS they got land use change map. They also got the average LST through the weight sum and standard deviation of pixel by pixel in each land use and in 1990 and 1999. Based on mean LST values they calculate LST Change rate per land use and between 1990 and 1999. They have found that LST is in remarkable response to LUCC. On the whole, because of rapid growth of cities in 1990-1999, more farm land was needed so that land Use/cover changed remarkably and the average of LST rose about 10 °C within this period. What we can use from this study is the way they got average LST through the weight sum in each land use.

- **Dynamics of Land Surface Temperature in Response to Land-Use/Cover Change**

Zhou et al., (2011) examined how LST responded to urban growth, they retrieved spatial patterns of LST and land use for 1992 and 2006 from Landsat images dated 16 August 1992 and 19 May 2006. They classified TM images into five Land-use types, including built-up land, water, barren land, forest, and agriculture land. Then they characterized the land use types with Remote sensing indices, The NDBI (normalized difference built-up index) is an indicator of urban area, NDVI (Normalized Difference Vegetation Index) as greenness indicator and The MNDWI (Modified Normalized Difference Water Index) is selected to represent water areas. They overlay classified land-use maps and the derived LST layers to recognize their spatial patterns and to sample 5929 points distributed evenly in study area to do correlation analysis. To examine the effect of LUCC on LST pattern, land use change detection was performed. Changed areas were then overlaid with LST layers to calculate the LST differences between 1992 and 2006. They did correlation analysis between LST and three mentioned indices separately and then they used two global and local multivariate regression to model LST based on indices. Some of their results showed that LST increased about 3.4 °C and 1.9 °C, respectively, for forest and agricultural land that were converted into built-up areas. Among the three indices, NDBI had the strongest relation with LST. The way of categorizing land cover would be the most interesting point of this article which can help the current study.

- **Identification and analysis of urban surface temperature patterns in Greater Athens, Greece, using MODIS imagery**

Keramitsoglou et al., (2011) analyzed urban heat island phenomenon. They investigate 9-year temporal LST behavior got from daily LST retrievals of MODIS 3000 images in 1 km resolution and Coordination of Information on the Environment (CORINE) land cover data set. The study area is in Greater Athens, Greece which is a coastal city in central basin bounded by mountains and Saronic Gulf in the south west; it is bisected by small hills and under the effect of see-breeze. Thermal pattern analysis was done to select three hot spots to be analyzed about spatial-temporal trends. They masked out cloudy and obliquely land pixels and then for dealing with missing cells they applied averaging techniques on invalid pixels. Then they used smoothing pixel to remove extreme LST values. All pixels with LST higher than suburban LST plus 6 C were introduced as potential hot spots. Using object-based analysis, they grouped hot pixels and selected 4 hot spots (objects).Then they did spatial thermal analysis in hot spots and over a decade, they extracted thermal information like temporal min and max LST. Some of their interesting results were finding cooler pixels along the coastline, or observing lower LST in higher altitudes. They also found that during day time bare soil and sparse vegetation showed faster heating rate than urban areas, inversely later in the day and mostly at nights city center of Athens showed UHI (urban heat island) phenomenon. Finding cooler pixels near the sea or masking out cloudy pixels would be interesting points which can be used in further analysis.

- **The impact of land use and land cover changes on land surface temperature in a karst area of China**

Xiao et al., (2007) studied the impact of land use and land cover changes on land surface temperature in Guizhou Province in Southwest China including four counties. It is a mountainous agricultural province and about 73% of it is karst formation, including poljes, cockpits, towers and dolines. Three cloud-free Landsat TM scenes, acquired on November 7, 1991, December 5, 1994, and December 19, 2001, were obtained for this study. The satellite images were corrected to remove atmospheric effects and georectified with control points. Then all the data were projected to a common UTM coordinate system. Using hybrid image classification system, five land use/land cover (LULC) types were selected, including natural vegetation, water, agriculture, urban, and barren land. In the next step LST and NDVI were computed for each image and in each land use type and the correlation coefficient between NDVI and LST were found around 0.78. Their results showed that urban/built-up land increased by almost three times from 1991 to 2001, while agricultural land decreased at a similar rate of about 4% per year. Of all the LULC categories, urban and built-up had the highest average temperature, followed by forest, agriculture, and barren land. The conversion of forest and agricultural land into urban/built-up land increased the amount of LST. The average LSTs for urban and built-up land increased by 1.1, 1.5, 1.4, and 1.2 K from 1991 to 2001 and in four counties.

- **Time Series Processing of MODIS Satellite Data for Landscape Epidemiological Applications**

Neteler (2005) analyzed time series of MODIS LST and NDVI/EVI satellite data in Province of Trento, Italian Alps with GRASS GIS software (Geographic Resources Analysis Support System) to do an epidemiological study about the exposure risk to Lyme and tick-borne encephalitis (TBE) diseases. They did Pre-Processing analysis of MODIS Data for GIS Usage. At first they used "MODIS Reprojection Tool" (MRT) to reproject images to UTM; moreover using MRT output images will be in standard data formats such as Geo TIFF. Then they did the pixel-wise application of the quality maps (QA) with reprojected LST maps to limit low quality cells. Then they applied one more quality filter due to removing thin cloud and high aerosol presence effects. To do so they applied outlier detection method to remove the minimum temperatures cells. In the next step they provide monthly LST values. Then to validate LST data they investigate mean monthly LST data with monthly mean temperatures of selected meteorological stations. And finally they tried to relate LST with mentioned diseases. Some of their results showed that just in months with nearly continuous cloud cover the mean temperatures deviate significantly from corresponded LST values. Using MRT software they reproject MODIS images to UTM and Geo TIFF format which can be considered in the current research.

- **Estimating Daily Land Surface Temperatures in Mountainous Environments by Reconstructed MODIS LST Data**

Neteler (2010) focused on estimating daily land surface temperatures in mountainous environments by reconstructed MODIS LST data from a total of 11,179 MODIS LST maps between 2000 and 2008. Study area was Northern Italy including the provinces of Trento, Bolzano and Belluno, and also parts of the regions of Friuli-Venezia Giulia, Lombardia and Veneto. They provided a new self-contained algorithm to reconstruct incomplete MODIS LST maps. Since the amount of available data was huge, reconstruction required to be automated. Their procedure included re-projection to UTM, filter out invalid pixels using quality assessment layer with applying the bit patterns of interest to LST maps, Nearest Neighbor (NN) resampling using MRT software, spatial oversampling to 200 m × 200 m resolution, applying several outlier detector filter, filling holes in the original LST maps, volumetric splines interpolation and checking the results with weather station data. Some of their results showed that between 32% and 41.5% of each altitudinal zone has good pixel coverage between 2000 and 2008 for the study region. The way of managing MODIS time series in this study will be useful for further researches.

- **Estimating the Urban Heat Island in residential areas in the Netherlands using observations by weather amateurs**

Wolters and Brandsma (2012) investigated the effect of urban heat island in the Netherlands; they analyzed over 200 amateurs weather stations to find 19 suitable stations. Then they used a linear model to estimate urban heat islands and they found r2 = 0.7

between the summer-averaged UHI and the population density. It was found that UHI in summer increases with decreasing wind speed and cloudy cover, and with increasing sea level air pressure. In spring and autumn the UHI was lower than in summer and in winter there was no significant UHI. The fact that in summer UHI is more intense will be good motivation to focus on summer season for some LST analysis.

- **Measurement and statistical modeling of the urban heat island of the city of Utrecht (the Netherlands)**

Brandsma and Wolter (2012) analyzed high-resolution measurements of temperature and humidity taken on a bicycle in the morning and afternoon. The sampling was done along a 14 km transect through the city of Utrecht to describe and model the UHI intensity between 2006 and 2009. Representative route was determined with fixed points every 10 m for both the early morning and afternoon transect. Two multiple linear regression models have been proposed to describe the mean and maximum nighttime UHI intensity profiles with area-averaged sky-view factors and land use (build-up, vegetation and open water) of the city Utrecht. Land use was expressed as fractions summing up to 1. The fractions are denoted as FB (fraction build-up), FV (fraction vegetated), and FW (fraction open water). Furthermore a non-linear model is constructed that relates the temperature difference between the warmest and coldest part along the profiles to wind speed and cloudiness. Their results showed that the difference between the warmest and coolest temperatures along the transect is about 1.5 for the mean nighttime profiles and 0.6C for the daytime profiles. Also their results showed less UHI in more windy and cloudy weather situation. They relate UHI with wind speed which can be used in this study.

- **Quantifying urban heat island effects and human comfort for cities of variable size and urban morphology in the Netherlands**

Steeneveld et al., (2011) studied the urban heat island phenomenon. The aim of this study was to quantify the canopy layer urban heat island which is done in the Netherlands based on observations by a network of hobby meteorologists and three weather stations. They related the UHI to the amount of green cover, presence of water bodies, and population densities. The majority of the largest cities in the western part like Rotterdam, Delft, The Hague, Leiden, and Haarlem have been included in this study. They also quantified the sensitivity of the recorded UHI to mean wind speed and daily solar radiation. Some of their results showed that average maximum UHI during a diurnal cycle is 2.3 Kelvin, while the average 95 percentile over all cities is 5.3 K. They relate UHI to wind and population density.

- **Exploring indicators for quantifying surface urban heat islands of European cities**

To validated LST data they examined temporal pattern and variation of LST with air temperature and soil moisture. All monthly MOD and MYD LST data from 2000 to 2006 were analyzed and temporal and spatial behavior of LST of winter wheat and grassland were studied. Some of their results showed that in the growing season, the wheat field has a well-defined cool anomaly, and after harvesting it showed warm anomalies. Another observation was that cool and warm anomalies have strong interannual variability.

- **Direct impacts on local climate of sugar-cane expansion in Brazil**

Loarie et al., (2011) analyzed the effect of sugar cane and natural vegetation land cover changes on LST temporal behavior in the Brazilian Cerrado, which is the largest savanna region in South America between 2000 and 2008. The fraction of sugar cane and natural vegetation were calculated to be matched with 1 km^2 grid cells of MODIS swath. For each 1 km pixel, they derived time series of 1 km MODIS LST (MOD11, 2000_2008 every 8 days), evapotranspiration, albedo, and enhanced vegetation index. Then they calculated fractional change in natural vegetation and fractional change in sugar cane with changes in the MODIS behavior. Then a regression slopes was calculated for each MODIS variable as a function of fractional changes and compare these fractional changes with changes in MODIS LST and other variables. Some of their results revealed that conversion from crop and pasture land to sugar cane leads to local cooling effects and conversion of natural vegetation to sugar cane leads to local warming.

1.2. Problem statement

The Netherlands is a small country with a relatively large population. Due to industrialization and population increase, its land use and land cover patterns are changing. Historical land use changes in the Netherlands mostly stem from the biophysical conditions like soil type and landform limitations, while recent land-use conversions are because of accessibility e.g. rail infrastructure, spatial policies, and neighborhood interactions (Verburg et al., 2004). Since there is a fixed amount of land, increase or decrease of each land use will affect other land uses. The most common land conversion is from agriculture (cropland and pastures) to urban. Based on a report of the Organization for Economic Co-operation and Development (OECD, 2008e), the Netherlands is the most urbanized country and has the second highest population density of all 34 OECD countries. An understanding of how land use changes occur and what are the impacts of these changes are important in different aspects of environmental management issues such as microclimate changes. One consequence of shifting from natural to urban surfaces is higher thermal inertia of urban surfaces which leads to higher land surface temperature during nights. Although a number of researches have proved the effect of land use on land surface temperature in different parts of the world (Keramitsoglou et al., 2011; Zhou et al., 2011), this study aims at quantifying this relationship in the Netherlands. Discovering a temporal relationship between land use change and land surface temperature can be an important input to predict future land warming. This study may provide practical information for urban planners, natural resources managers and environmental experts to manage natural landscapes to be sustainable and healthy.

1.3. General objective

The aim of this study is to investigate the effect of land use conversions on land surface temperature (LST) in the Netherlands between 2000 and 2008. LST is derived from satellite images, and the change of the LST pattern in response to land use change is explored by using GIS and remote sensing techniques.

1.4. Specific objectives

I. To analyze land use changes in the Netherlands between 2000 and 2008 using detailed land use maps (BBG).
II. To evaluate the temporal behavior of MODIS day and night time land surface temperature for different land uses.
III. To examine the changes in temporal behavior of land surface temperature in relation to land use conversions.

Chapter 2

Material

2.1. Study area

The Netherlands is a country in Western Europe which borders the North Sea to the north and west, Belgium to the south and Germany to the east, see Fig. 1. Its climate is temperate maritime (nationsonline.org). About 16 million people live in an area of about 40,000 km^2; the economic heart and most urbanized parts of the country is Randstad which comprises the major cities of Amsterdam, Rotterdam, Utrecht and The Hague and has around 5 million inhabitants (de Nijs et al., 2004).

Figure 1 - The Netherlands and it is location,
taken from http://wwwnc.cdc.gov/travel/destinations/netherlands.htm

2.2. Data Collecting

In this research different data sources were used which are shown in Tab. 1.

Table 1-Data which are used in this thesis

Data type	Data source	Product name	Platform	Projection system	Type	Res(m)/Scale	Temporal interval	Temporal coverage
Land surfaces temperature	NASA website	MODIS LST/MOD11A2	Terra	sinusoidal projection	Raster/HDF	1000m	8 Day	2000 onward
Land use	Land Use Base of Statistics Netherlands	BBG land use map	-	RD-New	Vector	1:10,000	2 or 3 years	1996,2000, 2003,2006, 2008

2.2.1. Land Surface Temperature Data onboard

NASA launched the Earth Observing System's flagship satellite "Terra" on December 18, 1999. Terra has a sun-synchronous, near polar, circular orbit which passes the earth from north to south. It crosses the equator in the morning (10:30 a.m.) and visits the entire Earth's surface each 1 to 2 days. Terra carries five sensors including ASTER, CERES, MISR, MOPITT and MODIS(NASA, 2013).

In this study data derived from the Moderate Resolution Imaging Spectroradiometer (MODIS) product is used. MODIS has a 36 spectral band spectrometer. MODIS thermal infrared (TIR) bands are used for LST retrieval. MODIS provides a global data set every 1-2 days. LST computation is based on Split Window algorithm.

The methodology used for the calculation of the LST maps is based on the Split Window Technique (SWT). Using the SWT, the LST is calculated as (Ts), (Jiménez-Muñoz et al., 2008):

Ts (land surface temperature) = $T_i + c_1 (T_i - T_j) + c_2 (T_i - T_j)^2 + c_0 + (c_3 + c_4 W)(1 - \varepsilon) + (c_5 + c_6 W)\Delta\varepsilon$ where:

T_i and T_j : at-sensor brightness temperatures at the SW bands i and j (in Kelvin)
ε: the mean emissivity, $\varepsilon = 0.5(\varepsilon_i + \varepsilon_j)$,
$\Delta\varepsilon$: the emissivity difference, $\Delta\varepsilon = (\varepsilon_i - \varepsilon_j)$,
W is the total atmospheric water vapor content (in grams per square centimeter),
$c_0 - c_6$: the SWT coefficients

In the case of the MODIS sensors i and j are bands 31 and 32, respectively. The LST pixels in MODIS scenes are retrieved from brightness temperatures in bands 31 and 32. Band width for band 31 is 10.780–11.280 μm and for band 32 it is 11.770–12.270 μm.

MODIS LST data products are generated as a series of seven products, MOD11L2, MOD11A1, MOD11B1, MOD11A2, MOD11C1, MOD11C2 and MOD11C3. Generally each LST product in the sequence is built from the previous LST products. The first LST product, MOD11L2, is the LST at 1km spatial resolution for a swath. MOD11_L2 LST is constructed using the MODIS sensor radiance data product (MOD021KM), the geolocation product (MOD03), the atmospheric temperature and water profile product (MOD07L2), the cloud mask product (MOD35L2), the quarterly land cover (MOD12Q1), and snow product (MOD10L2) (Wan, 2007). MOD11L2 product is prepared by the generalized split-window LST algorithm. MODIS swath LST values are retrieved in pixels which:

- are land or inland water.
- are in clear-sky conditions at a confidence (defined in MOD35) of >=95% over land <= 2000m or >= 66% over land > 2000m, and at a confidence of >= 66% over lakes.
- have nominal Level radiance data in bands 31 and 32.

The next MODIS LST product is MOD11A1. The daily MOD11A1 LST product is generated from MOD11_L2 products results of a day. For preparing the MOD11A1 LST product the scientific data sets of all pixels in MOD11_L2 are mapped onto grids in the sinusoidal projection and the LST values of overlapping pixels in each grid are averaged with overlapping areas as weight (Wan, 2007).

After MOD11B1, V5 MOD11A2 product is the fourth LST product which is used in this study. Production of MOD11A2 is done by using a simple average method in the current algorithm for the MOD11A2 product for each 8 days (from two to eight days). The MOD11A2 MODIS LST products are archived in Hierarchical Data Format - Earth Observing System (HDF-EOS) format files, including global metadata and scientific data sets (SDSs) with local attributes. The SDSs in the MOD11A1 product include LST_Day_1km, QC_Day, Day_view_time, Day_view_angl, LST_Night_1km, QC_Night, Night_view_time, Night_view_angl, Emis_31, Emis_32, Clear_ sky_ days, Clear_ sky_ nights, as shown in Tab. 2.

Table 2 - The SDSs in the MOD11A2 product.

SDS NAME	LONG NAME	NUMBER TYPE	UNIT	VALID RANGE	FILL VALUE	SCALE FACTOR	ADD OFFSET
LST_Day_1km	Daily daytime 1km grid Land-surface Temperature	uint16	kelvin	7500-65535	0	0.02	0
QC_Day	Quality control for daytime LST and emissivity	uint8	none	0-255	0	NA	NA
Day_view_time	(local solar) Time of daytime Land-surface Temperature observation	uint8	hrs	0-240	255	0.1	0
Day_view_angle	View zenith angle of daytime Land-surface Temperature	uint8	deg	0-130	255	1.0	-65.0
LST_Night_1km	Daily nighttime 1km grid Land-surface Temperature	uint16	kelvin	7500-65535	0	0.02	0
QC_Night	Quality control for nighttime LST and emissivity	uint8	none	0-255	0	NA	NA
Night_view_time	(local solar) Time of nighttime Land-surface Temperature observation	uint8	hrs	0-240	255	0.1	0
Night_view_angle	View zenith angle of nighttime Land-surface Temperature	uint8	deg	0-130	255	1.0	-65.0
Emis_31	Band 31 emissivity	uint8	none	1-255	0	0.002	0.49
Emis_32	Band 32 emissivity	uint8	none	1-255	0	0.002	0.49
Clear_sky_days	the days in clear-sky conditions and with validate LSTs	uint8	none	0-255	0	NA	NA
Clear_sky_nights	the nights in clear-sky conditions and with validate LSTs	uint8	none	0-255	0	NA	NA

MOD11A2 product local Attributes included the coefficients of the calibration which converts the SDS value to real LST value in kelvin. For example the valid range of LST in MODIS LST maps is between 7500 and 65535. Converting to kelvin, these values should be multiplied to the scale factor of 0.02 which is available in local attributes (Wan, 2007). MODIS HDF files are shown by a rather long name, the breakdown of MODIS filenames is (MODIS overview, USGS, 2011):

MOD11A2.A2000065.h18v03.005.2007176163054.HDF

MOD11A2: MODIS product group and processing level

A2000065: year and Julian day of granule capture
h18v03: number of tile in MODIS tiling system
005: version of processing code
2007176163054: time stamp of processing

USGS EROS Center published a Quality Assurance Tutorial in the year of 2012. Based on this report all MODIS land products have accompanying quality assurance (QA) information. HDF data sets have different Science Data Sets (SDS) besides at least one QA data layer. QA layer includes file-level metadata, pixel-level metadata and Land Data Operational Product Evaluation (LDOPE) web information. File-level metadata contains the summary of a file data quality; while pixel-level metadata is another important accompanying product for applications based on time-series analysis. They help users to be sure about data consistency or data quality Tab. 3. Pixel-level metadata includes two types:

- o Containing binary encoding of different information sources
- o Including single information source like pixel reliability in vegetation indices etc.

Table 3 - Bit flags defined for SDSs QC_day and QC_Night in MOD11A2. Note that bit 0 is the least significant bit.

bits	**Long Name**	**Key**
1 & 0	Mandatory QA flags	00=LST produced, good quality, not necessary to examine more detailed QA 01=LST produced, other quality, recommend examination of more detailed QA 10=LST not produced due to cloud effects 11=LST not produced primarily due to reasons other than cloud
3 & 2	Data quality flag	00=good data quality 01=other quality data 10=TBD 11=TBD
5 & 4	Emis Error flag	00=average emissivity error <= 0.01 01=average emissivity error <= 0.02 10=average emissivity error <= 0.04 11=average emissivity error > 0.04
7 & 6	LST Error flag	00=average LST error <= 1K 01=average LST error <= 2K 10=average LST error <= 3K 11=average LST error > 3K

LST is retrieved from MODIS TIR data only in clear-sky conditions. Cloudy pixels must be skipped in the LST processing, because the thermal infrared signals cannot pass through clouds besides the fact that the probability of cloudy conditions is usually more than 50% at the regional and global scales (WAN et al., 2004). In cloudy pixels cloud-top temperatures are measured instead of land surface temperature. So using cloud masking, MODIS products are retrieved only in clear-sky conditions. Clear-sky pixels defined by MODIS cloud mask in V5 daily LST is at confidence of >= 95% over land <= 2000m, confidence of >=

66% over land > 2000m and at confidence of >= 66% over lakes (Wan, 2007). But still there are some low quality and undetected cloudy pixels of each LST map marked in an attaching quality assessment (QA) layer of MODIS MOD11A2 product. By using this QA layer, low quality pixels can be filtered out (Neteler, 2010). In this study MODIS LST data is retrieved from two online sources. The first is the website of university of Oklahoma, available at http://www.eomf.ou.edu/visualization/gmap/, in earth observation and modeling part, MOD11A2 data are available for each MODIS pixel. In this website data can be downloaded as ASCII Table, CSV Table, and series of graphs, including data on selected tile and pixel. The second source is http://reverb.echo.nasa.gov/reverb/datasets, this website provides temporal and spatial criteria for searching needed LST images, and so 8-day HDF LST images are downloaded from this source. MODIS LST data are arranged in a universal tiling system, tiles are 10 degree by 10 degree and the tile h18v03 is covering the Netherlands, which is used to retrieve LST values Fig. 2.

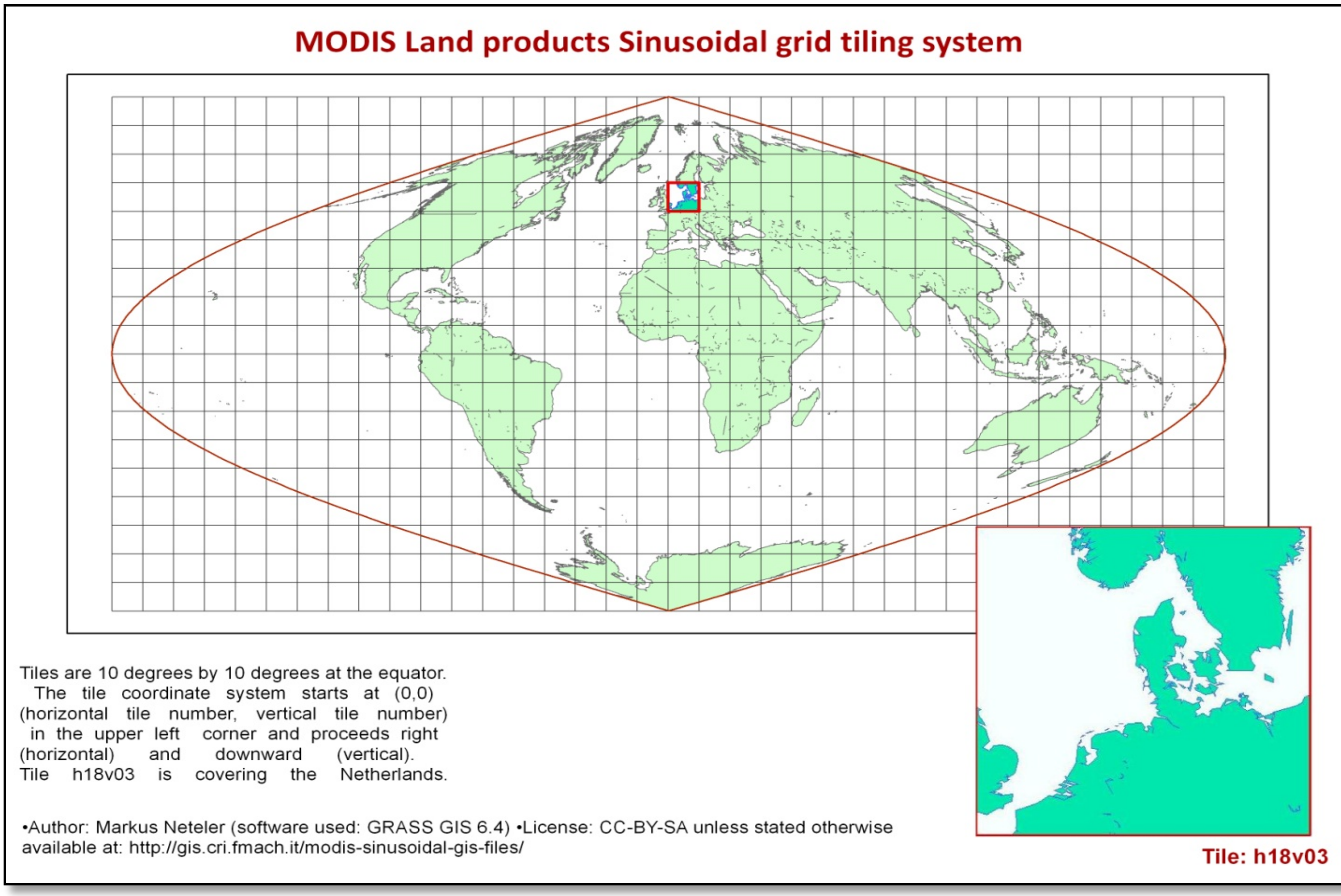

Figure 2-MODIS universal tiling system.

2.2.2. Land use data:

The spatial land use database of Statistics Netherlands (NL: BBG, Bestand Bodemgebruik), is a frequently updated dataset of land use information in the Netherlands. The first version of the BBG is for the year 2000 and also contains an interpretation of the year 1996. For the creation of its basic geometry visual interpretation of aerial photography and the Dutch topography map were used. The Dutch digital topographic map is available in vector format at a scale 1:10.000m (Van Leeuwen et al., 2011). BBG land use maps are available in shape-file format, consisting of polygon features with a scale of 1:10.000. After the year 2000 every two or three years a new updated version of BBG was created, including 2000, 2003, 2006 and 2008. The individual BBG maps contain 37 land use types, grouped into eight main categories (Linke, 2008). It emphasizes on urban land use and contains only few classes in rural areas; moreover areas smaller than 0.5 hectare are excluded (Koomen et al., 2006).

Chapter 3

Methodology

3.1. Analyze land use changes in the Netherlands between 2000 and 2008 using BBG data set

BBG land use maps of the years 2000, 2003, 2006 and 2008 were used to assess land use changes. Multiple land uses can be present in one 1-km^2 LST pixel and each of the land use classes can affect the LST mixed value. So it was needed to have land use change maps with the same resolution as the LST images (1-km^2), including areal proportions of each land use within each LST pixel. It was also useful to evaluate what the abundance of each land use was within a specific LST pixel. The sub-pixel heterogeneity in the characterization of land use changes was captured for the MODIS grid pixels. In other words, per MODIS 1-km^2 grid pixel the percentage of different land uses was determined for the years of 2000, 2003, 2006, and 2008. Fig. 3 is shown as an example of sub-pixel land use heterogeneity. Land surface temperatures represent average temperatures within a pixel which may be composed of several land use types. This can be done by determining the coverage ratios of different land use types within individual MODIS pixels.

Figure 3 - land use percentages per pixel; the figure has four pixels and each pixel represent the areal proportions of each land use in the left represented map.

Fig. 3 Shows as an example of sub-pixel land use heterogeneity of 4 MODIS pixels. For example the above left pixel is composed of 32% build-up area, 25% water, 15% agriculture, 28% forest, and 0% recreation and greenhouse farming. LST represents the average temperature within a pixel which may be influenced by several land use types. Determining the coverage ratios of different land use types within an individual MODIS pixel helps to find the role of each separate land use in governing the pixel LST value.

Dutch BBG land use map contains 8 main classes: Traffic, Build-up areas, Semi Build-up areas, Recreational, Agricultural, Forest and natural open land, and Inland waterway and offshore. These classes were reclassified to new categories in which different classes had different heat capacity, emissivity and reflection characteristics. The BBG land use maps were re-classed into 6 classes, using the dissolve function of Arc Map (ESRI 2011. ArcGIS Desktop: Release 10. Redlands, CA: Environmental Systems Research Institute). These 6 classes are supposed to influence LST differently, and thus they are considered as different classes. Recreation area is a mixed land use class. It can consist of water, or building area or other land use types. The reason for separating recreation area as different group is to separate green patches and corridors from the urban, thus distinguishing the vegetation role in mitigating land surface temperature. In other words, by separating cooling spots from build-up areas, the behavior of urban LST would be studied in a better way. Additionally, the traffic class was excluded from analysis. The reason is that this class does not contribute significantly in terms of areal percentage, to the MODIS grid cell. BBG Class codes of 70, 71, 80, 81 and 82, were also excluded, as can be seen in Tab.4. The reason was absence of LST data in these class codes. Next step was extracting different land use classes as separate shape files. Because the changes of each land use had to be studied and mapped separately. This step was achieved using export function of Arc Map. Considering 4 land use maps (4 years) and 6 classes, 24 shape files were produced for further analysis.

Table 4 - New and old classes of BBG land use.

New class		BBG land use attributes, old class		
New code	**BBG new classes**	**BBG Main group**	**BBG Class code**	**BBG Description**
1	Build-up area	***1. Traffic***	**10**	**Railroad**
			11	**Road**
			12	**Airport**
		2. Build-up areas	20	Residential
			21	Commercial
			22	Public services
			23	Welfare provision
			24	Industrial
		3. Semi Build-up areas	30	Dumping site
			31	Scrapheap
			32	Cemetery
			33	Raw-material producing area
			34	Building land
			35	Semi-paved other land
2	Recreational area	4. Recreational	40	Park
			41	Sports field
			42	Allotment
			43	Daytrip area
			44	Long-stay recreational area

Table 4, continue: New and old classes of BBG land use

<table>
<tr><td>3</td><td>Greenhouse farming</td><td>5. Agricultural</td><td>50</td><td>Greenhouse farming</td></tr>
<tr><td rowspan="3">4</td><td rowspan="3">Open agriculture</td><td rowspan="3">5. Agricultural
6. Forest and natural open land</td><td>51</td><td>Other agricultural area</td></tr>
<tr><td>61</td><td>Dry open land</td></tr>
<tr><td>62</td><td>Wet open land</td></tr>
<tr><td>5</td><td>Forest</td><td>6. Forest and natural open land</td><td>60</td><td>Forest</td></tr>
<tr><td rowspan="12">6</td><td rowspan="12">Inland waterway and Offshore area</td><td rowspan="12">7. Inland waterway
8. Offshore</td><td>70</td><td>Ijsselmeer/Markermeer</td></tr>
<tr><td>71</td><td>Closed inlet</td></tr>
<tr><td>72</td><td>Rhine/Meuse</td></tr>
<tr><td>73</td><td>Randmeer</td></tr>
<tr><td>74</td><td>Reservoir</td></tr>
<tr><td>75</td><td>Recreational inland water</td></tr>
<tr><td>76</td><td>Inland waterway for mineral extraction</td></tr>
<tr><td>77</td><td>Sewage farm</td></tr>
<tr><td>78</td><td>Other inland waterway</td></tr>
<tr><td>80</td><td>Waddensea/Eems/Dollard</td></tr>
<tr><td>81</td><td>Oosterschelde</td></tr>
<tr><td>82</td><td>Westerschelde</td></tr>
</table>

3.1.1. MODIS grid shape file preparation

As discussed in the data collecting section (section 2.2.), in the global MODIS LST tiling system, the Netherlands is located in tile h18v03. This tile is gridded in a network of approximately 1Km by 1Km (see Fig. 4). To extract this network, one MODIS LST image was converted to vector format. Using the clip function in ArcGIS, the grid was then clipped with the Netherlands boundary. This grid involved 4073 grid cells. Afterwards, a field was added to the attribute table of the grid shape file, and unique identification codes were assigned to every single pixel. This identifier column was needed for tracking and identifying individual grid cells in further analysis. For the field geometry, “grid cell area” and “XY coordinates at centroid” fields were also added to the Dutch grid shape file in the attribute table. XY coordinates of the grid cells were later on needed to extract corresponding LST values, and cell area was needed to calculate land use percentage coverage.

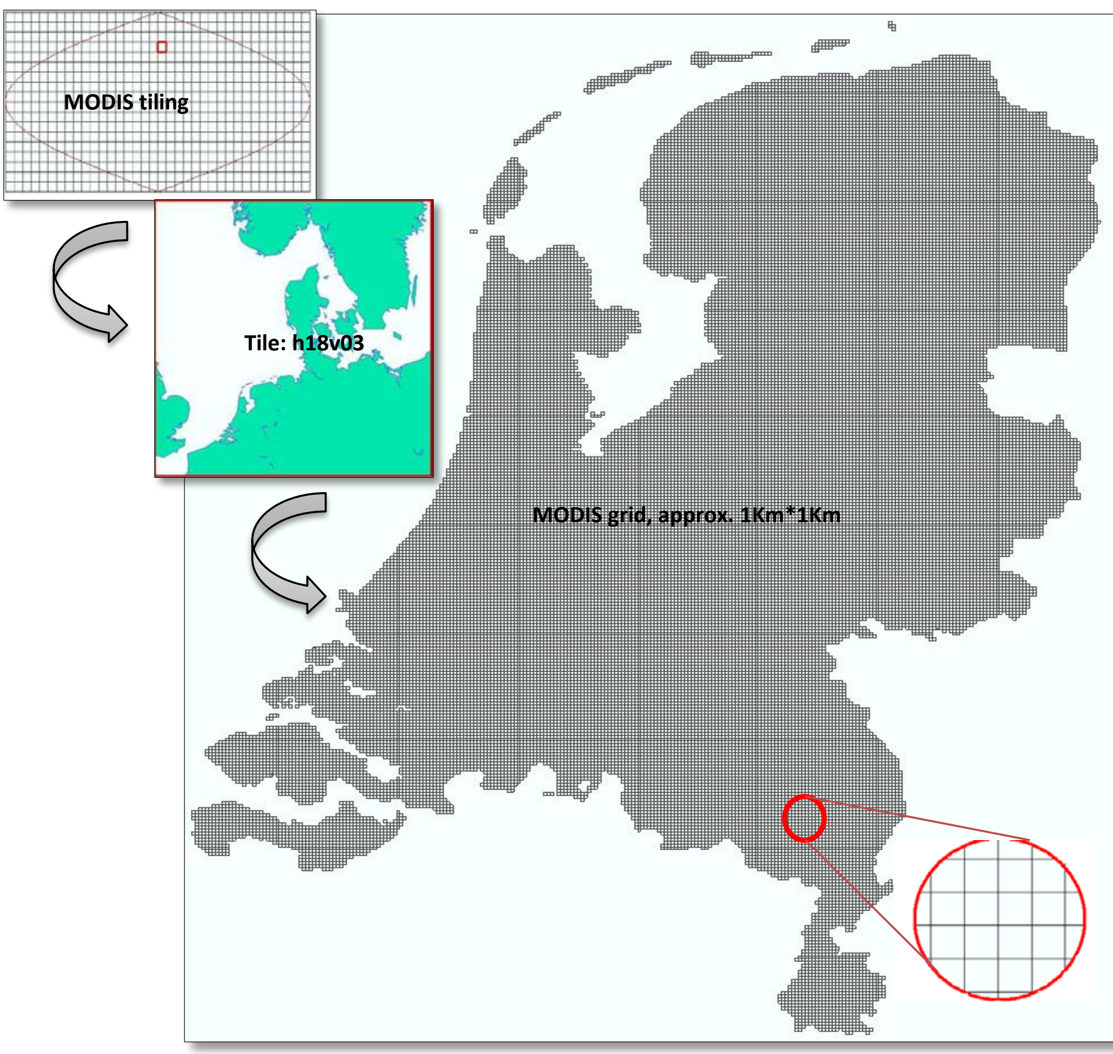

Figure 4 - the MODIS global tiling system, the tile in which the Netherlands is located and the prepared MODIS grid map.

The grid was then clipped by all 24 land use shape files separately. For example, it was clipped with the forest shape file of the year 2000 and named “forest_2000_clip”. Afterward, a new field named “land use area” was added to “forest_2000_clip” shape file and filled with area values and field geometry. In the next step, the attribute table of “forets_2000_clip” shape file was joined with the Dutch grid shape file attribute table. Then, a new column was defined in the joined table and named “land use percentage”. This new column was filled by using the field calculator. The loading formula was: “land use area” divided by “grid cell area” and multiplied by 100. This approach was repeated for the other 23 land use shape files from the different years. The attribute tables of prepared shape files where then exported in dbf format. Afterwards, an excel sheet was organized for each land use class, including the percentage of each year. To detect land use changes, land use percentage change columns were computed and added to the excel sheets. For example, the coverage percentage of forest in 2000 was subtracted from forest coverage in 2003 to make a forest land use change column from the period of 2000 to 2003. The same process was repeated for other land use types and years. The maximum and minimum values of percentage change columns were selected as MODIS grid cells with sharp land use changes. Following the same concept, cells with zero change value from different years were filtered by the Excel (Microsoft. (2010). Microsoft Excel [computer software]. Redmond, Washington: Microsoft) filter option and named as fixed land use MODIS cells.

3.1.2. Preparing land use change maps

The change columns of the Excel sheets for every single land use class were joined, creating a grid shape file attribute table. Land use change maps were then produced based on land use percentage change columns. Land use change maps were created for to the time periods of 2000-2003, 2003-2006 and 2006-2008. 18 land use change maps were made for six land uses and three time periods. The land use change maps illustrate the percentage of land use change in every single MODIS grid pixel in three time periods.

The results of these steps were:

I. Fractional land use change maps (land use class percentage coverage change in MODIS pixels) of the periods 2000-2003, 2003-2006 and 2006-2008.

II. A Dutch MODIS grid shape file

3.2. Temporal behavior of MODIS land surface temperature for different land uses

3.2.1. Retrieve LST data

To examine the temporal variation of surface temperature in relation to different land use types, the MODIS data from 2000 to 2008 were used. LST values per pixel were extracted from Oklahoma website available at: http://www.eomf.ou.edu/visualization/gmap/. Fig. 5 shows the interface of the Oklahoma website..

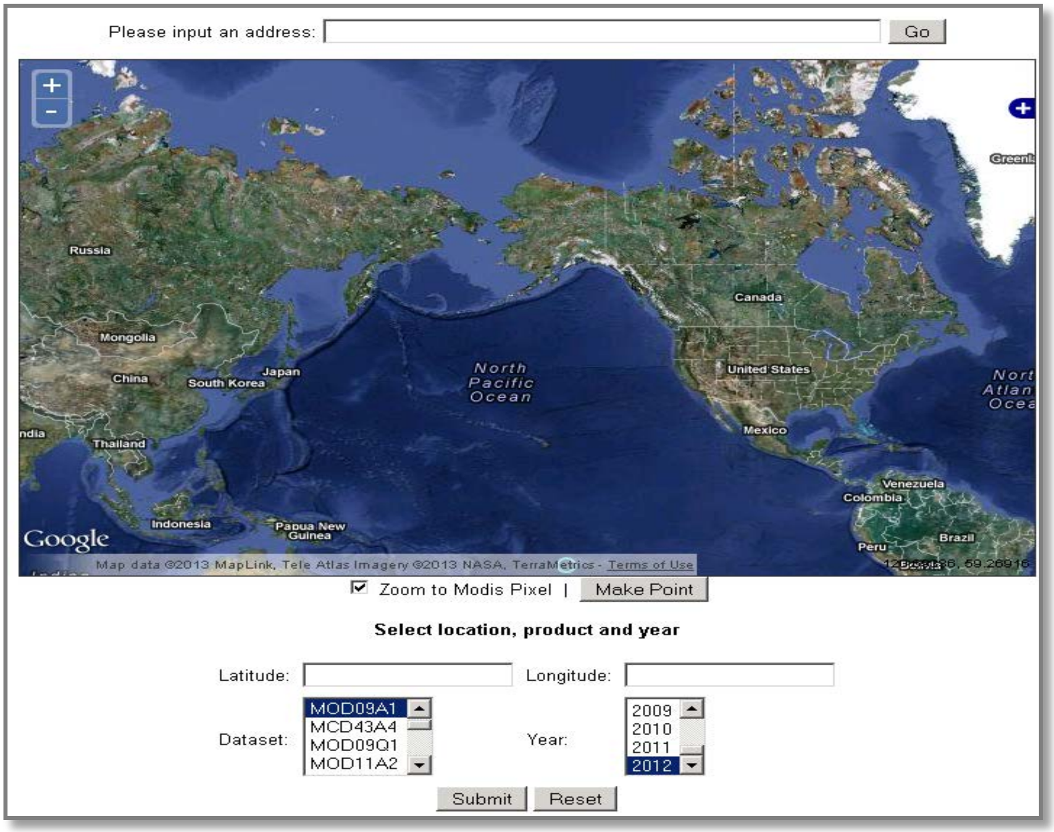

Figure 5 - The Oklahoma website, Retrieving LST values by pixels XY coordinates. Entering the longitude and latitude of each pixel, MOD11A2 LST values get extracted.

To retrieve LST values, MODIS pixel locations were entered based on the geographic coordinates (Latitude and Longitude). For each pixel, LST values were retrieved from 2000 to 2008 with 8-day intervals and in ASCII Table format. The tables were converted to Excel format. The raw LST values were multiplied by the scale factor of 0.02. The scale factor was defined in the LST product user manual (Zhengming, 2007). Afterwards, the LST values were subtracted by 273.15 to be converted from Kelvin to degrees Celsius.

3.2.2. Pre-assessment of LST data quality

LST images are equipped with a quality flag header. It means that for all LST pixels there is an attached quality value. The decision to accept or reject LST qualities depends on research objective. To decide which qualities to be included, a pre-analysis test was applied.

10 LST pixels which were evenly distributed in the whole Netherlands were selected (see Fig. 6). The LST values for these cells were extracted from 2000 to 2008 with an 8-day interval.

Figure 6 - The spatial distribution of sampled LST pixels for quality assessment pre-analysis.

Then, for each cell all available quality flags from 2000 to 2008 and their corresponding percentage were extracted (see Tab. 5). For example for the first point in the table 5, 46% of extracted LST values have the quality of zero, 4% the quality of 2 or 3, and 50% have 65 as their quality value. For every selected cell, the percentages of all available flag values were calculated. The next step was computing the mean percentage of each quality for all selected cells. For example 3.75% of all the extracted LSTs (from all of 10 pixels) have the quality of 81.The best quality is flagged as zero (Zhengming, 2007) which contributes 46.1% of the LST values. The second biggest quality group is flag 65, with 39.4% contribution percentage. The flag 65 has the medium quality. Due to low contribution percentage of lower qualities (for example quality 17 has 1.95% contribution in all the sampled cells from 2000 to 2008), the defined objectives and the scale of study, quality flags were all accepted except flags 2 and 3. Pre-assessment had shown that LST value for quality flags of 2 and 3 is zero. These zero values were filtered out in further analysis.

Table 5 - Percentages of different MODIS LST quality values in our sample points from 2000 to 2008.

Point	MODIS pixel Cell(row, column)	2000-2008 Quality (Bit position)					
		0	**2,3**	**17**	**65**	**81**	**145**
1	(871, 409)	46%	4%	-	50%	-	-
2	(831, 510)	51%	9%	-	40%	-	-
3	(1044, 445)	54 %	10%	-	36%	-	-
4	(1039, 262)	56%	8%	-	36%	-	-
5	(966, 385)	11%	11%	19%	20%	37%	2%
6	(921, 462)	53%	9%	-	38%	-	-
7	(948, 330)	50%	7%	-	43%	-	-
8	(930, 347)	42%	11%	-	47%	-	-
9	(790, 384)	44%	6%	0.5%	49%	0.5%	-
10	(841, 453)	54%	11%	-	35%	-	-
Mean percent for 10 pixel from 2000 to 2008		46.1%	8.6%	1.95%	39.4%	3.75%	0.2%
0: good quality, average LST error <= 1◦K 2,3: not produced due to cloud effects, pixel values are zero 17: other quality, average LST error <= 2◦K 65: other quality, average LST error <= 2◦K 81: other quality, average LST error <= 2◦K 145: other quality, average LST error <= 3◦K							

3.3. Evaluation of temporal behavior of land surface temperature in relation to land use conversions

To determine the temporal variation of the surface temperature, surface temperature is plotted at eight-day intervals during the years 2000–2008. Land surface temperatures represent average temperatures within a pixel which may be composed of several land use types. To examine weather different land uses have different LST values, and to see if there is any change of LST values through time (from 2000 to 2008), 27 representative cells were selected. These cells had fixed land use from 2000 to 2008. The representative cells were including of all land uses. Each land use had 5 cells apart from recreation areas that were represented by 2 cells. For the recreation class 5 pixels were not available. Representative cells had even distribution in the whole Netherlands. The temporal pattern of LST was analyzed with time plots which showed how LST behaves through time. After quality assessment and rejecting poor pixels (filtering out 2 and 3 quality flags in Excel), the temporal behavior of LST was plotted for single location pixels. LST values were extracted for every single representative cell from 2000 to 2008. Data were converted to excel format. Zero LST values were filtered out. Afterwards, a table was formed of 6 land use classes and their corresponded LST values. Using SPSS 17 (SPSS Inc, 2008) and a one-way ANOVA function, Analysis of variance was tested. The ANOVA was used to test the hypothesis that several means of different land use classes are equal.

In addition to determining if differences exist among the means, post hoc tests were applied to see which means that were differing, and where the difference among the means lie. The ANOVA results were analyzed using the Bonferroni post hoc test (Newsom, 2006). The Bonferroni is possibly the most frequently used post hoc test, because it is very flexible and simple to compute (Newsom, 2006). To visualize LST temporal behavior, LST time plots were plotted for all the 27 cells (see Fig. 7). Time plots showed the yearly and seasonal behavior of LST from 2000 to 2008. For each time plot, a graph trend equation was calculated. Later on the trends were used to examine if there was any relationship between LST values for different years when land use was fixed. This analysis was done for night LST values. To investigate if the LST variation was associated only with changes in land-use condition, LST time plots were plotted.

To visually assess LST trends in the cells with land use changes, 12 cells with sharp land use changes were selected. The selection of the 12 cells was based on availability of cells with sharp land use changes. These cells were in fact the maximum and minimum values of land use percentage change columns (see section 3.1.1). The LST values for these cells were extracted. LST time plots then were plotted from 2000 to 2008. To prove whether LST behavior was changed due to land use changes, LST values before and after land use change were tested using a Z-test (two- sample for means).

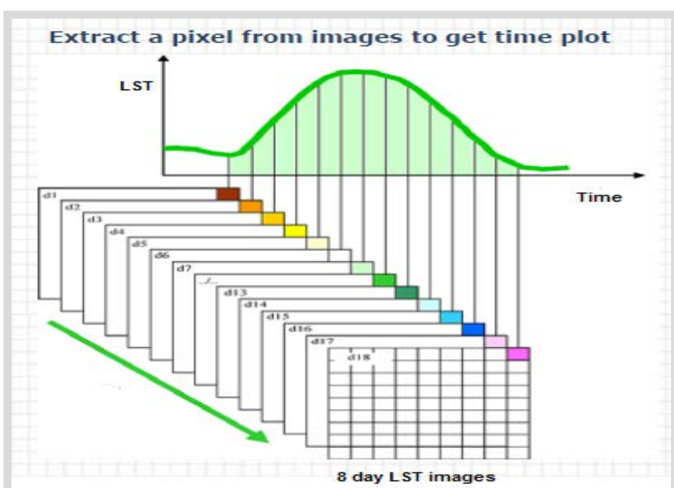

Figure 7 - Time plot per pixel from a time-series, modified from FAO (2010). For any selected pixel, the LST values were extracted from 2000 to 2008. Then the values were plotted versus time.

3.4. Evaluation of spatial behavior of land surface temperature in relation to land use conversions

3.4.1. Retrieving LST values from LST images

The satellite data used for this study were MODIS LSTs, and the product was the 8-day 1 km MOD11A2, averaging LSTs in the daily product MOD11A1 over 8 days. The 8-day composites of these LST HDF images were downloaded for the period from 2000 to 2008 from the reverb data gateway. 400 HDF images with 8-day intervals were downloaded from 2000 to 2008, see example in Fig. 8 LST images were then converted from the HDF-EOS format to GeoTIFF. The conversion was done for night LST header. This was achieved using the HEG software (HDF-EOS to GeoTIFF conversion tool). Only night LST images were selected for further analysis. During the day different land use classes absorb the sun energy, which is related to their heat capacity. During night times, the collected heat will be released as so called emissivity. The emissivity is captured by the night LST values while there is no heat absorption from the sun. This justifies why the night time LST values were selected to check weather different land uses have different land surface temperature.

Figure 8 - Sample night LST image tile and the position of the Netherlands boundary in it.

3.4.2. Computation of annual LST mean values

The images of the years 2003, 2006 and 2008 were selected to calculate the yearly mean LST values. This because in these years both LST data and BBG land use maps were available. LST values for the year 2000 started from 65th day of the year, so the year 2000 was excluded although a BBG land use map was available. Due to the nature of LST data, there are lots of zero values in LST images. These zero values are in fact quality flags of 2 and 3. These zero values could skew the surface analysis. The next step was thus filtering out these zero values from the LST images. To achieve this, a raster attribute table was defined for all the images. Afterwards, using the raster calculator and the Outras = SetNull (Inras1==0, Inras1) equation, all the zero values were converted to NO Data. Later, using the spatial analyst tool and cell statistic function, the yearly mean LST was calculated for the years of 2003, 2006 and 2008. Then the 3 yearly mean LST raster files were converted to point shape files, using the raster to point function of ArcGIS. These point shape files were then crossed with MODIS grid shape file using the intersection function of ArcGIS. The final result was a Dutch MODIS grid shape file for which all the pixels have land use coverage ratio and mean yearly LST.

3.4.3. Pearson's correlation analysis

LST pixel values and their corresponding land use percentage values were extracted in ArcGIS. These data series were processed to determine the relationship between LST and percentage of different land use types in SPSS. To better understand how LST dynamics were associated with land use, correlation strength between LST and the percentage of each land use was examined. Simple statistical analysis was used to find probable interconnections between LST and land use. In this phase of the analysis, the mean yearly LST and the percentage of different land uses for all pixels were available in the attribute table of MODIS grid shape files and for the years of 2003, 2006 and 2008. The attribute table then was exported to Excel sheets. To check the linear association between mean LST and the percentage of different land uses, Pearson's correlation between land use and mean LST was tested. However, if the data consist of underlying groups, then it is important to decompose the "total" correlation into components that measure the correlation within the groups, and the correlation between the groups (Marzban, 2013). The land use percentage data were grouped. Groups were formed based on land use percentage from zero to 10%, 10-20%, 20-30%, 30-40%, 40-50%, 50-60%, 60-70%, 70-80%, 80-90% and above 90%. The result was 10 groups for each land use class and for the three years of 2003, 2006 and 2008. The between-group correlation was obtained by averaging the land use percentage and LST values for each group. In other words, each group was represented by the average of the corresponding land use percentage and LST values. Pearson's correlation coefficient was computed once again for the prepared groups. Later on land use change and mean LST change from 2003 to 2006 and from 2006 to 2008, were computed and added to the excel sheet. The next set of analyses tested Pearson's correlation, first between all land use percentage changes and LST changes, and then between land use percentage changes above 20 percent and the corresponding LST change values.

3.4.4. Multiple regression analysis

The correlation indicates the strength of linear association between paired variables. Correlation is unable to show the interconnected effects of various land uses (Su, 2012). For example, consider one pixel which is occupied 50% by water and 50% by greenhouse farming. Due to the compensating effect of these two land use types on LST value, the LST value of this pixel doesn't show the real effect of inland water nor greenhouse farming. A multiple linear regression model was thus applied. The conventional regression model for a study is expressed as:

$$y=\alpha+\beta X$$

In which y (dependent variable) can be the land surface temperature, x can represent the percentage cover of land use (independent variables), and α is the intercept of the regression model. The regression reveals the form of linear relationship that best predicts LST from the values of land use percentage.
In this study stepwise regression was used. Stepwise is a regression model with sequentially adding or removing variables based on the t-statistics of their estimated coefficients (SPSS Statistics Base 17.0 User's Guide).

One aim of this study is that land thermal environment would be monitored and assessed by land use qualitatively. The prepared tables of MODIS pixel's land use percentage and LST values were imported into SPSS. Stepwise multiple linear regressions were then used to predict how the percentages of different land uses affect the mean LST in each pixel. Regression was repeated for the years 2003, 2006 and 2008. Mean yearly LST was considered as the dependent variable and the percentage contribution of different land use groups as the independent variables. The regression table had 4075 pixels of LST and corresponding land use percentage.

3.4.5. LST aggregation analyses, spatial mean, zonal statistic

To summarize the values of LST within each province and to provide tangible and practical information for decision making, zonal statistic methods were used. The spatial mean LST was then computed for all Dutch provinces (see Fig. 9). To achieve this, yearly mean LST raster files of the years 2003, 2006 and 2008 were used. To calculate the average LST of each province, the LST image values were converted to integer values, using the Int. function of spatial analyst tool in ArcGIS. Afterwards, applying zonal statistic function, the surface mean LST was calculated. The population density of Dutch provinces associated with each LST zone was then shown as a map to be compared with the LST map.

The mean LST for each province and the LST range for each municipality were calculated in the years of 2003, 2006 and 2008. To show weather the location of different land use classes related to mean LST values, the year 2006 was selected as a sample year. This was because the spatial pattern of different land uses was not very different from 2000 to 2008. In this year the distribution of different land uses, was illustrated with the background of mean LST.

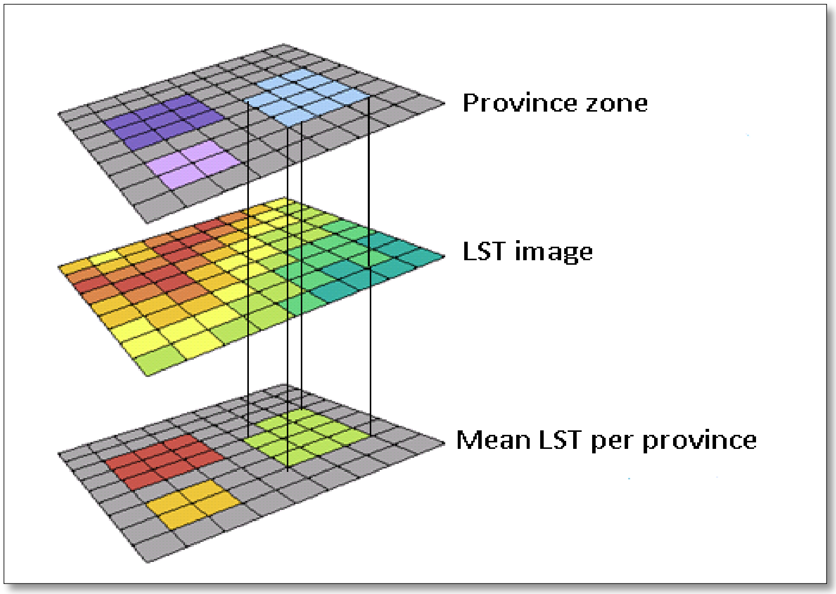

Figure 9 - Mean aggregation analysis (zonal statistic) of computing the mean LST for each province (modified from ArcGIS 10 help).

Chapter 4

Result and discussion

4.1. Analyze land use changes in the Netherlands between 2000 and 2008 in the context of LST pixels, using BBG data set.

Fig. 1 to Fig. 18 available in the appendix (Group. 4), show different land use changes for three time periods of 2000-2003, 2003-2006 and 2006-2008. Later on in this part, the amount of land use increase, land use decrease and the net land use change records in different time periods will be discussed. The change records are computed in the LST pixel scale. In other words, the change records are the sum of the increased, decreased or changed area of a land use which is computed based on all the Dutch LST pixels for each time periods. For example if it is argued that from 2000 to 2003, greenhouse farming has decreased by -1030.37 hectare and increased by 1694.784 hectare. It means in this time period, totally -1030.37 hectare of greenhouse farming is vanished from some pixels and at the same time it is expanded by 1694.78 hectare in other pixels of the country. Thus the net amount of change in this period is the absolute sum of decrease and increase, which is 2725.15 hectare. The border of the Netherland and the border of the Dutch LST grid map are not completely fitting. Therefore the change area records are subjected to be approximate.

Fig. 1 to Fig. 3 available in the appendix (Group. 4) show the spatial pattern of open agriculture. For all three periods open agriculture has a decreasing trend. The constructed line structures are observed in open agriculture change map in the first period. It shows bouwterrein areas were initially open agriculture. For the open agriculture class from 2000 to 2003, -34176.29 and 15873.19 hectare decrease and increase are observed. Net change of open agriculture class in this period is -18303.10 hectare. In the period of 2003 to 2006, -27928.69 and 10757.55 hectare are open agriculture decreasing and increasing values. In this period, total area of open agriculture decreased by -17171.14. From 2006 to 2008, the area of open agriculture in the Netherlands is decreased by -17158.16 hectare and increased by 7385.71 hectare.

Fig. 4 to Fig. 6 available in the appendix (Group. 4) show the spatial pattern of changing in forest land use. The density of changes is not high, but the trend is decreasing from 2000 to 2008. From 2000 to 2003, the forest class had -12800 hectare decrease and 9078.66 hectare increase of the area, in the context of MODIS LST grid shape file for the whole Netherlands. Totally, there is -3721.34 hectare decrease in forest land use from 2000 to 2003. In the period of 2003 to 2006, there is -7368.38 hectare decrease and 5771.49 hectare increase in the area coverage of forest land use in the Netherlands. The net forest change in this period is -1596.88 hectare. From 2006 to 2008 the forest has decreased by-2715.95 and has increased by 2726.86 hectare in the whole country.

Fig. 7 to Fig. 9 available in the appendix (Group. 4) show the greenhouse farming changes in the context of MODIS pixels. As the figures show the concentration of greenhouse farming changes is in the western part of the country, especially from 2000 to 2003. In the period of 2003 to 2006, a southward trend of greenhouse expansion is observable. In the third period, the spatial expansion is mostly to the north of the country. From 2000 to 2003 greenhouse farming has decreased by -1030.37 and increased by 1694.784 hectare. In the second period change records of -833.49 and 1417.63 hectare decrease and increase in greenhouse farming are calculated. From 2006 to 2008 greenhouse has decreased by -683.966 and increased by 1222.30. Fig. 10 to Fig. 12 available in the appendix (Group. 4) show the recreation area which is sparsely changed in the whole country. From 2000 to 2008, the amount of changes has reduced.

Fig. 13 to Fig. 15 available in the appendix (Group. 4) show the spatial change pattern of buildup area. The map clearly shows some linear patterns of buildup area change. Possible explanation for linear change patterns is infrastructure development. This is because the build-up class has included “bouwterrein” class. bouwterrein areas are temporary buildup area to support infrastructure development. The lines in the map are an east-west rail connection for goods between approximately Rotterdam and Nijmegen and their surrounded bouwterrein area. In the period of 2003 to 2006, and after completing the road construction, this lines conversion gets back. In the third period, a hot urbanized spot is observed in the northern east part of the Netherlands. This part is related to the project Blauwestad (2011-2012), in the Province of Groningen. Build-up area has a net increasing trend from 2000 to 2008. In the first period it has decreased by-11534.47 hectare and increased by 24234.32 hectare. From 2003 to 2006, build-up area has decreased by -9207.84 and increased by 20525.18 hectare. In the third period, decrease of -8342.54 and increase of 14003.18 hectare are observed. In the past, in The Netherlands, number of households increased faster than the population; the trend is slowing down to some extent, but still there is a extensive growth in the number of households, which results in 39,000 to 85,000 additional hectares for residential land use by 2030 (Muhammad, 2007).

Fig. 16 to Fig. 18 available in the appendix (Group. 4) illustrate the change patterns of Inland water class in three periods of 2000-2003, 2003-2006 and 2006-2008. In the first period the change pixels are mostly reddish, which shows a clear increasing trend. In this period inland water has decreased by -1234.46 hectare and increased by 3728.803 hectare. In the second period, a hot reddish spot of inland water is observable in the north eastern part of the country. Tracing the same pixels in open agriculture map in the same time period, one can see these cells are abundant farms. This area is in fact under construction of the project Blauwestad in the Province of Groningen to make attractive living in that area around a new lake. The introduction of new water to the inexpensive agricultural land of Groningen might offer interesting prospects for recreation and attractive locations for the construction of housing (World building directory, 2012). In the second period inland water has increased by 4096.70 hectare and decreased by -1386.35 hectare. In the third period, the rate of expansion lessened, and mostly lies in the south western part of the country. In this period, there is -575.53 hectare decrease and 1639.352 hectare increase in the area coverage of inland water land use in the Netherlands.

Fig. 10 shows that from 2000 to 2008, the net area change of open agriculture and forest has a decreasing trend. Meanwhile, build-up area, recreation area, greenhouse faming and inland water and offshore areas are increasing. The sharpest decrease from 2000 to 2008 is for open agriculture and the largest increase in the same period is for build-up areas.

Fig. 11 shows the magnitude of land use changes from 2000 to 2008. In other words, change here is the absolute sum value of the positive and negative changes of each land use from 2000 to 2008. Open agriculture has the highest change which is followed by build-up area, forest, recreation area, inland water and greenhouse farming. For greenhouse farming the amount of net land use change is approximately 4 times smaller than the amount of absolute land use change. The reason could be due to managerial strategies and policy decisions related to land use management. Based on Verburg et al., (2004), the most important driving factors of current land use changes in the Netherlands are spatial policies, accessibility, and neighborhood interactions.

Totally from 2000 to 2008, green house farming has changed by 6882.56 and has increased by 1786.89, inland water class has increased by 6268.513 and has changed by 12661.209, build-up area is changed by 87847.539 and increased by 29677.83 hectare, and recreation area has changed by 28566.61 hectare and has increased by 8550.82 hectare. In total, from 2000 to 2008 there are 113279.61 changes in open agriculture land use, for the forest in the same period; there is 40461.36 hectare change and -5307.31 hectare decrease in the amount of forest area in the whole country. Verburg et al., (2004), argued that urbanization is the most important process of land-use change in the Netherlands .

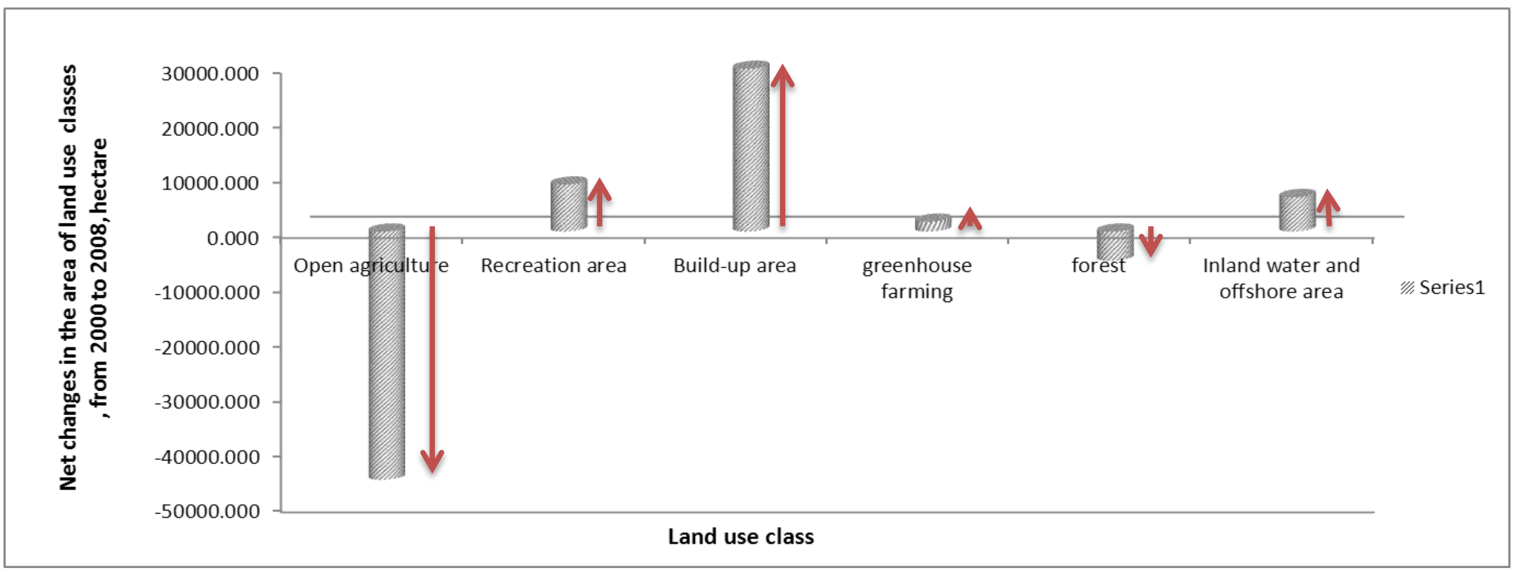

Figure 10 - Net land use change from 2000 to 2008, hectare

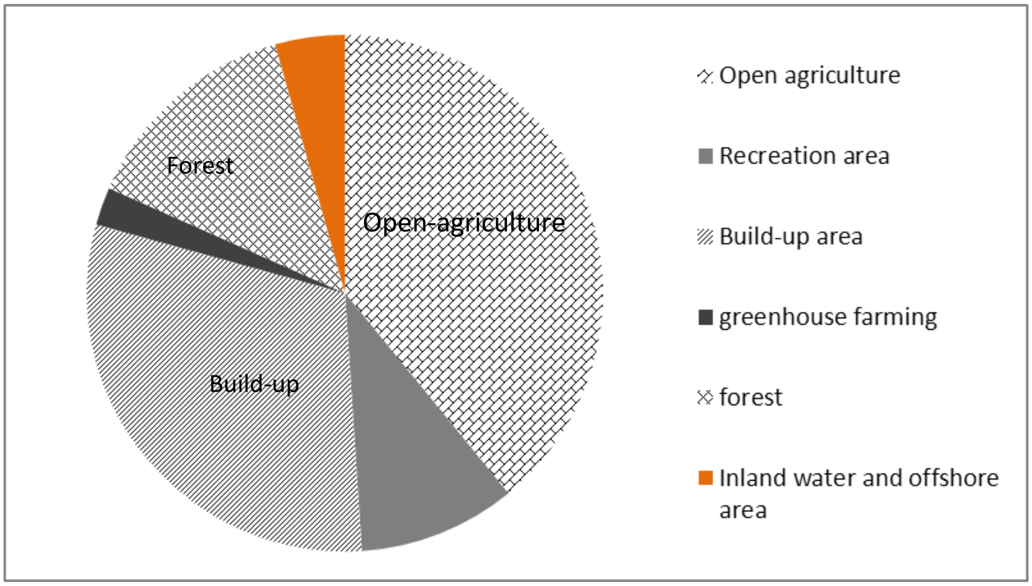

Figure 11 - Absolute land use change from 2000 to 2008, hectare

As the land use analysis demonstrates, urbanization had an increasing trend from 2000 to 2008 in the Netherlands. One of the important environmental consequences of urbanization is the urban heat island (UHI). UHI is defined as a phenomenon in which the urban environment is warmer than surrounding rural areas (Voogt and Oke, 2003). UHI is a relative phenomenon which gets worse when the skin temperature of the urban and its surrounding land use is highly different. The spatial arrangement of Dutch land uses, shows a common pattern of central urban areas which are surrounded by open agriculture farms. Thus increasing build-up area in on hand and decreasing open agriculture land use on the other hand could enhance the UHI phenomenon. Based on Fig. 12, the Netherlands has a high percentage for withdrawal of farming from 2000 to 2006 which supports the result of the current research.

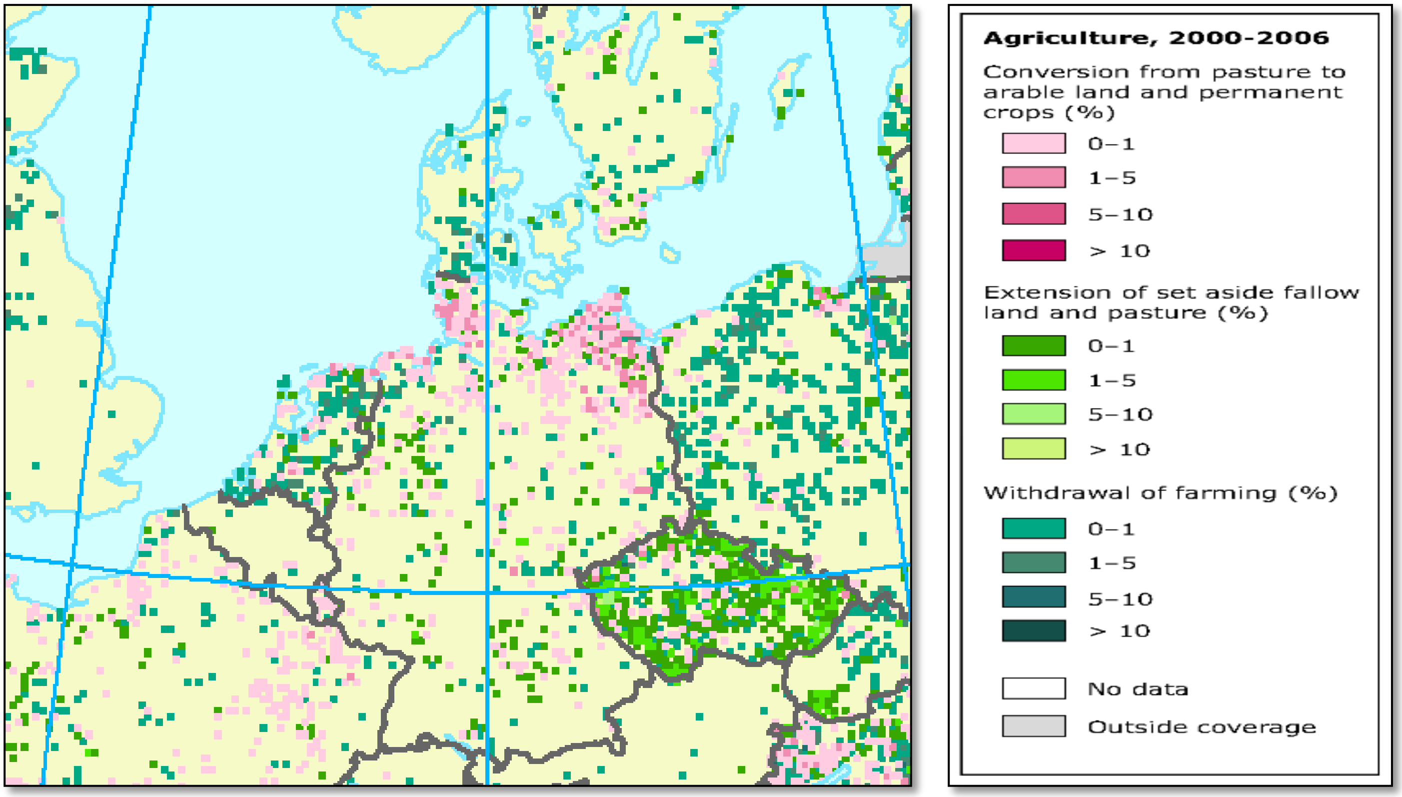

Figure 12 - The distribution and intensity of selected Land Cover Flows (LCF) in agricultural area between 2000 and 2008. The map is refined from Corine dataset source, available at: http://www.eea.europa.eu/data-and-maps/figures/agriculture-clc-change.

4.2. temporal behavior of MODIS land surface temperature for different land uses

Twelve pixels, with severe land use change were selected to show the LST change behavior. For one of them LST is not available due to the cloudy condition. Fig. 13 shows one sample of 11 prepared graphs.

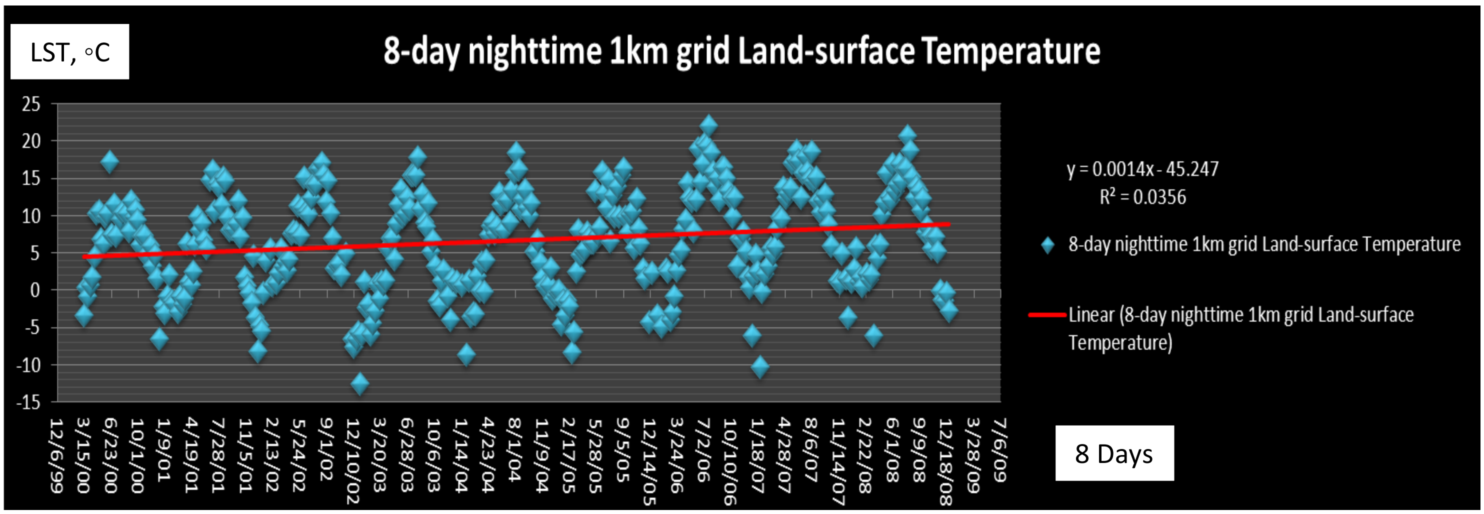

Figure 13 - LST time plot of a MODIS pixel in which land use has changed from 2000 to 2008 (Latitude: 53.1875 Longitude: 7.04413)

Other 10 graphs are provided in the appendix (Group 1 and Group 2). Fig. 13 shows that the surface temperature varies with respect to land use changes; the sample graph shows the behavior of LST in one pixel from 2000 to 2008. In the period of 2000 to 2003, the percentage of inland water in this pixel is zero percent.

As Tab. 6 indicates, the percentage coverage of inland water is increasing. The term "percentage cover" used hereafter in this study is defined as the percentage of a land use type within a pre-defined area, which is the area represented by a MODIS LST pixel of satellite sensor image. In 2006, 78 percent of the cell is occupied by water. At the same time the LST values started to increase. To see whether the increase in LST is statistically significant, a two-tail Z-test is applied.

Table 6 – The percentage of inland water in the selected pixel in the years of 2000, 2003, 2006 and 2008

MODIS, l mod11a2 Cell	MODIS FID	Longitude	Latitude	%inland water2000	% inland water2003	% inland water2006	% inland water2008
817, 506column):	1542	7.04413	53.1875	0.000(mainly open agriculture)	0.000(mainly open agriculture)	77.932	77.932

Tab. 7 indicates the result of Z-test between LST values before and after land use change. Based on this table, the mean LST value for the period of 2001 to 2003 is 5.16 degree Celsius. The mean value is increased by 3.45 degree Celsius in the period of 2006 to 2008.
Therefore the mean LST value in the pixel in 2000 and 2003 with zero percent inland water is 5.16 degree Celsius. The mean LST value in the same pixel but after changing it's land use pattern (78 % increase in inland water) is 8.16 degree Celsius. The Z-test is applied for the mean LST values before and after the land use change. The null hypothesis claims that the means are equal. P value is less than 0.01. Thus the mean of two communities are statistically different at the level of 0.01.
In some pixels, although they have sharp land use changes, there is no statistically significant difference in the amount of LST before and after land use change. In fact just in two cases of all 11 pixels the result of z-test is significant. One possible explanation is that in some pixels, although the percentage of changes is high, the land use types which are switched, have similar LST values, like open agriculture and forest. For the pixel which is shown above both, the type and the amount of land use change are strong. Some types of land use changes are in fact change in the use of the surface, not in the cover of it. For example a forest patch in 2003, which is still forest in 2006, but is interpreted as recreation area. Another example is vegetative land uses. Although they are categorized in different land use groups, they have similarities in the amount of LST. Hence the LST time plots don't show a significant increasing or decreasing trend, while land use is sharply changing.

Table 7 - The result of Z-test for LST values before and after the land use change

z-Test: Two Sample for Means		
	8-day nighttime (2001,2002,2003)	8-day nighttime(2006,2007,2008)
Mean	5.164109	8.617538
Known Variance	45.32	48.44
Observations	129	130
Hypothesized Mean Difference	0	H0: m1=m2 (rejected) H1: m1 <> m2 (accepted) z> z Critical two-tail P value< α=0.01
z	-4.05884	
P(Z<=z) one-tail	2.47E-05	
z Critical one-tail	2.326348	
P(Z<=z) two-tail	4.93E-05	
z Critical two-tail	2.575829	

Fig. 14 shows the LST trend, from 2000 to 2008.The selected pixel is fully covered by forest from 2000 to 2008, Tab. 8. The value of R^2 is 0.000009, which is not statistically significant. The slopes of the trends are also near zero. It means in the selected pixel, there is no significant change of LST, while the land use is untouched. 27 representative cells were selected for fixed land use pixels. The result of R^2 values for all the 27 time plot is 0.00. It means that for the selected 27 sample pixels, when land use is stable, there is no significant change of LST from 2000 to 2008. Fig. 14 is shown as an example, and other 26 LST time plots are provided in the appendix (Group 1 and Group 3).

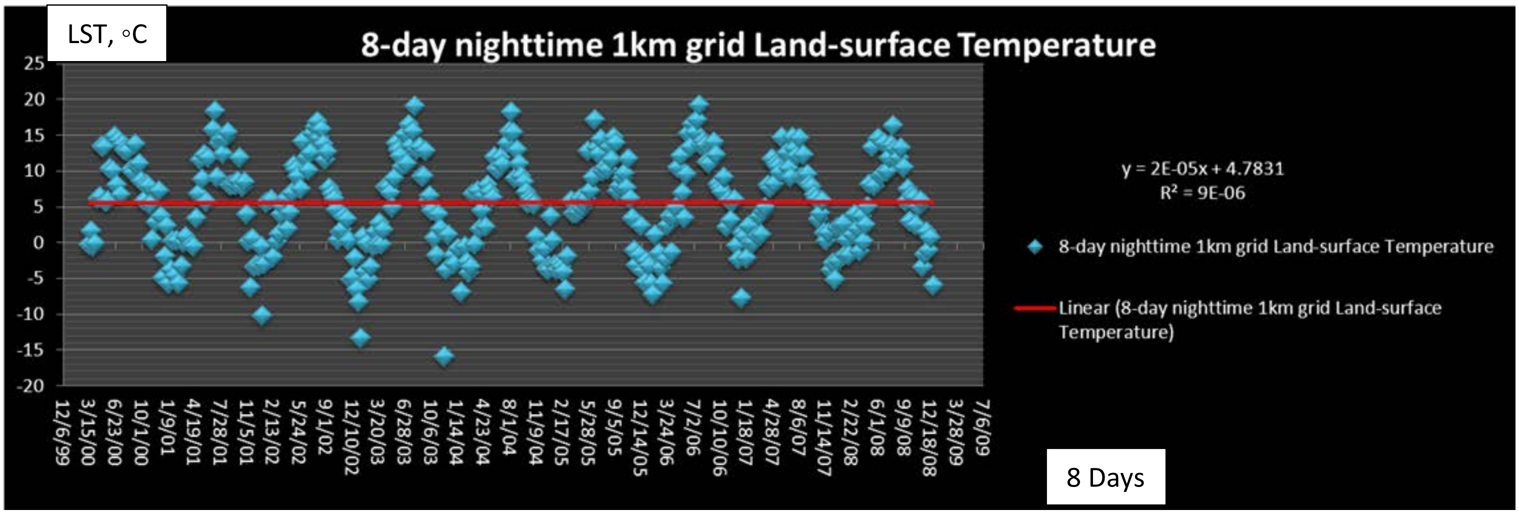

Figure 14 - LST time plot of a MODIS pixel in which land use has no land use change from 2000 to 2008 (Latitude: 52.3292 Longitude: 6.44304)

Table 8 - The land use coverage of selected pixel from 2000 to 2008

MODIS, Tile: h18v03	MODIS FID	Longitude	Latitude	%forest 2000	%forest 2003	%forest 2006	%forest 2008
Cell (row, column): 920, 472	6886	6.44304	52.3292	100.000	100.000	100.000	100.000

4.3. Evaluation of spatial behavior of land surface temperature in relation to land use conversions.

4.3.1. ANOVA test for night time LST

ANOVA is a statistical method used to compare the means of two or more groups. Tab.9 shows the descriptive analysis of nigh LST values of 27 fixed land use pixels. The column called count is the number of LST values extracted from fixed land use pixels from 2000 to 2008. For example, in five pixels with entirely open agriculture land use from 2000 to 2008, 1498 LST values are extracted. The column sum is the sum of all night LST values for each land use. Dividing the sum columns by the number of involved pixels, arithmetic mean is computed. The lowest mean LST is observed in forest, followed by open agriculture, recreational area, greenhouse farming, build-up area and inland waterway and offshore area.

The warmest land use during the nights is Inland waterway and offshore area. Water has an extremely high heat capacity J/kg/◦C (Sharp, 2001); this means that water can absorb a lot of energy before it increases temperature. During the day time water absorb a high amount of heat. During night time, it emits the highest land surface temperature comparing to other land uses. This response is due to a rather high thermal inertia, relative to typical land uses. Thus, it heats less during the day and keeps that heat more at night and has the highest night LST. Forest has the lowest night LST. It is related to cooling effect of evaporation and evapotranspiration.

Table 9 - descriptive analysis of nigh LST values

	SUMMARY					
	Groups	*Count*	*Sum*	*Arith. Mean*	*Variance*	*Std. Dev.*
1	Open agriculture, 5 pixels	1498	7089.94	4.733	44.585	6.677
2	Build-up area, 5 pixels	1894	13540.68	7.149	51.906	7.205
3	Recreational area, 2 pixels	725	3843.99	5.302	54.894	7.409
4	Greenhouse farming, 5 pixels	1969	10457.79	5.311	36.062	6.005
5	Forest, 5 pixels	1385	6042.57	4.363	59.287	7.700
6	Inland waterway and Offshore area, 5 pixels	1571	12598.19	8.019	56.292	7.503

Tab. 10 shows the result of applying the ANOVA test. F statistic indicates the amount of overlap group distributions. If the differences between groups are higher than the differences within the groups, the F value gets larger and the null hypothesis gets rejected. The null hypothesis for F test claims that all the means are equal. The alternative hypothesis argues that not all the means are equal and at least one of them is different. Tab. 10 indicates that the F test is significant at the level of 0.01 and null hypothesis is rejected.

Table 10 - The result of ANOVA test for night LST

	Sum of Squares	df	Mean Square	F	Sig.
Between Groups	16244.701	5	3248.940	65.800	.000
Within Groups	446110.511	9035	49.376		
Total	462355.211	9040			

As discussed above, null hypothesis is rejected. Clearly there is a difference among the groups. Additional analysis, called post hoc tests, is done to determine where the differences lie. Fig. 15 shows the mean value of forest and open agriculture is very similar. Greenhouse farming and recreational area also show similarities in mean value.

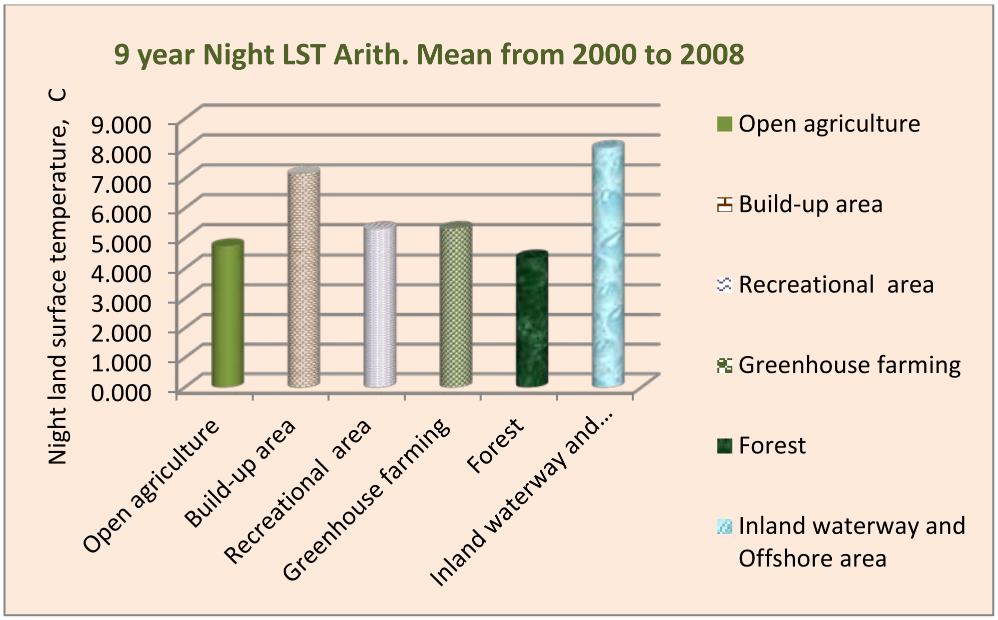

Figure 15 - Night LST arithmetic mean for different land uses

To capture statistically significant differences between the mean values of land use groups, Bonferroni analysis is applied. Tab. 11 shows the result of Bonferroni test. If the sig. column (the P value) is less than 0.01 or 0.05, the results are statistically significant at the 0.01 and 0.05 significance level. Open agriculture group is significantly different from build-up area and inland waterway and offshore area groups at the 0.01 level. While there is no statistically prove to consider open agriculture, recreational area, greenhouse farming and forest as different groups. Build up area is statistically significant (P = 0.01) from all other land use groups. Recreation area group is different from build-up are and Inland waterway and offshore area groups at significance level of the 0.05. It´s mean is considered significantly different from forest (P = 0.05). Green house farming is significantly different from build-up are, inland waterway and offshore area and forest groups. Forest is a separate group from build-up area, inland waterway and offshore area and greenhouse farming at the 0.01 significance level. Forest group also differs from recreational area (P = 0.05). Inland waterway and offshore area is significantly different from all other groups at the 0.01 level. In summary, build-up and Inland waterway and offshore area are considered as separate groups.

Table 11 - The result of Bonferroni test for night LST

(I) landuse	(J) landuse	Mean Difference (I-J)	Std. Error	Sig.
1 Open agriculture	2	-2.412*	.243	.000
	3	-.565	.318	1.000
	4	-.574	.241	.258
	5	.374	.262	1.000
	6	-3.282*	.254	.000
2 Build-up area	1	2.412*	.243	.000
	3	1.847*	.307	.000
	4	1.838*	.226	.000
	5	2.786*	.248	.000
	6	-.870*	.240	.004
3 Recreational area	1	.565	.318	1.000
	2	-1.847*	.307	.000
	4	-.009	.305	1.000
	5	.939	.322	.053
	6	-2.717*	.315	.000
4 Greenhouse farming	1	.574	.241	.258
	2	-1.838*	.226	.000
	3	.009	.305	1.000
	5	.948*	.246	.002
	6	-2.708*	.238	.000
5 Forest	1	-.374	.262	1.000
	2	-2.786*	.248	.000
	3	-.939	.322	.053
	4	-.948*	.246	.002
	6	-3.656*	.259	.000
6 Inland waterway and Offshore area	1	3.282*	.254	.000
	2	.870*	.240	.004
	3	2.717*	.315	.000
	4	2.708*	.238	.000
	5	3.656*	.259	.000

4.3.2. ANOVA test for day time LST

Tab. 12 shows the descriptive results of analyzing 27 homogeneous land use MODIS LST pixels. Build-up area has the largest day LST. Inland waterway and offshore area has the least day LST. It is because of high heat capacity of water. As Tab. 12 indicates, water has the minimum day LST mean. Water can be considered as a cooler land use during the day. As discussed from night ANOVA analysis, water has the largest night LST among all land use types. Build-up area has the largest day LST. The findings of the current study are consistent with those of Weng et al., (2004) who found that commercial and industrial land had the highest temperature followed by residential land; the lowest temperature was observed in forest and then in water bodies. The present findings seem to be consistent with other research of Guo (2012) which found that built-up areas with paved roads and residential and factory buildings have significant higher surface temperatures than other land cover types. Based on their study, vegetation have the lowest surface temperatures.
Possible explanation for high mean LST of paving materials is that paving and building materials are mostly dark and have a large heat capacity in one hand and a low reflectivity on the other hand (Mallick, 2009). Moreover, natural land covers benefit from cooling effect of soil moisture, evaporation and transpiration.
Lowest day time LST in the current study is for green house land use. The reason is that greenhouse farming houses have highly reflective roofs. The variance value of LST has the largest amount for build-up area, indicating that these surfaces experience a wide variation in land surface temperature which could be because of different construction materials.

Table 12 - descriptive analysis of day LST values

SUMMARY				
Groups	*Count*	*Sum*	*Arith. Mean*	*Variance*
Open agriculture, 5 pixels	1859	25806.03	13.882	75.38114
Build-up area, 5 pixels	707	12083.37	17.091	110.6373
Recreational area, 2 pixels	1822	28032.6	15.386	82.37462
Greenhouse farming, 5 pixels	1838	23253.18	12.651	75.32547
Forest, 5 pixels	1800	23423.64	13.013	71.6768
Inland waterway and Offshore area, 5 pixels	1871	21870.19	11.689	49.70682

Tab. 13 shows the ANOVA test result for daytime LST. The result shows that the F value is statistically significant ($p = 0.01$). Thus the null hypothesis is rejected and at least the mean of one of the land uses is not equal to zero. In other words, not all the means are equal and at least one of them is different.

Table 13 - The result of ANOVA test for day LST

	Sum of Squares	df	Mean Square	F	Sig.
Between Groups	23681.851	5	4736.370	64.309	.000
Within Groups	728401.816	9890	73.650		
Total	752083.667	9895			

Fig. 16 shows some similarities between the mean values of different land uses. For example, the mean day LST value for greenhouse farming and forest are almost the same. To find weather the near values are in the same groups, post hoc analysis is done. The lowest mean LST is observed in inland waterway and offshore area, followed by greenhouse farming, forest, open agriculture, recreational area and build-up area. The findings of the current study are consistent with those of Zhou et al., (2011), who found that the amount of LST becomes higher as the land use changed from vegetated areas to built-up lands. Campbell (2002) argued that temperature of different bodies is a function of their internal properties including heat capacity, inertia and thermal conductivity. Build-up area has the highest day LST, which can be due to reduction of the water storage that strengthen the sensible heat flux (Zhou, et al, 2011) .Non-evaporating and non-transpiring surfaces like p aving and building materials have high absorptivity, high thermal capacity and low albedo. Based on NCHRP (2004), asphalt pavement has low conductivity (0.76-1.4 W/mK) which prevents the absorbed energy from being conveyed elsewhere; high absorptivity (0.85-0.93) of solar radiation coupled with relatively high thermal capacity (921-1,674 J/KgK) allows asphalt pavements to stock thermal energy and reach relatively high temperature – usually higher than the neighboring air. Fig. 16 also shows that open agriculture has a larger mean LST than forest. This finding corroborates the ideas of Wickham (2012), who found that the average annual land surface temperature for cropland is higher than average surface temperatures for forest. This finding furthermore supports previous research of Davin and Noblet-Ducoudré (2010). They argued that evapotranspiration from forest produce a larger cooling effect than croplands. For dense forest canopy, LST is collected from forest canopy. Therefore to compare forest with open agriculture, type of forest (evergreen, deciduous), and type of open agriculture (winter or summer farms) should be considered. Seasonal analysis can capture these variations better than annual LST values. In general, forest albedo is lower than cropland albedo. The color of soil, its water content and snow cover are among other important factors which impact surface characteristic (Bonan, 1997).

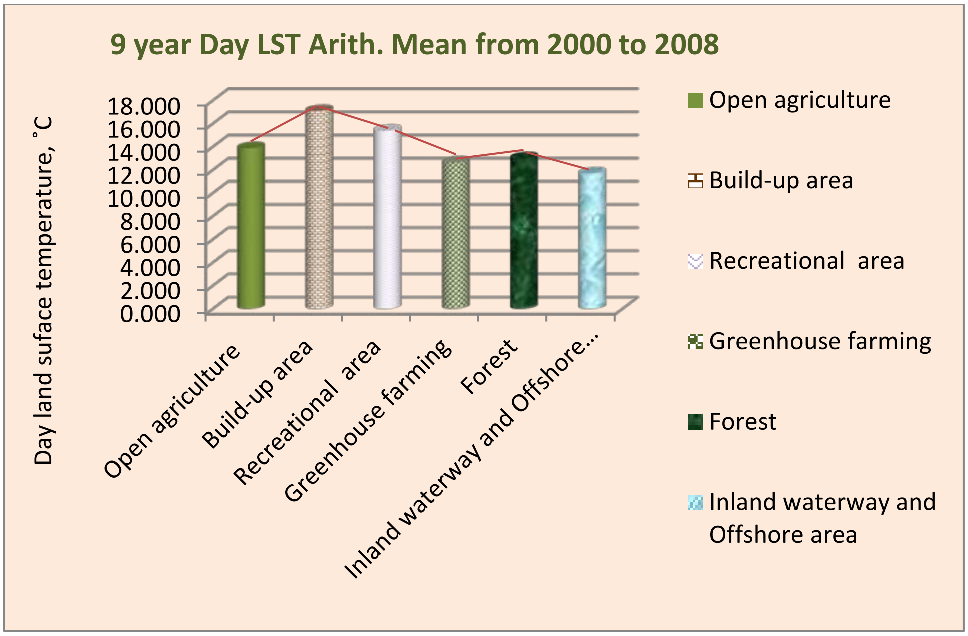

Figure 16 - Night LST arithmetic mean for different land uses

The LST shows similarities for forest, greenhouse farming, inland water and open agriculture. To allocate statistically different groups to these land use types, post hoc analysis is done. Tab. 14 shows the result of a Bonferroni test. Open agriculture is statistically different from forest at the significance level of 0.05, which supports the result of Wickham (2012). Open agriculture is separated from all other land use types at the 0.01 significance level. Build up area, inland waterway and offshore area and recreational area are considered as distinct land use groups (P = 0.01). Greenhouse farming is disjointed from all land use types (P = 0.01), except forest. Forest is statistically different from build-up area, recreational area and inland waterway and offshore area at the level of 0.01. Forest and open agriculture are allocated to different groups at significance level of 0.05. In summary, forest and greenhouse farming are considered as a jointed group. However, the findings of the current part do not support some of the previous research of Quattrochi and Ridd (1998) that argued that thermal responses for vegetation can be highly different as a function of the biophysical properties of the vegetation. For any surface material, certain internal properties play important roles in governing the temperature of a body at equilibrium with its surroundings (Campbell, 2002). These thermal properties vary with soil type and its moisture content (Sandholt et al., 2002). Biophysical characteristics of different vegetation types affect the thermal behavior of different green land covers (Weng, 2004).

Table 14 - The result of Bonferroni test for night LST

(I) land use	(J) land use	Mean Difference (I-J)	Std. Error	Sig.
1 Open agriculture	2	-3.206*	.379	.000
	3	-1.500*	.283	.000
	4	1.234*	.282	.000
	5	.872*	.284	.032
	6	2.196*	.281	.000
2 Build-up area	1	3.206*	.379	.000
	3	1.705*	.380	.000
	4	4.440*	.380	.000
	5	4.078*	.381	.000
	6	5.402*	.379	.000
3 Recreational area	1	1.500*	.283	.000
	2	-1.705*	.380	.000
	4	2.734*	.284	.000
	5	2.372*	.285	.000
	6	3.697*	.282	.000
4 Greenhouse farming	1	-1.234*	.282	.000
	2	-4.440*	.380	.000
	3	-2.734*	.284	.000
	5	-.362	.285	1.000
	6	.962*	.282	.010
5 forest	1	-.872*	.284	.032
	2	-4.078*	.381	.000
	3	-2.372*	.285	.000
	5	.362	.285	1.000
	6	1.324*	.283	.000
6 Inland waterway and Offshore area	1	-2.196*	.281	.000
	2	-5.402*	.379	.000
	3	-3.697*	.282	.000
	4	-.962*	.282	.010

5	-1.324*	.283	.000

4.3.3. Comparing day and night analysis

Tab. 15 and Fig. 17 indicate the difference between day and night LST values for different land uses. LST is normally defined as soil surface temperature for the bare soil surface. For dense vegetated ground, LST is the canopy surface temperature and for sparse vegetated LST is determined by the mixed temperature of the vegetation canopy, vegetation body and the soil surface (Qin and Karnieli 1999).

Build-up area and open agriculture has the largest LST difference between day and night values. One interesting point is inland water LST pattern. Inland water has the maximum night LST, minimum day LST and the minimum LST difference between day and night. This is because the water temperature changes slowly due to high thermal inertia and convection (Sun, 2012). After inland water the lowest mean difference is for greenhouse farming, followed by forest, open agriculture, build-up area and recreational area. The present findings seem to be consistent with other research of Kant et. al (2009), which found commercial/industrial and high dense builtup area to have high surface temperature values during day time, compared to water bodies, agricultural cropland, and dense vegetation. They also argued that night LST values are higher in dense built-up and water bodies, than in dense vegetation and agricultural cropland. Recreation is a mixed land use and it is not easy to interpret its LST behavior. The mean day and night LST difference of forest is 8.65 degree Celsius which is less than the open agriculture with 9.14 degree Celsius. Based on Goulden et. al (2006), and due to night drainage of cold air from upper canopy layer to ground level, upper levels of canopy are warmer than forest ground level. This process is more sensible in intact forests rather than sparse and short vegetation. Based on the process described above, intact forest shows a higher night LST than short vegetation and bare ground. Consequently the LST difference between day and night is lower (Goulden et al., 2006). The reason is that satellite sensors only measure the temperature of the top of forest canopies. High difference between open agriculture and build-up area LSTs can cause a strong UHI between build-up area and the surrounding open agricultural farms (Xu, 2010). Based on table 15, the difference between build-up area and open agriculture land uses is 3.20 degree Celsius for day time and 2.41 degree Celsius for night time.

Table 15 - The mean difference between day and night LST

	Arith. Mean(day)	*Arith. Mean(night)*	Arith. Mean (Day-Night)
Open agriculture	13.882	4.733	9.149
Build-up area	17.091	7.149	9.942
Recreational area	15.386	5.302	10.084
Greenhouse farming	12.651	5.311	7.340
Forest	13.013	4.363	8.650
Inland waterway and Offshore area	11.689	8.019	3.670

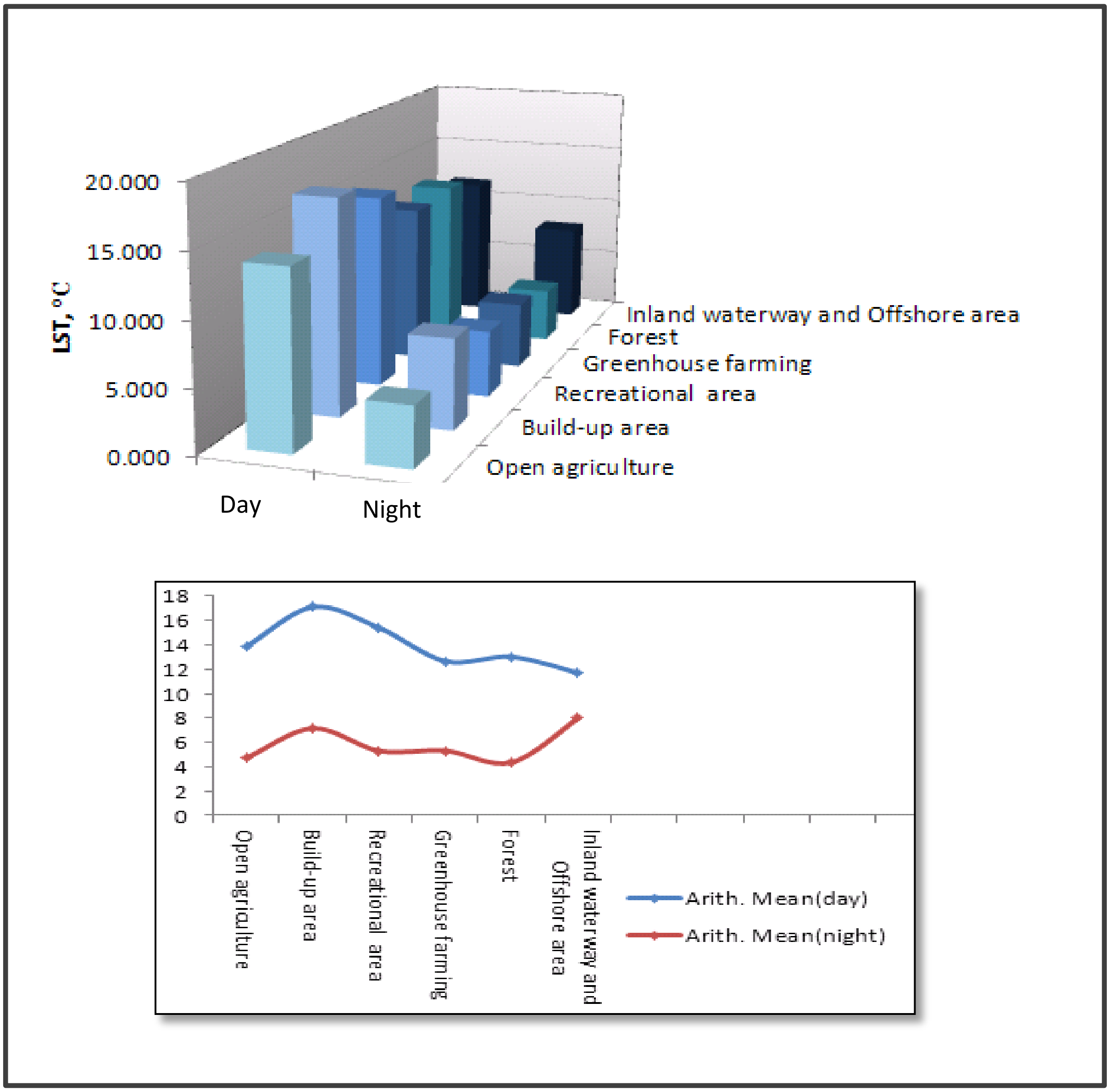

Figure 17 - The mean difference between day and night LST, Figure shows the difference between mean day and night LST for different land use types

4.3.4. Correlation analysis

"The linear association between two continuous quantities is often assessed in terms of Pearson's correlation coefficient, r" (Marzban, 2012).

As tab. 16 shows, the result of correlation between land use groups and mean LST is statistically significant, but not strong. The significance is shown with one star for the level of 0.05 and with two stars for the level of 0.01. As is expected from physical considerations, all of the associations of vegetative land uses (forest, open agriculture) are negative. Based on Weng et al., (2004), LST is negatively correlated with green vegetation pixel fraction and positively correlated with impervious surface percentage. Shading and evapotranspiration would contribute to reduce the land surface temperature. Open agriculture has the strongest relationship with night LST. Open agriculture is the dominant land use and its dominant presence could affect the mixed LST value of each pixel in a strong way. The associations of inland waterway and offshore area and build-up area are positive. The weakest relationship (r= -0.01) is observed in greenhouse farming. One possible explanation is the small percentage coverage of greenhouse land use. When the percentage of a land use within a LST pixel is low, the mixed LST value is mostly under the effect of other land uses which skew the correlation analysis. Correlation coefficients are checked with t-tests to be statistically significant. All coefficients are significant at the level of 0.01 or 0.05. The only case which is not statistically proved is recreation area in the year of 2008.

However, in some cases the data are not homogeneous and consist of different groups. It is important to break the "total "correlation into within and between group correlations. In other words, by observing only the total correlation the fact of strong correlation between groups and weak correlation within groups will be disregarded (Marzban, 2013).

Table 16 - Pearson correlation coefficient between land use percentage and mean LST including all the pixels

All cells			
Yearly mean night LST, land use percentage			
	2003	2006	2008
Open agriculture	-0.48**	-0.36**	-0.38**
Forest	-0.06**	-0.12**	-0.14**
Build-up area	0.37**	0.31**	0.33**
Greenhouse farming	-0.01*	-0.01*	-0.02**
Inland waterway and offshore area	0.32**	0.26**	0.28**
Recreation area	0.23**	0.18**	0.14

Tab. 17 shows the result of correlation after grouping the data. New correlations are statistically significant and highly strong. One possible explanation is that the mix value of

LST in each pixel is under control of all land uses types. One or two percent presence of a land use in a pixel cannot insert a sharp effect on LST. So grouping the land use data percentage, for each group there would be a representative mean value. These mean values are correlated with corresponding mean LST. After grouping the data, in each group there is higher participation of each land use in the context of one pixel, which can affect the mixed LST value of each pixel more significantly. Capturing these underlying groups, strong correlation coefficients are observed. It is worth to mention that a relationship can be strong and not significant. The reason is the size of sample. For small samples, it is easy to produce a strong correlation (by chance). Thus the correlation coefficients should be tested to check whether they are significant or not. Tab. 17 shows that the correlation coefficients are significant. The only exception is recreation area. The reason is that recreation is a mixed land use, which can not be interpreted as a pure land use class. For all other land uses, there is a noticeable change in the strength of correlation coefficient before and after grouping the percentage data.

Table 17 - Pearson correlation coefficient for grouped pixels

All cells , grouped Yearly mean night LST, land use percentage			
	2003	2006	2008
Open agriculture	-0.99**	-0.98**	-0.98**
Forest	-0.89**	-0.91**	-0.91**
Build-up area	0.72*	0.97**	0.97**
Greenhouse farming	-0.90**	-0.99**	-0.85**
Inland waterway and offshore area	0.90**	0.89**	0.87**
Recreation area	0.41	0.23	0.19**

To see the relationship between the percentage of land use changes and the corresponding LST changes for each pixel, a correlation test is applied. Tab. 18 shows the result. A possible explanation for the weak and inconsistent relationships is that small changes in land use can not cause sharp changes in LST. In the pixels with small amount of land use changes, LST is mainly under the effect of dominant land uses. These small changes affect the correlation analysis and skew the results of correlation. Therefore the correlation coefficients are not strong while they are often significant.

Table 18 - Pearson correlation coefficient for land use change and LST change

Correlation coefficient, r		
Yearly mean night LST change, land use percentage change		
	2003-2006	2006-2008
Open agriculture	-0.03**	0.00
Forest	0.01**	0.00
Build-up area	0.01*	0.01*
Greenhouse farming	-0.01**	-0.02**
Inland waterway and offshore area	-0.03**	0.01**
Recreation area	-0.00	0.00

Tab. 19 shows the result of a correlation analysis when the pixels with land use change above 20 % are selected. Results indicate how stronger land use changes affect the amount of changes in LST. For most land uses, the correlation coefficient is improved. For forest and inland waterway and offshore areas group, the numbers of cells above 20 percent changes from 2006 to 2008 were not enough to do correlation test. An interesting point is how inland water coefficient is changed from two sets of the correlation analysis of land use change. Including all percentage changes, the coefficient for inland water is -0.03. After grouping the cells with changes above 20%, the coefficient improves up to +0.56. The context of all land use changes is a pixel with a fixed area. So, when one land use is increasing, at the same time the percentage of other land uses are changing. Therefore the amount of LST is under control of both increasing one specific land use and changing other land uses. As the ANOVA test proved, water has the biggest night LST. The reason behind the situation that LST is decreasing while inland water is increasing is due to complexity and types of other land use changes. For example, in one pixel there is 5 percent increase in inland water but at the same time 50 percent increase in open agriculture. The amount of LST change is under control of both 5% increase water and 50% increase of open agriculture. The power of 50% is much higher than 5%, so in that pixel LST is decreasing while inland water is increasing. This could be an explanation for the negative sign of correlation between LST and inland water. Once pixels with change in inland water above 20%, are selected, the LST changes show a stronger coefficient. The reason is that the percentage of inland water change is high enough to affect LST and so the correlation is stronger and positive. The number of cells and the sample size are decreased, so significance of new correlation coefficients should be checked. Among all land uses, inland water from 2003-2006 and build-up area from 2006-2008 are statistically significant at the level of 0.01. Other coefficients are not significant at 0.01 or 0.05 levels.

Table 19 - Pierson correlation coefficient for land use changes above 20% and corresponding LST changes

Correlation coefficient, changes above 20 %		
Yearly mean night LST change, land use percentage change		
	2003-2006	2006-2008
Open agriculture	0.04	0,00
Forest	-0.23	Not enough cells
Build-up area	0.08	0.26**
Greenhouse farming	-0.23%	-0.36
Inland waterway and offshore area	0.56**	Not enough cells
Recreation area	0.33	0.20

4.3.5. Multiple regression analysis

I. The result of stepwise regression model for the year 2003

Tab. 20 indicates the descriptive statistics for the year 2003. Open agriculture has the largest mean and standard deviation. The mean value indicates that in average 67 percent of all the LST pixels in the Netherlands are spatially occupied by agriculture. Open agriculture is the dominant land use, and in most of pixels there is a high percentage of agriculture. Although other land use types are changing in a pixel, the dominant occupant has a dominant effect on LST of this pixel. In other words the final mixed value of LST for each pixel is strongly under the effect of dominant land use or dominant change. Standard deviation indicates the variety of data. The second highest percentage is build-up area by 10.54 percent, which is still near 6 times smaller than open agriculture. The mean area of build-up area is followed by forest, inland water, recreation area and greenhouse farming. The main existence of open agriculture can skew the role of other land uses in the amount of mixed pixel LST.

Table 20 - Descriptive Statistics for night annual LST of the year 2003

	Mean	Std. Deviation	N
Mean annual LST (◦C)	5.13	1.34	40732
Open agriculture %	67.43	33.02	40732
Forest %	9.68	20.09	40732
Greenhouse farming %	.44	3.99	40732
Recreation area %	2.61	6.79	40732
Build-up area %	10.54	21.25	40732
Inland water %	4.03	11.83	40732

Tab. 21 shows the structure of 6 models of stepwise regression. The model descriptions are listed below:
1. Predictors: (Constant), open agriculture, 2. Predictors: (Constant), open agriculture, forest, 3. Predictors: (Constant), open agriculture, forest, build-up area, 4. Predictors: (Constant), open agriculture, forest, build-up area, greenhouse farming, 5. Predictors: (Constant), open agriculture, forest, build-up area, greenhouse farming, recreation area
6. Predictors: (Constant), open agriculture, forest, build-up area, greenhouse farming, recreation area, inland water and offshore area
The largest amount of adjusted R square is 0.35 %. It means that 35 percent of change in LST is explained by land use percentage changes for the year 2003. Model number 6 has the largest R square and the least error of estimates. So this model is the best regression fit of our data. This model includes all 6 land use types.

Table 21 - R square table for the regression models, year 2003

Model	R	R Square	Adjusted R Square	Std. Error of the Estimate
1	.484[a]	.234	.234	1.1728127
2	.576[b]	.331	.331	1.0957476
3	.589[c]	.348	.347	1.0824968
4	.595[d]	.354	.354	1.0768919
5	.599[e]	.359	.359	1.0727806
6	.600[f]	.360	.359	1.0725024

Tab. 22 indicates the ANOVA analysis for all the six regression models. The result of the ANOVA test shows that F statistic is statistically significant for all the regression models at the 0.01 level. It means the null hypothesis is rejected. Null hypothesis for the F-test claims that the model has no explanatory power. In other words, all the coefficients are zero. The alternative hypothesis argues that at least one coefficient is not zero. To check the coefficients one by one and to see which of them is zero additional t tests are applied.

Table 22 - ANOVA analysis between regression and residual, 2003

Model		Sum of Squares	df	Mean Square	F	Sig.
1	Regression	17118.715	1	17118.715	12445.543	.000[a]
	Residual	56023.690	40730	1.375		
	Total	73142.405	40731			
2	Regression	24240.605	2	12120.303	10094.676	.000[b]
	Residual	48901.799	40729	1.201		
	Total	73142.405	40731			
3	Regression	25417.362	3	8472.454	7230.295	.000[c]
	Residual	47725.042	40728	1.172		
	Total	73142.405	40731			
4	Regression	25911.462	4	6477.866	5585.830	.000[d]
	Residual	47230.942	40727	1.160		
	Total	73142.405	40731			
5	Regression	26272.557	5	5254.511	4565.733	.000[e]
	Residual	46869.848	40726	1.151		
	Total	73142.405	40731			
6	Regression	26298.011	6	4383.002	3810.440	.000[f]
	Residual	46844.394	40725	1.150		
	Total	73142.405	40731			

Tab. 23 contains the unstandardized and standardized coefficients and the corresponding t - test statistic. An unstandardized coefficient is based on original variables. A standardized coefficient is based on standardized values while each observation is subtracted by the sample mean and divided by the sample standard deviation (SPSS Statistics Base 17.0 User's Guide). The standardized coefficient removes the scale of units. The standardized coefficients show the sensitivity of LST in terms of changes of land uses. So in the sixth model and for one standard deviation increase in open agriculture, the model predicts that the LST will decrease by -.865 standard deviations. One standard deviation increase in forest, build-up area, greenhouse farming, recreation area and inland water will change the

LST by -.480, -.219, -.086, -.075 and .025 standard deviations respectively.

In the present study the unit of all independent variables is the same, so unstandardized coefficient are considered. The table also shows that the t-test is significant for all the models. In t-test, the null hypothesis claims that the coefficient is zero while the alternative hypothesis claims that the coefficient is not zero. All the independent variables are statistically significant.

The regression equation (6) is:

Equation (1):

LST (2003) = 8.002- .035X1 - .032X2 -.014X3 -.029X4 - .015X5+.003X6

X1 is open agriculture, X2 is forest, X3 is build-up area, X4 is greenhouse farming, and X5 is recreational area, and X6 is inland water.

This means that for each MODIS LST pixel, the amount of LST can be predicted by the above coefficients of different land uses.

The model predicts that for one unit increase in the percentage of open agriculture, the LST will decrease by 0.035, holding other land uses fixed. For one unit increase in the percentage of forest the LST will decrease by -.032, holding other land uses fixed. The same explanation is used for build-up area, greenhouse farming, recreation area and inland water with -.014, -.029, - .015 and +.003 values of regression coefficients respectively.

Multiple regression returns results for the combined influence of all land use types on the LST as well as the individual influence of each land use while controlling the other land uses. It is therefore a far more accurate method than running separate simple regressions for each land use. To see how different land uses effect the LST separately, the land use-LST scatter plots are drawn (Campbell, 2008).

Table 23 - Unstandardized and standardized regression coefficients, T-test, 2003

Model	Unstandardized Coefficients		Standardized Coefficients	t	Sig.
	B	Std. Error	Beta		
1	6.463	.013		489.232	.000
	-.020	.000	-.484	-111.560	.000
2	7.104	.015		477.268	.000
	-.026	.000	-.636	-141.084	.000
	-.023	.000	-.347	-77.017	.000
3	7.791	.026		297.379	.000
	-.033	.000	-.812	-113.986	.000
	-.030	.000	-.453	-81.363	.000
	-.013	.000	-.205	-31.690	.000
4	7.910	.027		296.333	.000
	-.034	.000	-.842	-116.402	.000
	-.032	.000	-.473	-84.081	.000
	-.014	.000	-.226	-34.682	.000
	-.028	.001	-.084	-20.641	.000
5	8.131	.029		276.795	.000
	-.036	.000	-.897	-114.209	.000
	-.033	.000	-.500	-86.087	.000
	-.015	.000	-.240	-36.692	.000
	-.030	.001	-.090	-22.233	.000
	-.016	.001	-.081	-17.713	.000
6	8.002	.040		198.903	.000
	-.035	.000	-.865	-83.155	.000
	-.032	.000	-.480	-67.253	.000
	-.014	.000	-.219	-27.630	.000
	-.029	.001	-.086	-20.811	.000
	-.015	.001	-.075	-15.894	.000
	.003	.001	.025	4.704	.000

Fig. 18: A-F illustrates relationships between pixel-average LST and within-pixel coverage ratios of different land use types. Each plot shows the behavior of night LST while the percentage of land use is changing from 0 to 100 percent in each pixel. Thus the X axis is the percentage of land use in each pixel and Y axis is the corresponding pixel-average LST value for that pixel. All MODIS LST pixels in the Netherlands are included. Fig. 18, part A shows that as the percentage of agriculture is increasing (in each pixel) the amount of mean yearly LST is decreasing. The density of the graph points indicates the large number of cells which are occupied by agriculture. The density of points is more near high percentage at the end of the X axis, which shows that the number of pixels with high agriculture percentage is more than cells with low percentage of agriculture. As mentioned in Tab. 20, open agriculture has the largest occupation mean of 67 percent of all the LST pixels in the Netherlands. The general pattern of the graph proves the negative association of LST and open agriculture. Fig. 18, part B shows the behavior of mean yearly LST, while the percentage of forest is increasing in the context of a LST pixel. The density of pixels is at the beginning of the graph (percentage below 20). By increasing the percentage of forest, the number of pixels and the mean LST are decreasing. It means the medium contribution of forest in LST pixels and negative relationship between forest and LST. Fig. 18, part C shows the least populated graphs, which is green-house farming. Fig. 18, part D shows how mixed LST will change when the percentage of recreation area is changing. For recreation area the trend is rising. Almost all the cells are concentrated at the percentage below 40%. The heterogenous concentration of points in the graphs may enhance the need of grouping the data. This finding about vegetation covers is in agreement with Guo et al (2012) findings that argued when the vegetation cover increase, the LST trend is opposite. The explanation for Fig. 18, part E is as the percentage of inland water is increasing, the LST value is rising. The density of the pixels is located before 20 %. It means that as the percentage of inland water land use in each pixel is going up, the number of pixels which are highly (more than 20%) covered by inland water is decreasing. The overall trend is increasing. Fig. 18, part F, indicates another populated graph. When the percentage of build-up area is increasing, the amount of mean LST is also increasing. This finding is in agreement with Guo et al (2012) findings which showed that when the coverage ratios of built-up increase, the LST goes up.

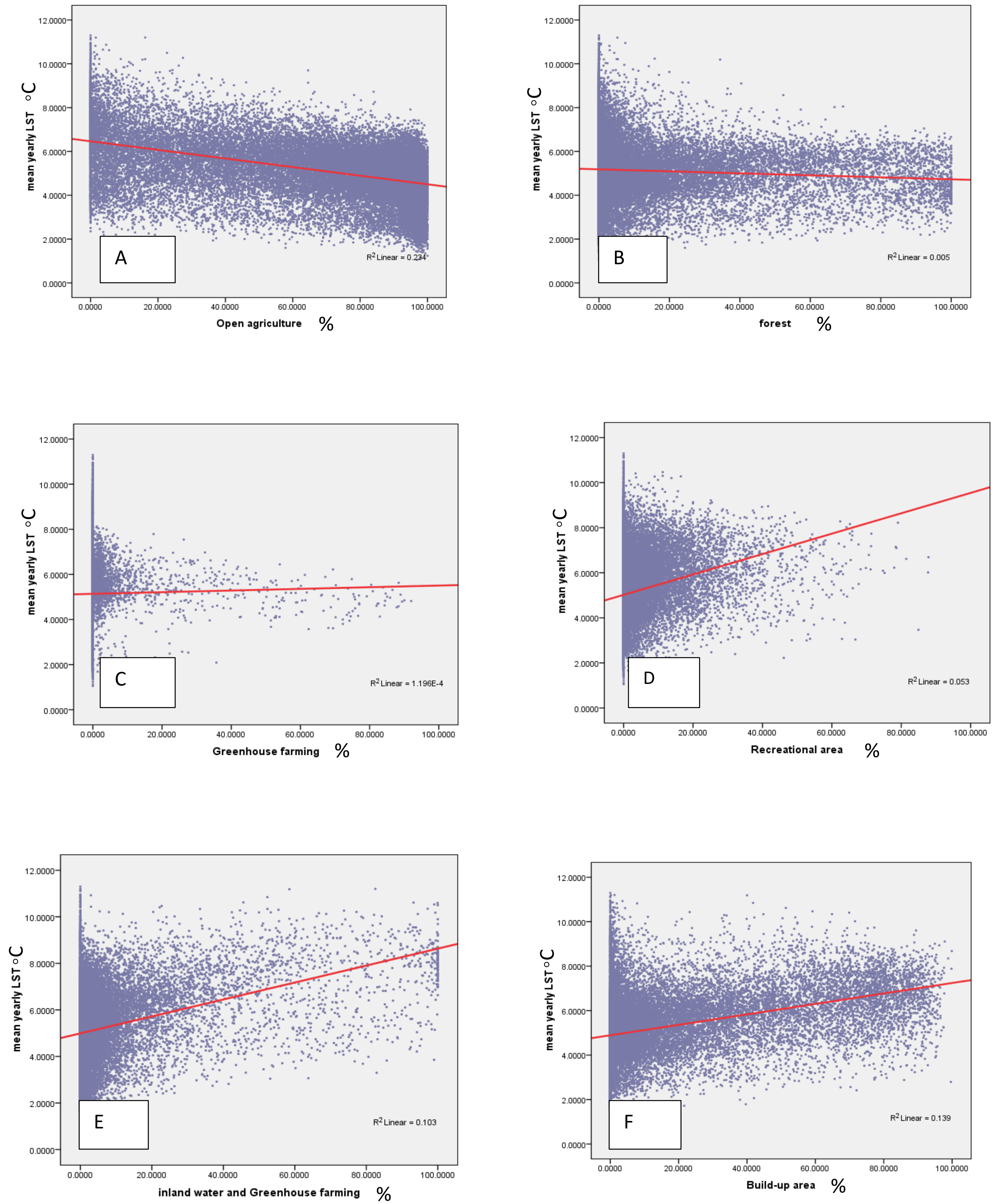

Figure 18 - illustrates relationships between pixel-average LST and within-pixel coverage ratios of different Land use types. A-F letters show percentage of different types of land uses in relation with LST

II. The result of stepwise regression model for the year 2006

Tab. 24 shows the descriptive statistics for the multiple regressions. The test is based on mean yearly LST as independent variable and the percentage of different land uses as dependent variables. The number of cells which involved in the analysis is 40732. Open agriculture is the most dominated land use with the biggest standard deviation. Greenhouse farming has the minimum contamination in the pixels and the minimum std. deviation. Among the analysis of entering and removing variables, inland waterway and offshore area is excluded from the analysis. It is because of its high error of estimate.

Table 24 - Descriptive Statistics for night yearly LST of the year 2006

	Mean	Std. Deviation	N
Mean LST	6.08449	1.285251	40732
Open agriculture	66.94030	33.211051	40732
forest	9.63962	20.077991	40732
Greenhouse farming	.45854	4.103221	40732
Recreational area	2.68401	6.930270	40732
Build-up area	10.86936	21.557325	40732
Inland waterway and Offshore area	4.11058	11.902724	40732

Tab. 25 shows the sequence of 5 selected models of stepwise regression. The model descriptions are listed below:

1. Predictors: (Constant), open agriculture
2. Predictors: (Constant), open agriculture, forest
3. Predictors: (Constant), open agriculture, forest, build-up area
4. Predictors: (Constant), open agriculture, forest, build-up area, greenhouse farming
5. Predictors: (Constant), open agriculture, forest, build-up area, greenhouse farming, recreational area

The fifth model has the lowest estimate of error and the highest r square value. The adjusted R square for the 5th model is .0256. It means in 2006, 25% of total variability of mean yearly LST is explained by the percentage of different land uses in the context of MODIS LST pixels. Therefore the 5th model, including open agriculture, forest, build-up area and greenhouse farming and recreational area as independent variables and mean yearly LST as dependent variable, is selected as the best model by step wise regression.

Table 25 - R square table for the regression models, year 2006

Model Summary				
Model	R	R Square	Adjusted R Square	Std. Error of the Estimate
1	.365[a]	.133	.133	1.196431
2	.483[b]	.234	.233	1.125247
3	.495[c]	.245	.245	1.117068
4	.503[d]	.253	.253	1.110952
5	.506[e]	.256	.256	1.108405

Tab. 26 shows that the result of the f-test for the 5 selected models. F values for all the models are significant. It means null hypothesis is rejected. The null hypothesis for the F-test claims that the model has no explanatory power and all the coefficients are zero. The alternative hypothesis claims that at least one coefficient is not zero.

Table 26 - ANOVA analysis between regression and residual, 2006

Model		Sum of Squares	df.	Mean Square	F	Sig.
1	Regression	8979.564	1	8979.564	6273.071	.000[a]
	Residual	58302.809	40730	1.431		
	Total	67282.373	40731			
2	Regression	15712.120	2	7856.060	6204.536	.000[b]
	Residual	51570.253	40729	1.266		
	Total	67282.373	40731			
3	Regression	16460.336	3	5486.779	4397.020	.000[c]
	Residual	50822.037	40728	1.248		
	Total	67282.373	40731			
4	Regression	17016.542	4	4254.135	3446.838	.000[d]
	Residual	50265.831	40727	1.234		
	Total	67282.373	40731			
5	Regression	17247.985	5	3449.597	2807.835	.000[e]
	Residual	50034.388	40726	1.229		
	Total	67282.373	40731			

Tab. 27 also shows that the T-test is significant for all the models and all the independent variable are statistically significant. The regression equation is:

Equation (2):
LST (2006) = 8.490 - .029 X1 - .031 X2 - .012 X3 - .031 X4 - .012 X5

X1 is open agriculture, X2 is forest, X3 is build-up area, X4 is greenhouse farming and X5 is recreational area.
This means for each MODIS LST pixel, the amount of LST is predicted by the modeled coefficients of different land uses. The equation shows how to predict the amount of LST based on the percentage of different land uses in a pixel

Table 27 - unstandardized and standardized regression coefficients, t-test, 2006

Model		Unstandardized Coefficients		Standardized Coefficients		
		B	Std. Error	Beta	t	Sig.
1	(Constant)	7.031	.013		527.104	.000
	Open agriculture	-.014	.000	-.365	-79.203	.000
2	(Constant)	7.639	.015		507.149	.000
	Open agriculture	-.020	.000	-.516	-107.421	.000
	forest	-.022	.000	-.351	-72.919	.000
3	(Constant)	8.184	.027		305.288	.000
	Open agriculture	-.026	.000	-.663	-86.591	.000
	forest	-.028	.000	-.438	-73.449	.000
	Build-up area	-.010	.000	-.171	-24.487	.000
4	(Constant)	8.311	.027		304.113	.000
	Open agriculture	-.027	.000	-.696	-89.554	.000
	forest	-.029	.000	-.460	-76.377	.000
	Build-up area	-.012	.000	-.195	-27.718	.000
	Greenhouse farming	-.029	.001	-.093	-21.229	.000
5	(Constant)	8.490	.030		281.029	.000
	Open agriculture	-.029	.000	-.743	-87.646	.000
	forest	-.031	.000	-.483	-77.441	.000
	Build-up area	-.012	.000	-.208	-29.329	.000
	Greenhouse farming	-.031	.001	-.099	-22.483	.000
	Recreational area	-.012	.001	-.067	-13.725	.000

Fig. 19, part A shows how LST changes when the percentage of agriculture is increasing. Agriculture is the dominant land use in the Netherlands. The red trend line has a falling trend, while the open agriculture percentage is increasing. The same falling trend can be realized for forest and green house farming land use types Fig. 19, part B and C. Inland water Fig. 19, Part E and build-up area Fig. 19, part F have rising trend. Recreation area is a mixed land use. In some pixels it is buildings, in some it is water and in other areas it is forest. Recreation is selected as a separate group to consider cooling effect of parks and recreation areas from build-up land use. For open agriculture, build-up area and forest land uses, larger number of pixels are involved and the graphs are very dense. For all land use types except open agriculture, when the land use percentage is lower than 40%, the pixel density is higher. In other words, from beginning to the end of trend line, the numbers of pixels are decreasing. For open agriculture the reverse is true. Grouping land use percentage, better correlation results can be captured.

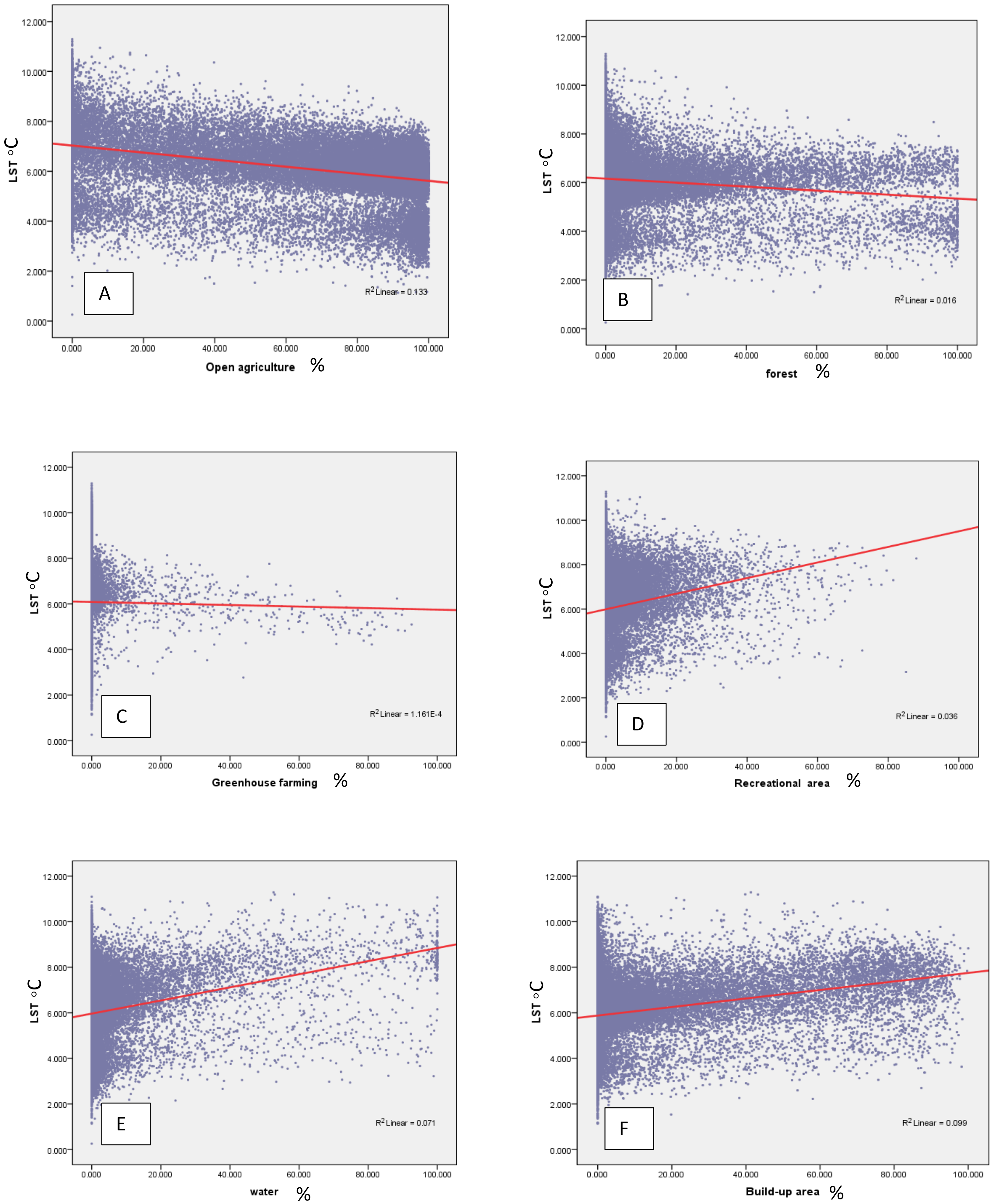

Figure 19 - Relationships between pixel-average LST and within-pixel coverage ratios of different Land use types. A-F letters show percentage of different types of land uses in relation with LST

III. The result of stepwise regression model for the year 2008

Tab. 28 shows the descriptive statistics for the multiple regression model of the year 2008. The test is based on mean yearly LST as independent variable and the percentage of different land uses as dependent variables. Open agriculture is the most dominated land use with the biggest standard deviation. Greenhouse farming has the minimum pixel contamination and the minimum std. deviation.

Table 28 - Descriptive statistics for night yearly LST of the year 2008

	Mean	Std. Deviation	N
Mean LST	6.01730	1.278438	40732
Open agriculture	66.66064	33.266766	40732
forest	9.63982	20.055373	40732
Greenhouse farming	.47393	4.170884	40732
Recreational area	2.72040	6.968323	40732
Build-up area	11.03155	21.719552	40732
Inland waterway	4.14100	11.927463	40732

Tab. 29 shows the arrangement of 6 models of stepwise regression. The model descriptions are listed below:

1. Predictors: (Constant), open agriculture
2. Predictors: (Constant), open agriculture, forest
3. Predictors: (Constant), open agriculture, forest, build-up area
4. Predictors: (Constant), open agriculture, forest, build-up area, greenhouse farming
5. Predictors: (Constant), open agriculture, forest, build-up area, greenhouse farming, recreation area
6. Predictors: (Constant), open agriculture, forest, build-up area, greenhouse farming, recreation area
, inland water

The sixth model has the lowest estimate of error and the highest r square. The adjusted r square for the 6th model is .287. It means in 2008, 28% of total variability of mean yearly LST is explained by the percentage of different land uses. So the 6th model is selected as the best close-fitting model by step wise regression.

Table 29 - R square table for the regression models, year 2008

Model	R	R Square	Adjusted R Square	Std. Error of the Estimate
1	.382[a]	.146	.146	1.181451
2	.510[b]	.260	.260	1.099975
3	.521[c]	.271	.271	1.091345
4	.531[d]	.282	.282	1.083323
5	.535[e]	.287	.287	1.079800
6	.536[f]	.287	.287	1.079583

Tab. 30 shows the result of F-test. F test for all the models is significant.

Table 30 - ANOVA analysis between regression and residual, 2008

Model		Sum of Squares	df	Mean Square	F	Sig.
1	Regression	9718.848	1	9718.848	6962.792	.000[a]
	Residual	56852.000	40730	1.396		
	Total	66570.848	40731			
2	Regression	17291.029	2	8645.515	7145.383	.000[b]
	Residual	49279.819	40729	1.210		
	Total	66570.848	40731			
3	Regression	18062.461	3	6020.820	5055.125	.000[c]
	Residual	48508.387	40728	1.191		
	Total	66570.848	40731			
4	Regression	18774.138	4	4693.535	3999.304	.000[d]
	Residual	47796.709	40727	1.174		
	Total	66570.848	40731			
5	Regression	19085.653	5	3817.131	3273.788	.000[e]
	Residual	47485.195	40726	1.166		
	Total	66570.848	40731			
6	Regression	19105.849	6	3184.308	2732.139	.000[f]
	Residual	47464.998	40725	1.166		
	Total	66570.848	40731			

Tab. 31 indicates that the t-test is valid for all the coefficients in all the models. It means all land use types influence the mean yearly LST in 2008.

Equation (3):
$$LST\ (2008) = 8.423 - .02\ X1 - .032\ X2 - .012\ X3 - .033\ X4 - .013\ X5 + .002 X6$$

X1 is open agriculture, X2 is forest, X3 is build-up area, X4 is greenhouse farming, and X5 is recreational area, and X6 is inland water.
In 2008, compared to 2006, water is included in the step-wise regression. The coefficient of inland water is 0.002. It means that for one unit increase in the percentage of inland water, the LST will increase by 0,002, holding other land uses fixed.

Table 31 - unstandardized and standardized regression coefficients, T-test, 2008

Model		Unstandardized Coefficients		Standardized Coefficients		
		B	Std. Error	Beta	t	Sig.
1	(Constant)	6.996	.013		533.651	.000
	Open agriculture	-.015	.000	-.382	-83.443	.000
2	(Constant)	7.634	.015		521.916	.000
	Open agriculture	-.021	.000	-.541	-114.832	.000
	forest	-.024	.000	-.373	-79.109	.000
3	(Constant)	8.186	.026		313.620	.000
	Open agriculture	-.027	.000	-.691	-91.946	.000
	forest	-.029	.000	-.462	-79.045	.000
	Build-up area	-.010	.000	-.175	-25.450	.000
4	(Constant)	8.331	.027		313.505	.000
	Open agriculture	-.028	.000	-.729	-95.688	.000
	forest	-.031	.000	-.487	-82.663	.000
	Build-up area	-.012	.000	-.203	-29.347	.000
	Greenhouse farming	-.032	.001	-.106	-24.625	.000
5	(Constant)	8.539	.029		290.758	.000
	Open agriculture	-.030	.000	-.784	-94.386	.000
	forest	-.033	.000	-.514	-84.291	.000
	Build-up area	-.013	.000	-.218	-31.341	.000
	Greenhouse farming	-.034	.001	-.112	-26.165	.000
	Recreational area	-.014	.001	-.079	-16.345	.000
6	(Constant)	8.423	.040		208.585	.000
	Open agriculture	-.029	.000	-.754	-68.331	.000
	forest	-.032	.000	-.495	-65.964	.000
	Build-up area	-.012	.000	-.198	-23.353	.000
	Greenhouse farming	-.033	.001	-.109	-24.688	.000
	Recreational area	-.013	.001	-.073	-14.646	.000
	Inland waterway	.002	.001	.023	4.163	.000

a. Dependent Variable: Mean LST

Fig. 20 illustrates relationships between pixel-average LST and within-pixel coverage ratios of different Land use types. All the graphs except open agriculture show a triangular pattern. It means the number of cells with low land use occupation is larger than high land use contamination. The same as 2003 and 2006, as the percentage of agriculture is increasing; the number of pixels which are contaminated with open agriculture is increasing while the amount of LST is decreasing. The reason behind branches in open agriculture graph can be different type of crops. Fig. 20, part B shows the trend of forest which has two branches at the end of the trend line. The explanation for this behavior is that satellite sensors only measure the temperature of the top of forest canopies and when the canopy of intact forests is thick enough, the LST would be collected from top of the canopy rather than the ground (Goulden et al., 2006). Different types of forest (ever green or deciduous) are not divided in this study. The canopy pattern and the color of different types of forests are different. This difference will be sharper during the winter. In other words contrasting reaction of mean yearly LST to increasing the percentage of forest could be due to different types of forests or their canopy cover type. Recreation area, inland water and build-up area land use groups, have the rising trend of LST while their percentage is increasing in context of one pixel. The concentration of the cells is higher for percentage below 40%. Greenhouse shows a falling trend.

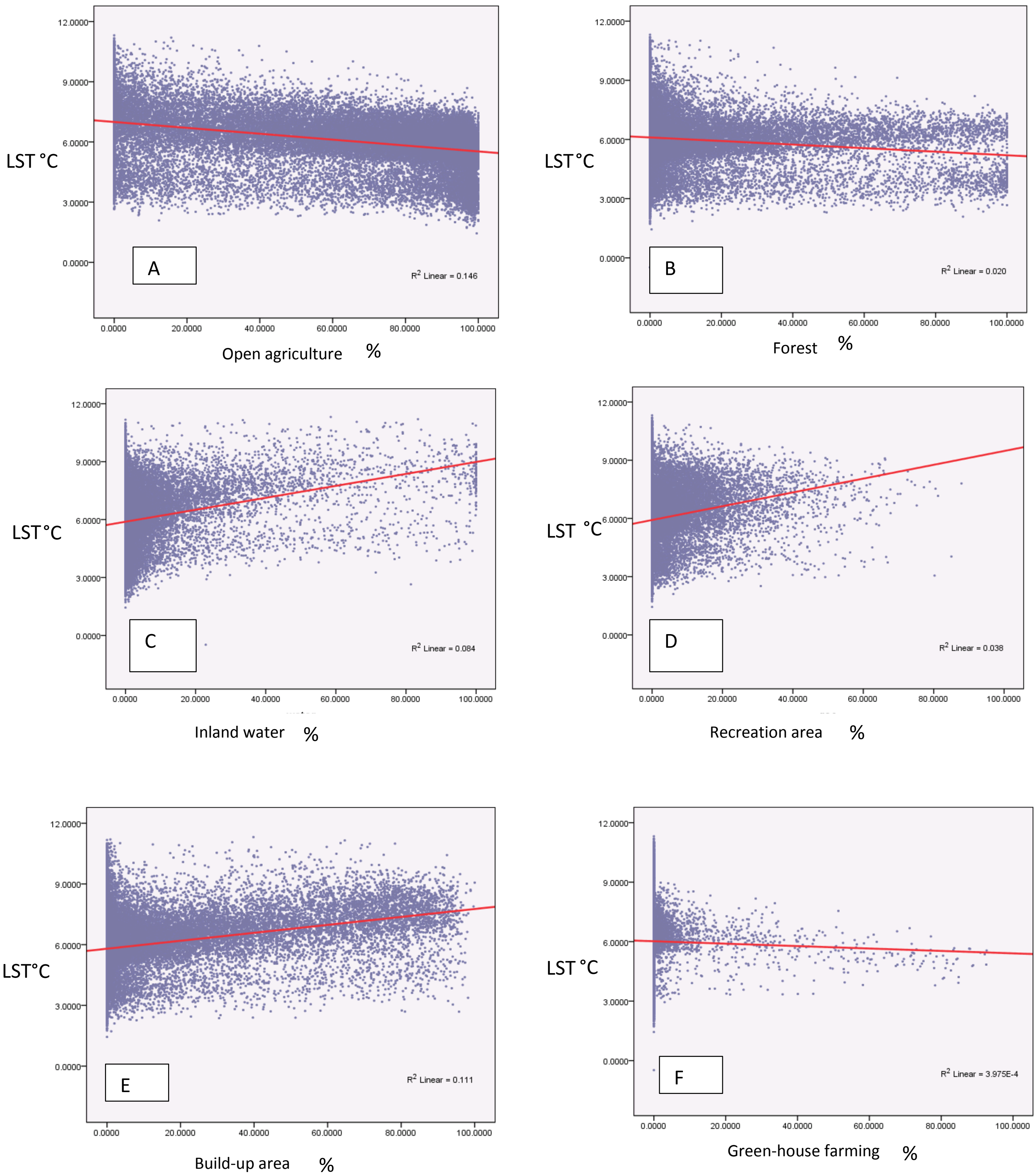

Figure 20 - illustrates relationships between pixel-average LST and within-pixel coverage ratios of different Land use types. A-F letters show percentage different types of land uses in relation with LST

4.3.6. The difference between scatterplots and regression analysis

Different type of information can be driven from scatterplots, including the rising or falling trends which show the sign of association between land use type and LST. The slope and intercept of graphs are also important. For example from 2003 to 2008 the amount of intercepts for all land use types are increased. The graphs also provide useful information about spatial arrangement and dominance of different type of land uses. For example it can be argued from the graphs that open agriculture is the dominant land use or the pixels covered by inland water are grouped to the percentage below 20 or 30 percent. The ramifications of some graphs like forest or open agriculture show the differences of LST for different type of forests or different type of seasonal or annual crops.

Comparing the result of regression coefficient with the scatter plots, some paradoxes should be discussed. For example the scatterplot of mean LST and the percentage coverage of build-up area indicate a rising trend for all three years of 2003, 2006 and 2008, whereas the regression coefficients for build-up area are negative for all these three years. The reason is that scatter plot attributes the mean LST of each pixel to its corresponding build-up area percentage, while in a multiple regression the mean LST values of each pixel is related to the percentage of different land uses. Although the percentage of build-up area is increasing in the fixed area of a pixel, the amount of LST for that cell is simultaneously under effect of other land use changes, and the pattern and the area of other land use types. Therefore in regression equation the sign of build-up area coefficient is negative.

Linear regression model applied in the current study is unable to show the correct association sign between LST and build-up area percentage coverage. This idea is supported by Guo (2012), who argued that the relationships of LST and build-up area index could not be expressed using the linear regression model by achieving R-square value less than 0.6 for determination of LST to build-up area index. He argued there might be more complicated unknown associations between these variables. Su et al (2012) tested a geographically weighted regression (GWR) between the percentage of different land covers and day LST and argued that built-up class was the only class with a positive slope parameter. In contrast to Su (2012) findings and similar to Sun (2011), however, in the current study built-up class has the negative coefficient.

There are several possible explanations for this result. One possible explanation is the dominant presence of open agriculture. The dominance and the power of negative association of open agriculture with LST can affect the sign of other land use coefficients. Sun et al (2011) revealed that dominant presence of forest and agriculture played important roles in moderating LST despite rapid urban development in Guangzhou. Inland water is not a dominant land use, but still has its positive sign. It may be because of the power of inland water, which makes it effective, though it is not the dominant land use in LST pixels. Thus due to the area coverage and the power of different land use types in a pixel there are some unknown complexity in the system which can not be captured by the linear regression model. As the scatter plot triangular patterns show, there are quiet large numbers of pixels with low percent (below 20%) of each land use. LST values of these pixels are mostly under control of the other 80% dominant land use types that affect the result of regression. In other words, the potential influence of different land uses on LST may largely be counteracted by the surrounding surface materials when the land use is not the dominant cover-type in the pixel area. “Satellite detection of LST based on mixed land use pixels has the risk of composite signatures, which are formed when pure spectral responses of specific land uses are disordered with the pure responses of other land uses in a pixel” (Weng, 2008). For pure pixels with one type of land use, it would be easier to discuss about how land use affect LST. Due to the rather large area of a pixel (approx. 1 km^2), the majority of pixels of MODIS LST at the 1000 m spatial resolution are mixed pixels. Most of the LST pixels are occupied by more than one land use type. The strength of this effect depends on the area, spatial pattern, adjacency and the power of different types of land uses to affect the amount of LST. The neighborhood effect can be additive or subtractive. For example for pixels on coastal margins or with a high percentage of inland water, differences between cropland and forest LST is very small (Wickham, 2012). This finding shows the complexity and the local effects of land use patterns in the context of one pixel. Using LST data from pixels with different land uses, and judge about how each type of land use affect the LST, would be tricky. However many statistical regressive methods do not yield good results under the condition of non-uniform land covers where vegetation cover is mixed with other land cover types, particularly in areas covered with mixture of water, bare soil and impervious components (Yang et al., 2011). Yang et al (2011) argued that using linear regression models ignoring sub-pixel temperature estimation may produce a large error. Here the resolution of land surface temperature is important. In finer resolutions it would be easier to find pure land use cells and so the results will be more accurate. (Frohn, 1998).

Fig. 21 indicates that mean yearly LST differs between different land use types. The largest mean night LST is for inland water and the second large LST is for build-up area.

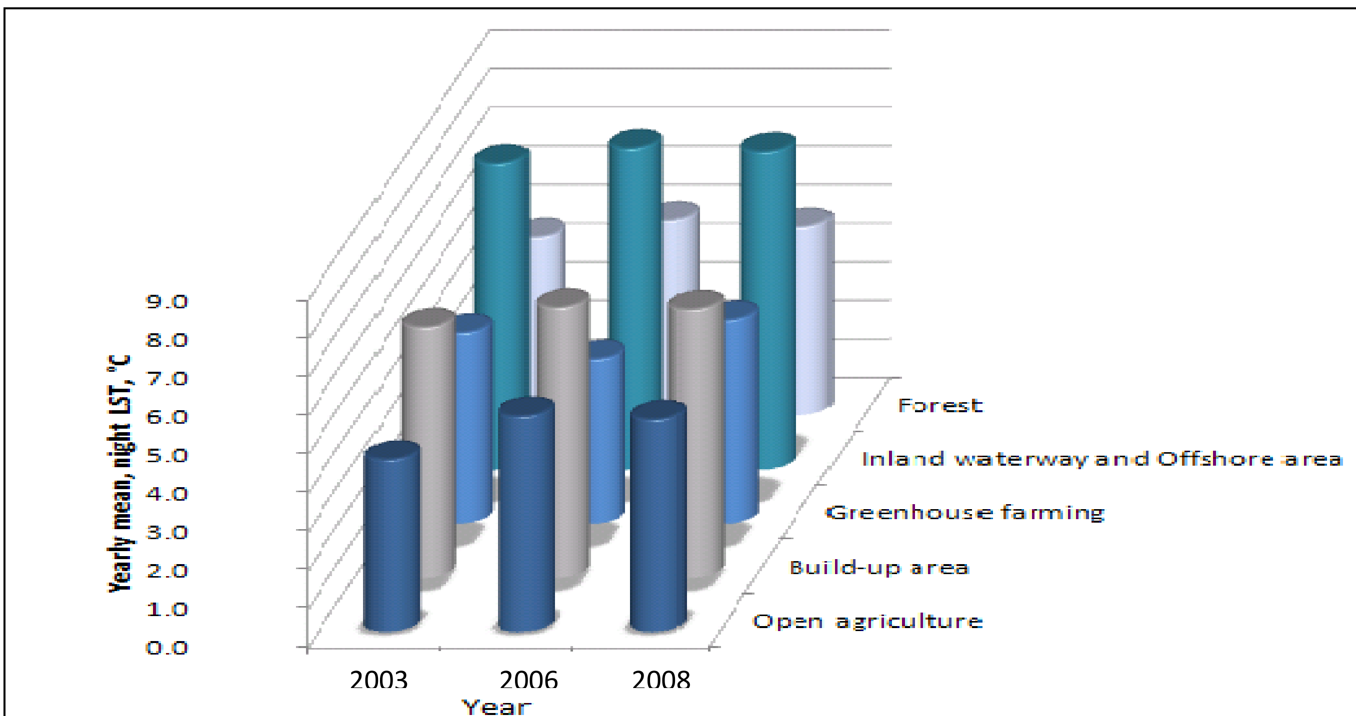

Figure 21 - Mean yearly LST of different land use types.

Thermal characteristics, conductivity, albedo, surface roughness and heat capacity are among the fundamental factors which affect the amount of LST of different land uses (Brovkin et al., 2004; Davin and Noblet-Ducoudréf, 2010). The spatial arrangement, area, adjacent land uses and connectivity of different land uses also impact on the mixed value of LST for each pixel. Van Leeuwen (2011) argued that LST is regulated by several parameters e.g. surface conductance, the amount of water available for evaporative cooling, wind speed, and surface roughness which regulates the power of sensible and latent heat fluxes.

Tab. 32 shows that the lowest LST in 2003 is observed in open agriculture, followed by forest, greenhouse farming, build-up area and inland waterway and offshore area. The pattern of 2006 is slightly different, where the lowest LST is found in greenhouse farming, followed by forest, open agriculture, build-up area and inland waterway and offshore area. In 2008, the lowest LST is for forest followed by greenhouse farming, open agriculture, build-up area and inland waterway and offshore area. These results are consistent with the study of Weng et al., (2004). They suggest that the higher biomass/vegetation abundance a land cover has, the lower the land surface temperature. Furthermore, vegetative land uses possessed a smaller mean value than inland water and build-up area. Forest has the least LST. This result may be explained by the fact that forests thick vegetation can decrease the amount of heat stored in the soil and surface structures through transpiration (Weng, 2008). A possible explanation for this is argued by Xiang (2006). They discussed that these changes can stem from the discrepancy in solar illumination, atmospheric influences, and soil moisture content in the different study years.

Table 32 - the average of mean yearly LST for different land use types for 2003, 2006 and 2008

	Mean LST for All the Pixels with Open agriculture >95%	**Mean LST for All the Pixels with Inland waterway and offshore area >95%**	**Mean LST for All the Pixels with Forest >95%**	**Mean LST for All the Pixels with Greenhouse farming >80%**	**Mean LST for All the Pixels with Build-up area >95%**
2003	4.45	7.90	4.59	4.93	6.48
2006	5.57	8.30	5.02	4.31	6.98
2008	5.49	8.21	4.85	5.27	6.93

4.3.7. LST Aggregation analyses, spatial mean

The zonal maps of the years 2003, 2006 and 2008 are provided. See Fig. 22 which shows the average of mean night yearly LST for each province. The maps for the years of 2003 and 2008 are provided in the appendix (Group 5). The values are LST original raw values. To convert to Celsius, each value should be multiplied by 0.02 and subtracted from 273.15 (Zhengming, 2007). Zuid-Holland for all the three years has the largest mean yearly LST. Noord-Holland and Noord-Brabant are among the high LST provinces. The most urbanized parts of the country is Randstad which comprises the major cities of Amsterdam, Rotterdam, Utrecht and The Hague and has around 5 million inhabitants (de Nijs et al., 2004). Fig. 23 shows the population density in the Netherlands. The highest density is for Zuid-Holland. It has the density of more than 1000 inhabitants per square kilometer. Comparing spatial LST figures with Fig. 23, it could be noted that in hot urbanized spots, the amount of mean LST is higher. Zhou (2011) argued that “apart from land-use change, urbanization with increased human population also contributes to the urban thermal environment change with the rising anthropogenic heat discharge.” To see how the spatial pattern of different land uses are related to mean LST, the year 2006 is selected as a representative year. The spatial pattern of different land use types from 2000 to 2008 is not very much different. Therefore the year 2006 is shown as a sample year.

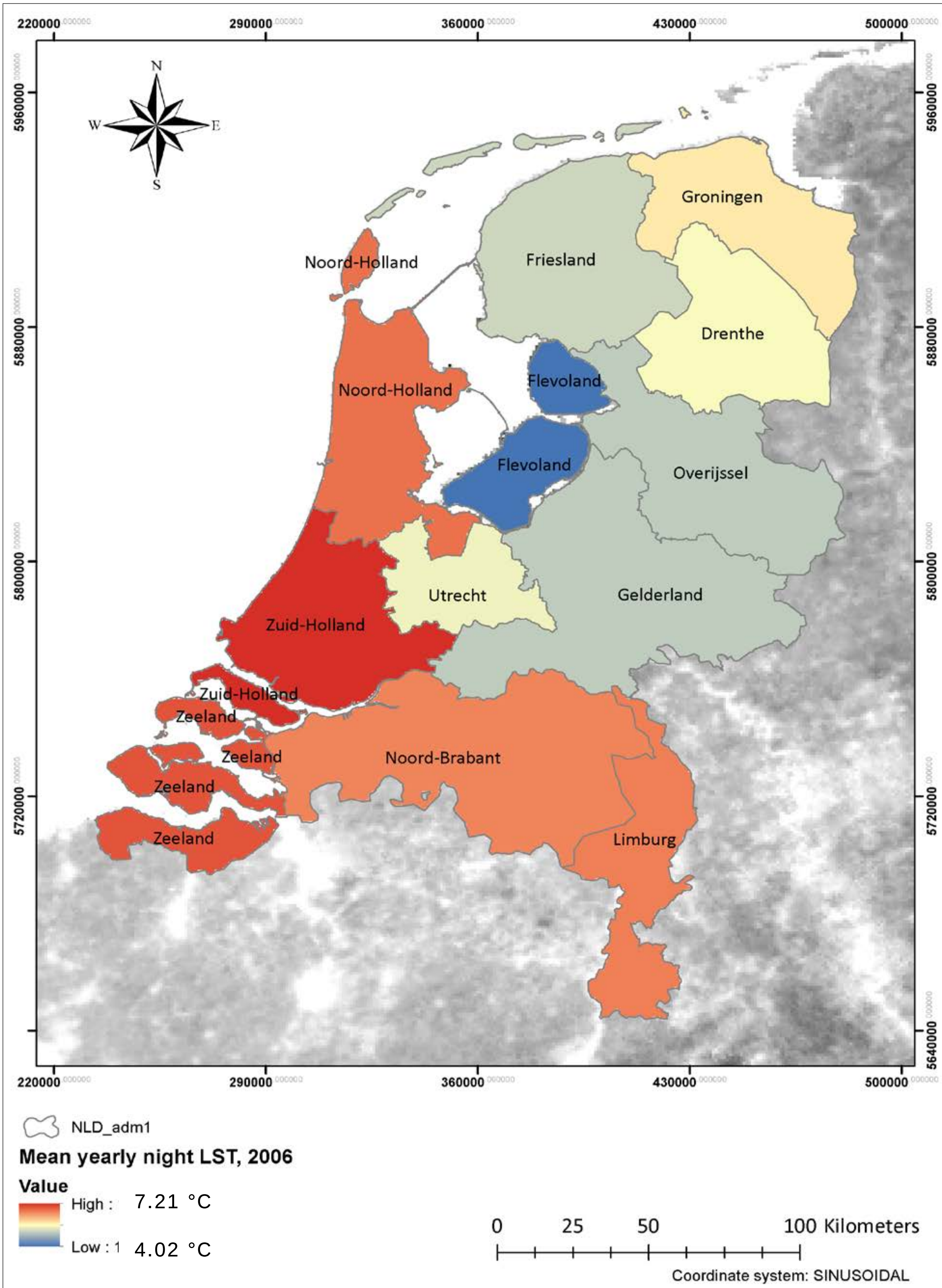

Figure 22 - The up-scaled mean yearly night LST mean to Dutch province scale, 2006

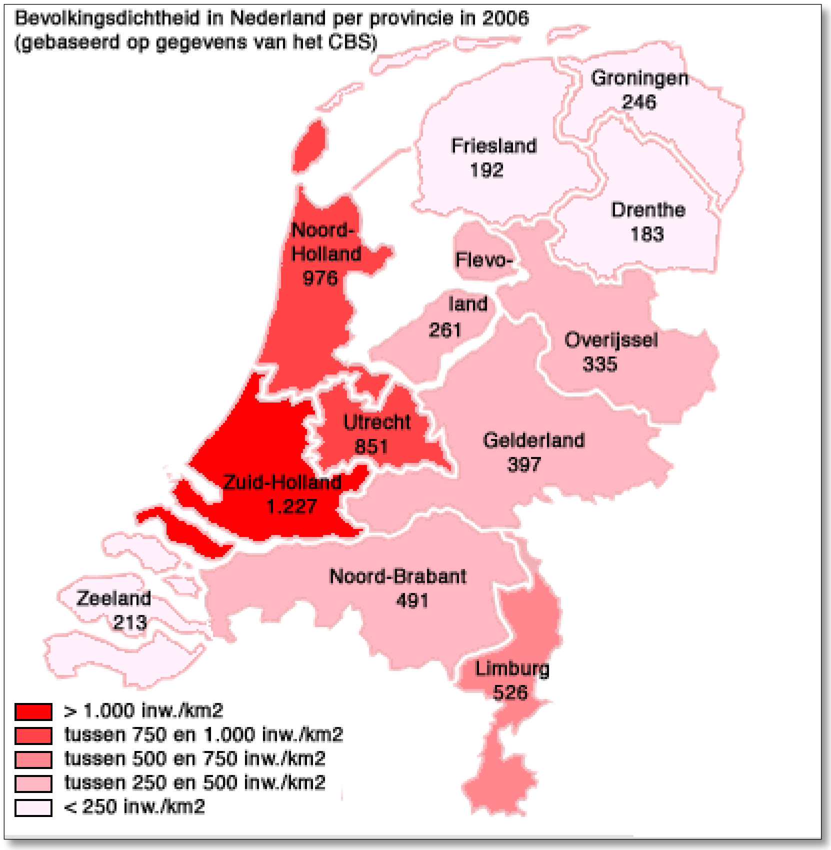

Figure 23 - Population density in the Netherlands by province in 2006 , Taken from: gebaseerd op gegevens van het CBS, available at http://schools-wikipedia.org/images/597/59738.png.htm

Tab. 33 indicates the annual mean value of LST for different provinces for the years of 2003, 2006 and 2008. Zuid-Holland has the highest LST value in 2003, 2006 and 2008. The range of LST for the year 2003 is from 3.39 to 6.39 °C. In the year 2006, it is ranging from 4.02 to 7.21 °C. The range for 2008 is from 4.15 to 7.05 °C. The mean LST value for each province can be a good decision-making factor and an environmental warning tool for urban and environmental planners.

Table 33 - The mean LST value for each province.

Province	Mean LST (◦C), 2003	Mean LST (◦C), 2006	Mean LST (◦C), 2008
Groningen	4.38	5.99	5.93
Drenthe	4.37	5.81	5.48
Overijssel	4.42	5.39	5.46
Gelderland	4.78	5.39	5.40
Noord-Brabant	5.83	6.64	6.62
Limburg	5.84	6.68	6.57
Friesland	4.21	5.49	5.39
Noord-Holland	5.83	6.78	6.68
Zuid-Holland	**6.30**	**7.21**	**7.05**
Zeeland	6.24	6.97	6.79
Utrecht	5.00	5.74	5.76
Flevoland	3.39	4.02	4.15

Fig. 24 shows the distribution and arrangement of open agriculture land use in 2006. Agriculture dominantly occupied most parts of the country. The figure indicates that open agriculture does not have strong presence in most red LST hot spots. In the circled part, although open agriculture has lying strongly, the degree of LST is relatively high. The reason is in this area that two land uses of open agriculture and build-up area are mixed. Therefore the cooling effect of open agriculture along with warming effect of build-up area in a compensating process, give an orange color to this area. The orange color has the medium amount of LST.

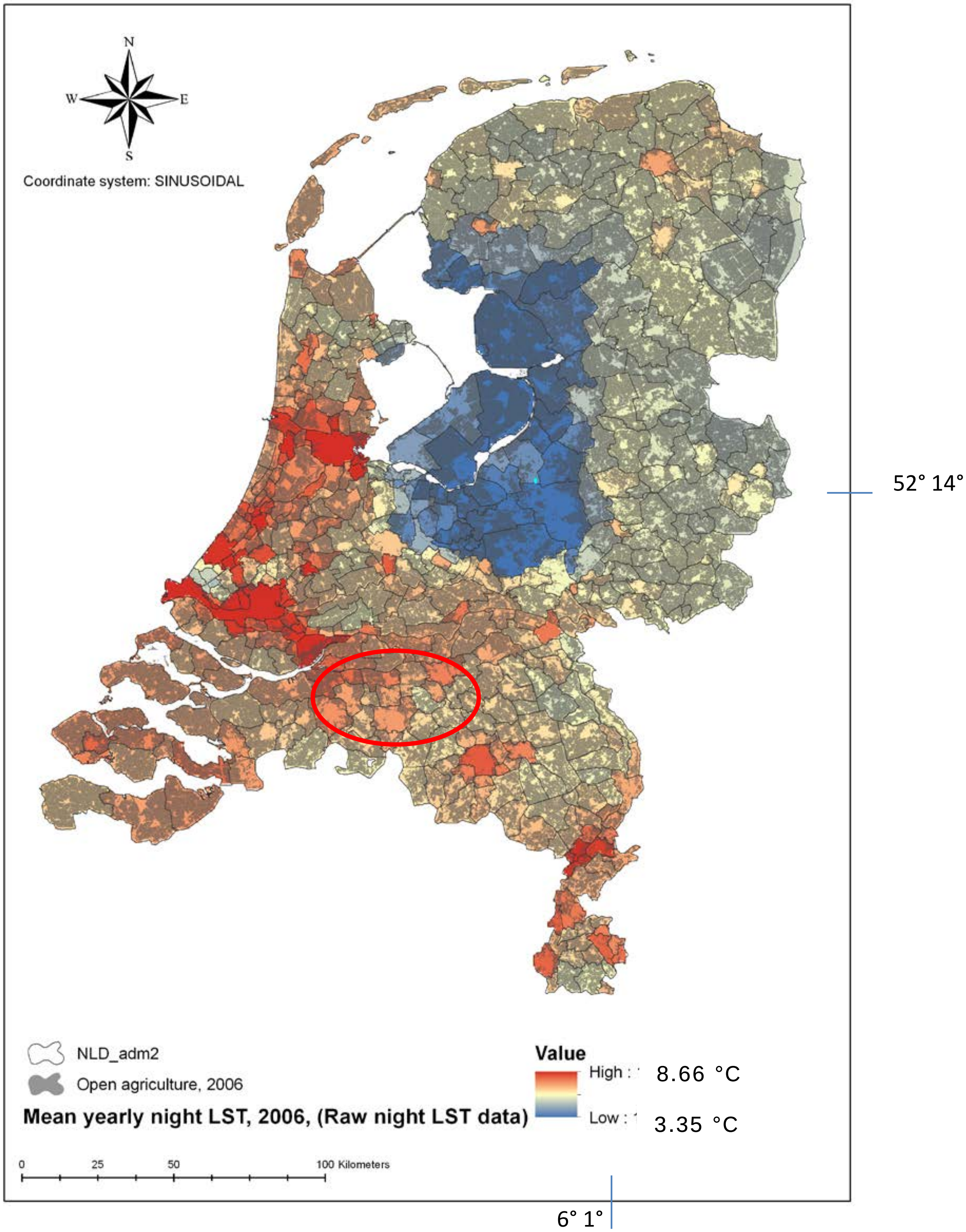

Figure 24 - The up-scaled mean yearly night LST mean to Dutch city scale and the spatial of pattern of open agriculture, 2006. In the circle area shows the mixture of open agriculture and build-up area which gives the orange tone to the area.

Fig. 25 shows, the spatial pattern of forest in the context of mean LST. The highest density of forest is located in the central blue part, which is categorized by low LST values. The presence of forest with other land uses in MODIS pixels can affect the strength of forest to decrease the amount of LST. This finding is in agreement with Sun et al., (2011), which showed that the peak of forest appeared in low and very low LST areas. They explained that it is because forest can moderate temperature.

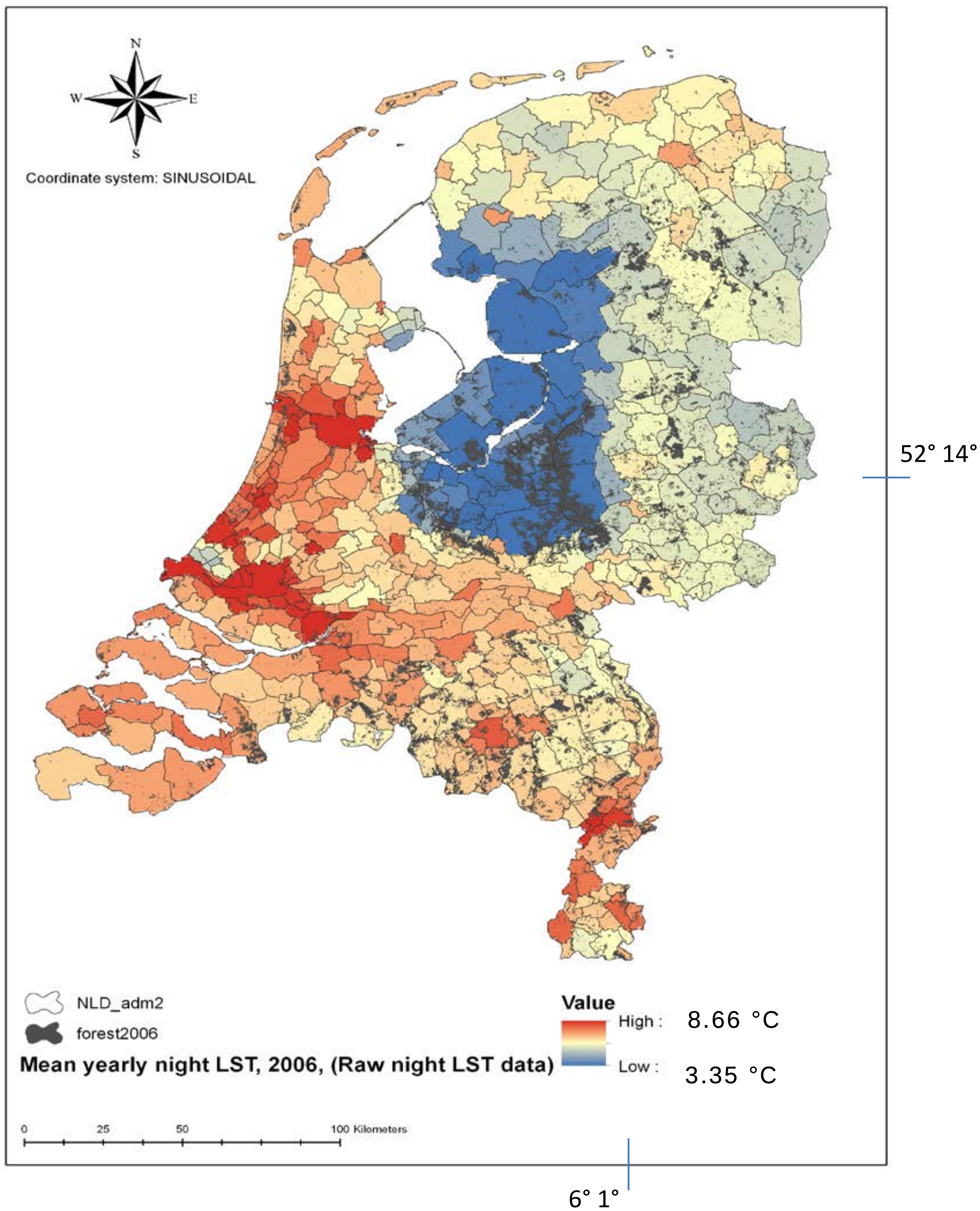

Figure 25 - The up-scaled mean yearly night LST mean to Dutch city scale and the spatial of pattern of forest, 2006

Fig. 26 shows the spatial pattern of inland water in 2006. Inland water is also mostly concentrated in the blue parts. And inland water has the highest night LST. Clarification is that the mean up-scaled LST is based on the political boundaries of the Dutch administrative polygon. In the blue parts (circle A) the urban sub-divisions are rather bigger than southern and western parts. In the blue region, inland water is mostly at the border of big municipalities. Consequently the warming effect of inland water is shared between large areas of the big polygons in which the dominant land use is open agriculture. In the circle B, inland water is in a smaller administrative polygon and can insert its warming effect in a strong way. The orange polygon in the circle B is dominantly occupied by open agriculture, and the reddish color is due to the presence of inland water.

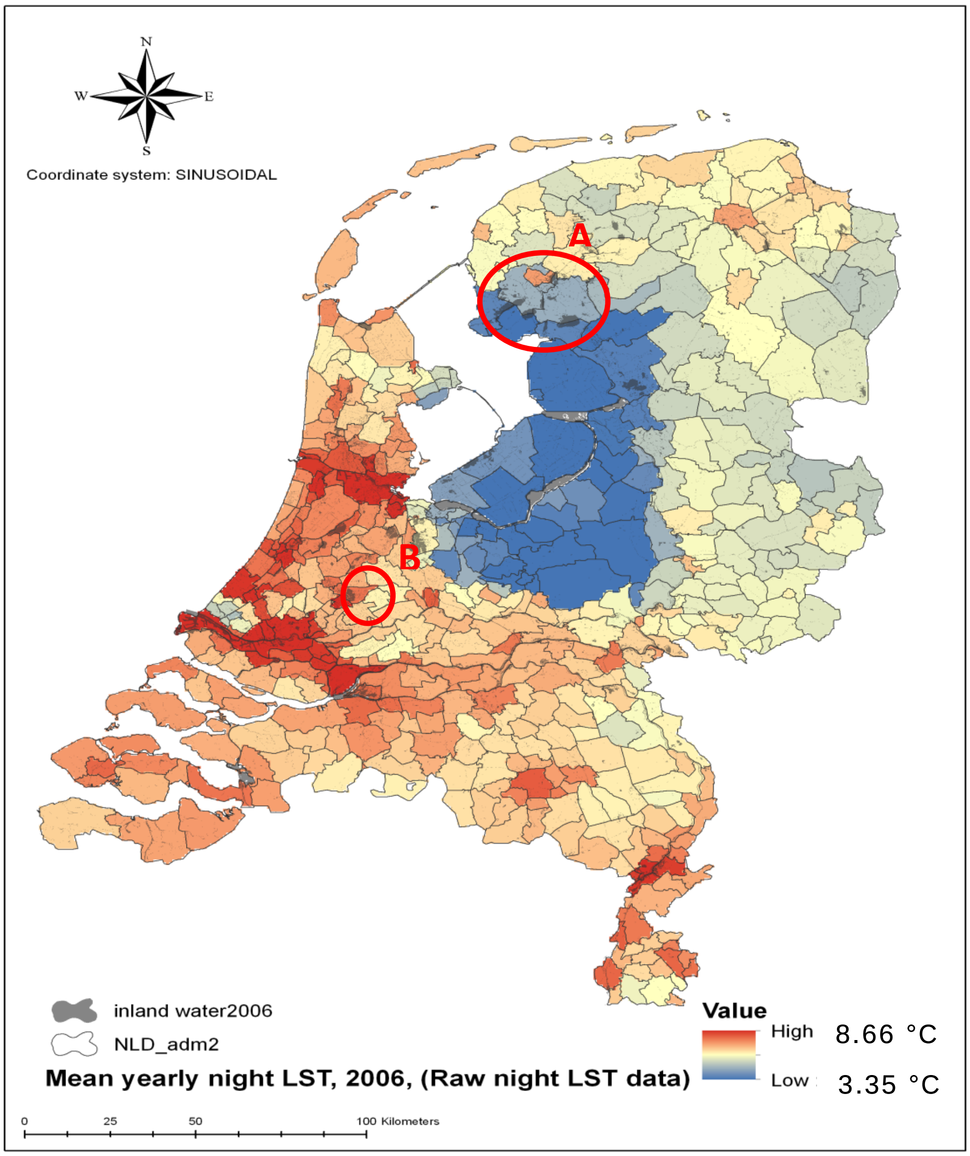

52° 14°

Figure 26 - The up-scaled mean yearly night LST mean to Dutch city scale and the spatial of pattern of inland water, 2006. Circle A shows inland water location in large municipalities, circle B show its location in smaller municipalities

Fig. 27 shows the build-up land use in the context of mean LST for each municipality. The greatest percentage of build-up area is positioned in high LST areas, indicating that high concentration of build-up area is mostly coincident with red high LST polygons. The span of build-up area and reddish color of mean polygons reveal the warming effect of building materials on land surface temperature. This finding supports the idea of Sun et al (2011), who found the maximum percentage of urban built-up land is located in high and very high LST areas.

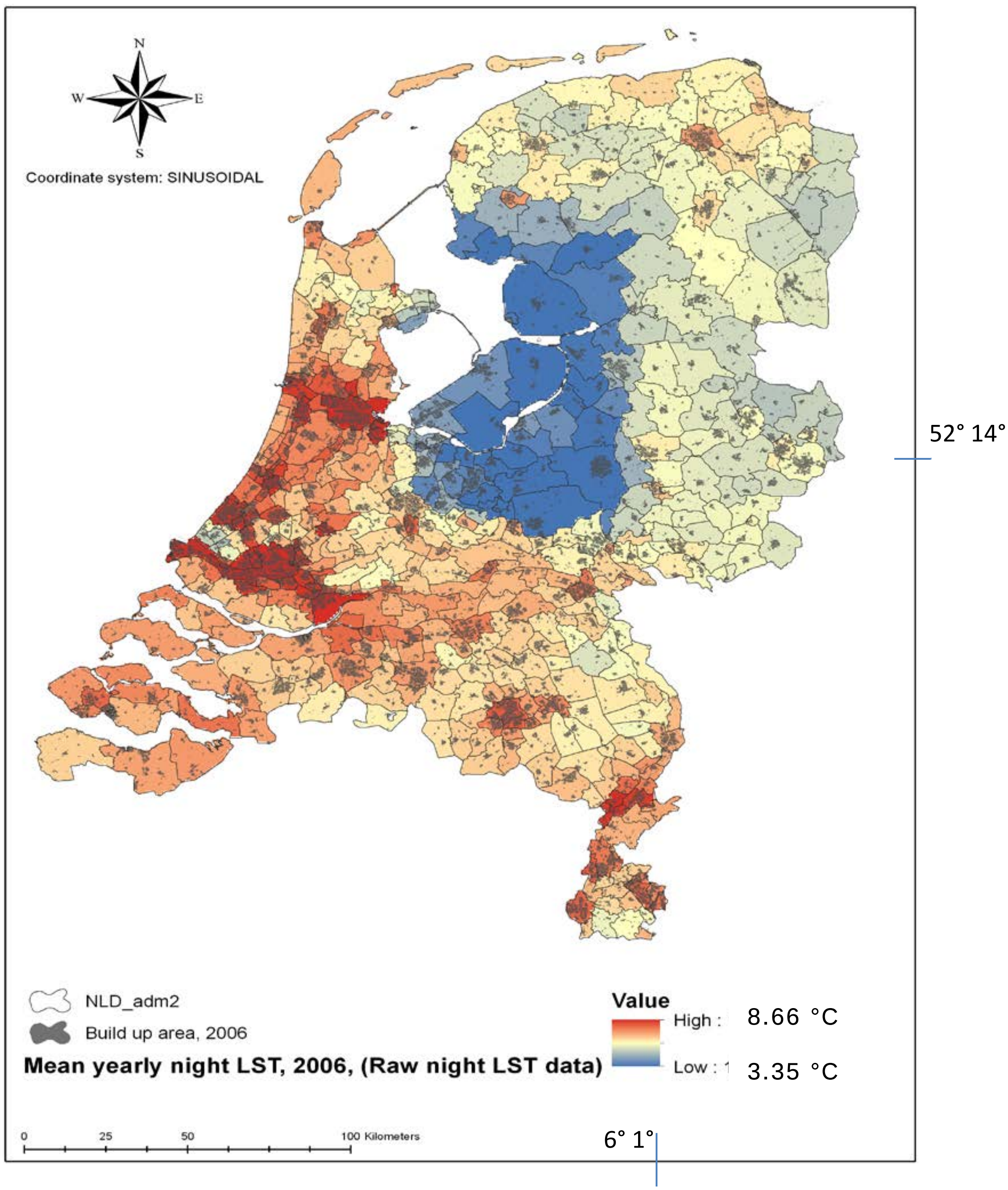

Figure 27 - The up-scaled mean yearly night LST mean to Dutch city scale and the spatial of pattern of build-up area, 2006

To show how recreation area affects the value of mean LST is very difficult from the Fig 28. One reason is that as argued before; recreation area is a mixed land use. The other reason is that recreation area has a low contribution in many LST pixels, comparing to dominant land uses. Moreover the spatial pattern of this land use is very well distributed in the whole country. Lack of hot spots of recreation areas in which some adjacent cells are fully occupied by recreation area limits any strong conclusion about this land use.

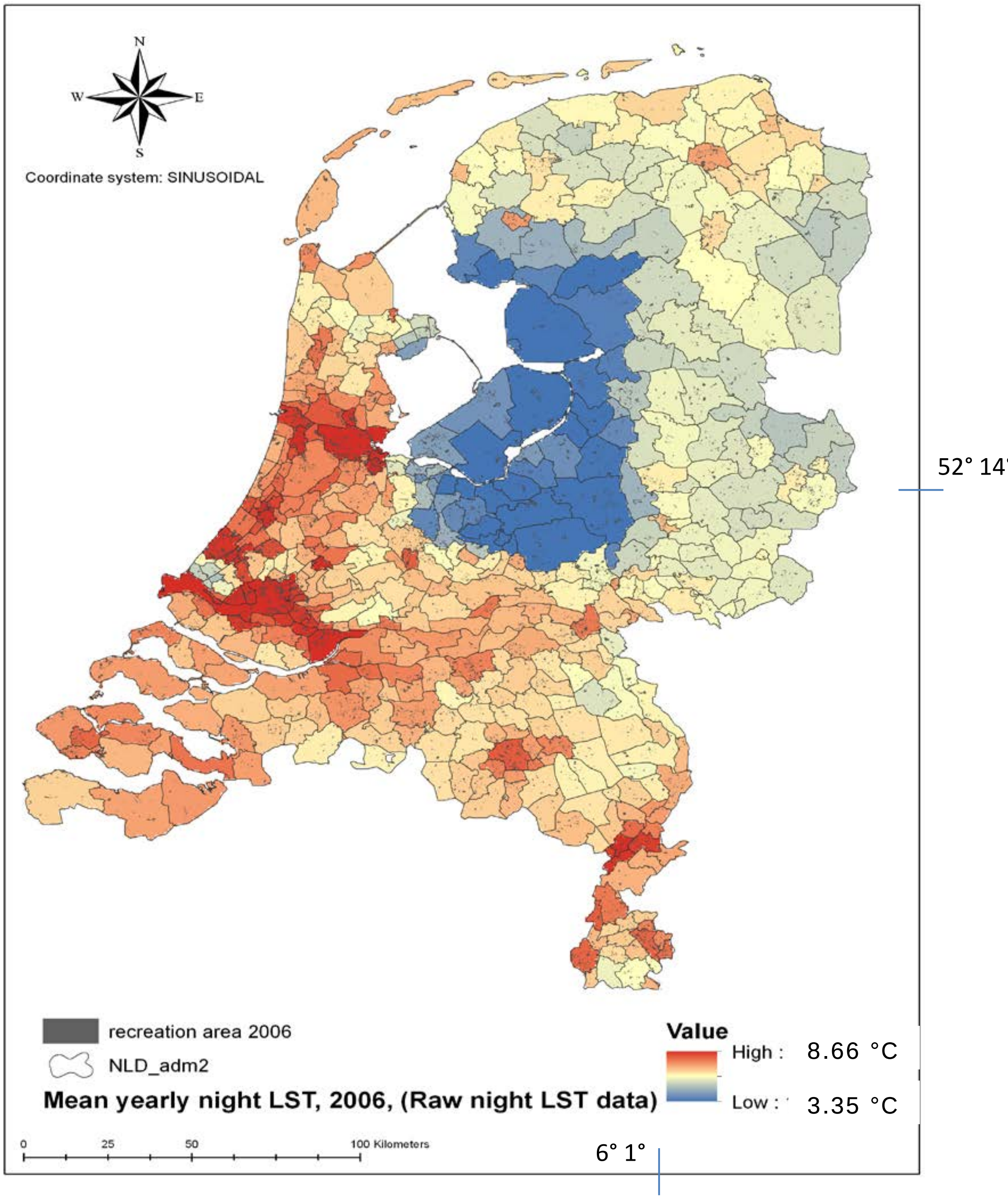

Figure 28 - The up-scaled mean yearly night LST mean to Dutch city scale and the spatial of pattern of recreation area, 2006

In case of greenhouse farming, although it has a low contribution in LST pixels, there are some dense spots which are highly occupied by greenhouse farming land use Fig. 29 Presence of these dense pure greenhouse spots in small administrative boundaries makes it easier to show how one specific land use can change the mean LST value. One of these areas is emphasized by the blue circle. Although the magnified area is surrounded by reddish urbanized land use, it has a low LST. This is due to high density of greenhouse farming houses. The roof of these houses has high reflection, so the amount of mean night LST is low.

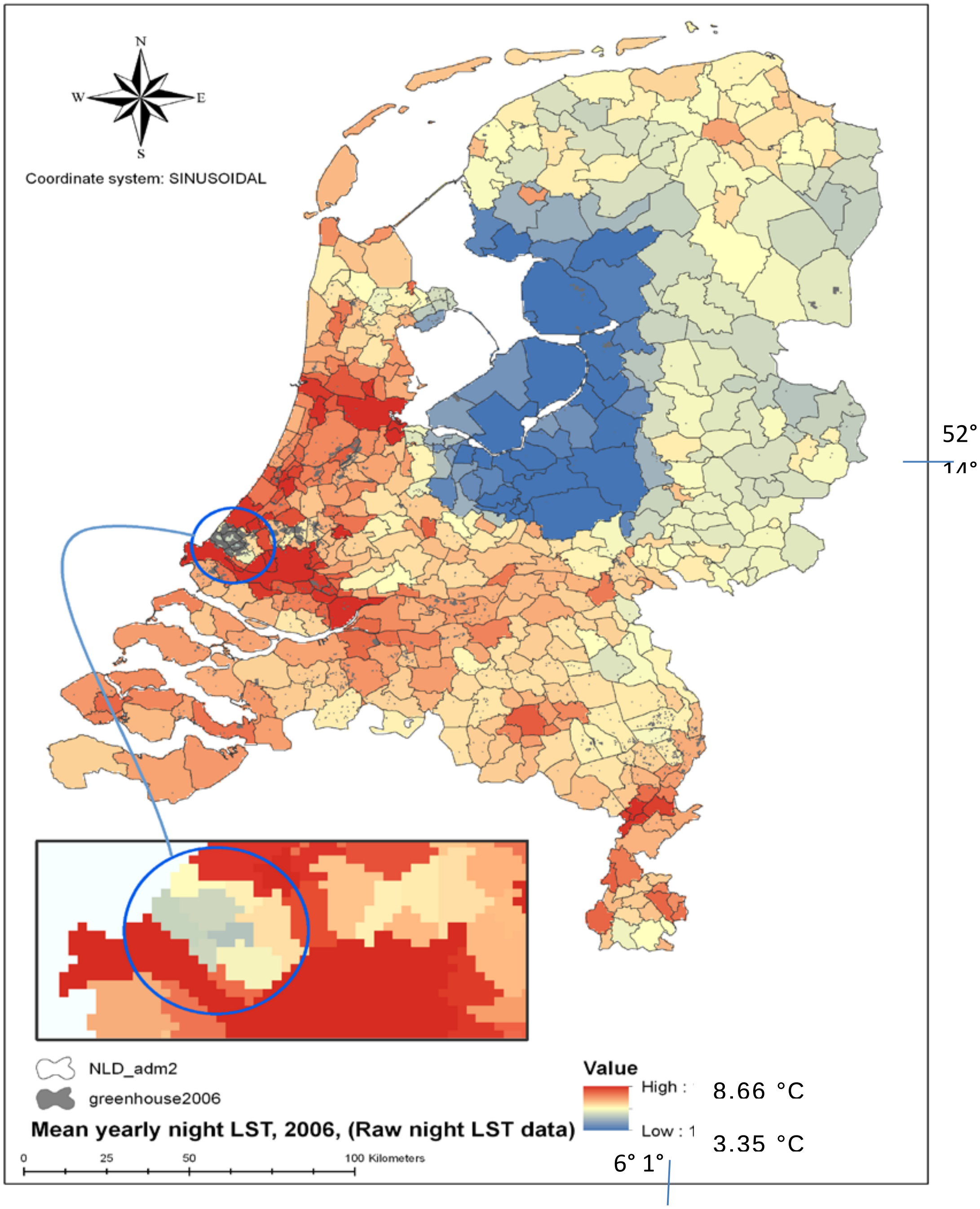

Figure 29 - The up-scaled mean yearly night LST mean to Dutch city scale and the spatial of pattern of greenhouse farming, 2006. The circle shows a bluish low LST municipality which is mostly covered by greenhouse farming

4.4. Conclusion

The above discussion has evaluated the effect of different land use types on land surface temperatures. The main findings of the study have fulfilled the aim and objective of this research. Through this analysis, the change pattern of different land use types was studied. Meanwhile the corresponded LST for each land use were extracted. To find any logical relationship, LST and coverage ratio of different land use types were statistically analyzed. The results have shown that from 2000 to 2008, open agriculture and build-up area had the largest land use change. In this period, open agriculture and forest were decreasing and all other land use types were increasing. The main increasing trend is for build- up area. Changing from natural land use types to building and paving covers lead to sharp changes in geophysical characteristic of the earth surface, including surface albedo, infiltration rate, runoff, evaporation and etc. which all can alter and get altered by LST. Results also have shown that inland water and offshore area had the biggest night LST, which was followed by build-up area. The lowest night LST was for forest class. During the day time, build-up area had the largest LST .The lowest day LST was for inland water and offshore area. So in one hand build up area is sharply increasing and on the other hand it is proved form ANOVA test that build up area has a high amount of LST. The mean yearly value of LST is calculated. This value can serve as a good managerial tool for urban planner and environmental scientists. Combining the result of land use analysis and mean LST can offer useful information to study urban heat island in the Dutch cities.

Zuid-Holland has the highest amount of LST from 2003 to 2008. The amount of LST for this province has increased from 2003 to 2008 by 0.75 ◦C which could be due to urbanization, population increase and also possible variations in weather temperature. In the same period Flevoland has the minimum amount of LST that is also increased from 3.39 ◦C in 2003 to 4.15◦C in 2008. The behavior of LST in 27 cells with fixed land use types does not show a significant slope, Which proves that weather condition does not affect LST in a meaningful way. The result of correlation for grouped data shows a strong and significant linear association between LST and the percentage of different types of land use. The sign of coefficient is positive for build-up area and inland water and offshore area. For open agriculture, forest, and greenhouse farming the reverse is true and the sign of association is negative. The result shows that strength of correlation was higher when land use data were grouped. Finally the thermal environment of the Netherlands in the years of 2003, 2006 and 2008 was described by regression analysis. Using these equations, the value of mean LST can be predicted in each cell that is based on coverage ratio of different types of land uses in that cell. These equations can be used to evaluate future land use scenarios and to plan a balanced spatial arrangement of land use types in which high LST values of hot land use types can be moderated by the coldest ones. To have a better understanding on how LST and land use types are related, future researches are needed in this criterion. It is recommended to study LST with a finer resolution of satellite images. It is suggested to examine the relationship between LST and weather temperature in the Netherlands for the next studies. It is also recommended to do the same study and for each province or municipality. Studying seasonal changes of LST and relating that to land use patterns is recommended. It is also advised to use Dutch future land use scenarios and relate it to LST values. Working in a smaller area, the number of land use types can be increased. For example, considering different types of forest or farming products. This study will be a significant endeavor in promoting global and regional climate models. This study will also be beneficial to the urban planners for future land use planning. Moreover, this research will provide recommendations on how to manage thermal environment of big cities in accordance to land use management. This study will be helpful to soil scientists and environmentalist in a way that it will provide critical information on surface temperature which affects soil moisture and thus the habitat of Soil micro-organisms, soil characteristic.

References

ArcGIS Desktop 10, ArcGIS Resource Center, available at: http://resources.arcgis.com/content/arcgisdesktop/10.0/about

Bonan, G.B. 1997. Effects of land use on climate of the United States. Clim. Change 37, 449–486.

Brandsma, T. and Wolters, D. 2012. Measurement and Statistical Modeling of the Urban Heat Island of the City of Utrecht (the Netherlands). Journal of Applied Meteorology and Climatology, 51(6), 1046-1060. doi: 10.1175/jamc-d-11-0206.1.

Brovkin, V., Claussen, M., et al. 2006. Biogeophysical effects of historical land cover changes simulated by six Earth system models of intermediate complexity. Climate Dynamics 26, 587-600.

Campbell, J.B. 2002. Introduction to Remote Sensing (3rd ed.).The Guilford Press, New York.

Campbell, D. and Campbell, S. 2008. Statlab Workshop Introduction to Regression and Data Analysis. StatLab Workshop Series 2008, available at: http://www.yale.edu/statlab.

Cao, X. M., Bao, A. M., et al. 2008. Land surface temperature in response to land use/cover change based on remote sensing data in Sangong River. In W. Gao & H. Wang (Eds.), Remote Sensing and Modeling of Ecosystems for Sustainability, 7083.

Davin, E.L. and De Noblet-Ducoudré, N. 2010. Climatic impact of global-scale deforestation: radiative versus non-radiative processes. Clim. 23, 97–112.

de Nijs, T. C., de Niet, R. et al. 2004. Constructing land-use maps of the Netherlands in 2030. Journal of Environmental Management 72(1–2): 35-42.

Dubayah, D. J. and Davis FW .1990. Topographic distribution of clear-sky radiation over the Konza Prairie.

European Commission/Joint Research Centre. 2006. Urban sprawl in Europe The ignored challenge, from website: http://www.eea.europa.eu/publications/eea_report_2006_10.

The European Environment Agency (EEA), Corine dataset, available at: http://www.eea.europa.eu/

FAO/ UNEP. 1996. 0ur land our future, FAO/AGLS .Rome. 48. P.

FAO/UNEP. 1999. Terminology for Integrated Resources Planning and Management. Food and Agriculture Organization/United Nations Environmental Program, Rome, Italy and Nairobi, Kenya.

Frohn, R.C. 1998. Remote Sensing for Landscape Ecology: New Metric Indicators for Monitoring, Modelling, and Assessment of Ecosystems. Lewis Publishers, Boca Raton, Florida.

Ge, J. 2010. MODIS observed impacts of intensive agriculture on surface temperature in the southern Great Plains. International Journal of Climatology, 30(13), 1994-2003. doi: 10.1002/joc.2093.

Goulden, M. L., Miller, S.D., et al. 2006. Nocturnal cold air drainage and pooling in a tropical forest. J Geophys Res-Atmos, 111(D8). doi: http://dx.doi.org/10.1890/05-1906.

Guo, Z. Wang, S.D., et al. 2012. Assess the effect of different degrees of urbanization on land surface temperature using remote sensing images. Procedia Environmental Sciences, 13, 935-942, doi:10.1016/j.proenv.2012.01.087.

Jiang, J., and Tian, G. 2010. Analysis of the impact of Land use/Land cover change on Land Surface Temperature with Remote Sensing. Procedia Environmental Sciences, 2(0), 571-575. doi: 10.1016/j.proenv.2010.10.062.

Jiménez-Muñoz, J. C. and J. A. Sobrino. 2008, IEEE Geoscience and Remote Sensing Letters, Vol. 5, No. 4, pp. 806-809,

Kantzioura, A., Kosmopoulos, et al. 2012. Urban surface temperature and microclimate measurements in Thessaloniki. Energy and Buildings, 44(0), 63-72. doi: 10.1016/j.enbuild.2011.10.019.

Kant, Y., Bharath, B.D., et al. 2009. Satellite-based Analysis of the Role of Land Use/Land Cover and Vegetation Density on Surface Temperature Regime of Delhi, India. Indian Soc. Remote Sens, 37, 201–214.

Keramitsoglou, I., Kiranoudis, C. T. et al. 2011. Identification and analysis of urban surface temperature patterns in Greater Athens, Greece, using MODIS imagery. Remote Sensing of Environment 115(12): 3080-3090.

Koomen, A. J. M., Nieuwhuizen, W., et al. 2006. Monitoring Landschap. Gebruik van steekproeven en landsdekkende bestanden. Wettelijke Onderzoekstaken Natuur & Milieu. Werkdokument 41, Project WOT-04-002 – 231701.01 Wageningen, the NetherlandsLe.

Linke, S. C. 2008. Local level application of the dynamic land use model METRONAMICA Assessment and modelling – a case study on the Dutch municipality Weert.

Loarie, S. R., Lobell, D. B., et al. 2011. Direct impacts on local climate of sugar-cane expansion in Brazil. *Nature Climate Change, 1*(2), 105-109. doi: 10.1038/nclimate1067.

Mallick R.B., Chen B. L., et. al. 2009. Harvesting energy from asphalt pavements and reducing the heat island effect. International Journal of Sustainable Engineering; 2(3), 214-228.

Marzban, C., R. Illian, D. et al. 2013. Within-group and between-group correlation: Illustration on noninvasive estimation of intracranial pressure. Submitted to the IEEE Journal of Biomedical and Health Informatics. (A related paper with more detail has not been submitted for publication).

MODIS overview. USGS, United States Geological Survey, Available at: https://lpdaac.usgs.gov/products/modis_overview.

Muhammad, S. 2007. Future urbanization in the Netherlands, under the influence of information and ommunication technologies. Urban and Regional Research Centre Utrecht (URU), Utrecht University, Faculty of Geosciences. Phd thesis.

NASA, EOS Project Science Office located at NASA Goddard Space Flight Center , from http://earthobservatory.nasa.gov/GlobalMaps/view.php?d1=MOD11C1_M_LSTDA.

NASA LP DAAC, USGS EROS Center, Sioux Falls, SD, 2012, MODIS Land Products Quality Assurance Tutorial: Part-1

National Cooperative Highway Research Program (NCHRP). 2004.Guide for Mechanistic-Empirical Design. Transportation Research Board, Washington, DC, Design Inputs,

Nationalonline data available at: http://nationalonline.org/.

Neteler, M. 2005. Time Series Processing of MODIS Satellite Data for Landscape Epidemiological Applications. International Journal of Geoinformatics 1.

Neteler, M. 2010. Estimating Daily Land Surface Temperatures in Mountainous Environments by Reconstructed MODIS LST Data. Remote Sensing Journal.

Newsom, 2006. USP 534, Data Analysis1, Post Hoc Tests. Available at : www.upa.pdx.edu/IOA/newsom/da1/ho_posthoc.doc.

OECD, 2008e, OECD review of regional innovation: north of England, UK, OECD publishing Paris.

Prata, A. J., V. Caselles, C. et al. 1995. Thermal remote sensing of land surface temperature from satellites: Current status and future prospects. Remote Sens. Rev., 12, 175–224.

Qin, Z., and Karnieli, A.1999. Progress in the remote sensing of land surface temperature and ground emissivity using NOAA-AVHRR. International Journal of Remote Sensing, 20, 2367-2393.

Quattrochi, D. A., and Ridd, M. K. 1998. Analysis of vegetation within a semi-arid urban environment using high spatial resolution airborne thermal infrared remote sensing data. Atmospheric Environment, 32, 19–33.

Rizwan, A. M., Dennis, L. Y. C. et al. 2008. A review on the generation, determination and mitigation of Urban Heat Island. Journal of Environmental Sciences 20(1): 120-128.

Sandholt, I., Rasmussen, K., et al. 2002. A simple interpretation of the surface temperature/vegetation index space for assessment of surface moisture status. *Remote Sensing of Environment*, 79, 213-224.

Sharp, K., A., 2001. Water: Structure and Properties. University of Pennsylvania. ENCYCLOPEDIA OF LIFE SCIENCES.

Schwarz, N., Lautenbach, S., et al. 2011. Exploring indicators for quantifying surface urban heat islands of European cities with MODIS land surface temperatures. [Article]. *Remote Sensing of Environment, 115*(12), 3175-3186. doi: 10.1016/j.rse.2011.07.003.

SPSS Inc. Released 2008. SPSS Statistics for Windows, Version 17.0. Chicago: SPSS Inc.

SPSS Statistics Base 17.0 User's Guide, available at: http://www.hks.harvard.edu/fs/pnorris/Classes/A%20SPSS%20Manuals/SPSS%20Statistcs%20Base%20User's%20Guide%2017.0.pdf

Statista, the leading German statistics portal, from http://www.statista.com/search/netherlands/cat/19/.

Steeneveld, G. J., Koopmans, S., et al. 2011. Quantifying urban heat island effects and human comfort for cities of variable size and urban morphology in the Netherlands. Journal of Geophysical Research-Atmospheres, 116. doi: 10.1029/2011jd015988.

Sun, Q., Wu, Z., et al. 2012. The relationship between land surface temperature and land use/land cover in Guangzhou, China. Environ Earth Sci, 65, 1687-1694, doi: 10.1007/s12665-011-1145-2.

Su, Y.F., Foody, G.M., et al. 2012. Spatial non-stationarity in the relationships between land cover and surface temperature in an urban heat island and its impacts on thermally sensitive populations. Landscape and Urban Planning, 107(2), Pages 172-180, doi:10.1016/j.landurbplan.2012.05.016.

van Leeuwen, T.T., Frank, A.J., et al. 2011. Optimal use of land surface temperature data to detect changes in tropical forest cover. JOURNAL OF GEOPHYSICAL RESEARCH, 116, G02002, doi:10.1029/2010JG001488.

Verburg, P. H., J. R. R. van Eck, et al. 2004. Determinants of land-use change patterns in the Netherlands. Environment and Planning B-Planning & Design 31(1): 125-150.

Voogt, J. A., and Oke, T. R. 2003. Thermal remote sensing of urban climates. Remote Sensing of Environment, 86, 370–384.

Wan, Z. 2007. Collection-5, MODIS Land Surface Temperature Products, Users' Guide.

Wan, Z. 2008. New refinements and validation of the MODIS Land-Surface Temperature/Emissivity products. Remote Sensing of Environment 112(1): 59-74.

Wan, Z., ZHANG, Y., et al. 2004. Quality assessment and validation of the MODIS global land surface temperature. International Journal of Remote Sensing. doi: 10.1080/0143116031000116417.

Wan, Z., 2003. *MODIS Land-Surface Temperature products users guide.* Electronic document: http://www.icess.ucsb.edu/modis/LstUsrGuide/usrguide.html.

Wang, W., S. Liang, et al. 2008. Validating MODIS land surface temperature products using long-term nighttime ground measurements. Remote Sensing of Environment 112(3): 623-635.

Weng, Q., Lu,D., et al. 2004. Estimation of land surface temperature–vegetation abundance relationship for urban heat island studies. Remote Sensing of Environment, 89(4),467-483. doi: 10.1016/j.rse.2003.11.005.

Weng, Q. and Lu, D. 2008. A sub-pixel analysis of urbanization effect on land surface temperature and its interplay with impervious surface and vegetation coverage in Indianapolis. International Journal of Applied Earth Observation and Geoinformation, 10(1),68-83,doi:10.1016/j.jag.2007.05.002.

Wickham, J., T. Wade, and K. Riiters. 2012 Comparison of cropland and forest surface temperatures across the conterminous United States. AGRICULTURAL AND FOREST METEOROLOGY. Elsevier Science Ltd, New York, NY, 166:137-143.

Wolters, D. and T. Brandsma. 2012. Estimating the Urban Heat Island in residential areas in the Netherlands using observations by weather amateurs. Journal of Applied Meteorology and Climatology, 51, 711-721, doi:http://dx.doi.org/10.1175/JAMC-D-11-0135.1.

World building directory, 2012, available at: http://www.worldbuildingsdirectory.com/.

Xiao,H. and Weng,Q. 2007. The impact of land use and land cover changes on land surface temperature in a karst area of China. Journal of Environmental Management,85(1),245-257, doi:10.1016/j.jenvman.2006.07.016.

Xiang, Q., Shan, H., et al. 2006. Impacts of land use and cover change on land surface temperature in Zhujiang Delta. Soil science society of china. Pedosphere, 16:6, 681-689.

Xu, Y., Qin, Z., et al. 2010. Spatial and Temporal Dynamics of Urban Heat Island and Their Relationship with Land Cover Changes in Urbanization Process: A Case Study in Suzhou, China. JOURNAL OF THE INDIAN SOCIETY OF REMOTE SENSING, 38(4), 654-663, do i**:** 10.1007/s12524-011-0073-7.

Yang,G., Pu,R., et al. 2011. Estimation of subpixel land surface temperature using an endmember index based technique: A case examination on ASTER and MODIS temperature products over a heterogeneous area. Remote Sensing of Environment, 115(5), 1202-1219, doi:10.1016/j.rse.2011.01.004.

Zhengming, W. and Dozier, J. 1989. Land-surface temperature measurement from space: physical principles and inverse modeling. Geoscience and Remote Sensing, IEEE Transactions on 27(3): 268-278.

Zhengming, W., 2007. Collection-5-MODIS Land Surface Temperature Products-Users' Guide. ICESS, University of California, Santa Barbara.

Zhou, X. and Wang, Y.C. 2011. Dynamics of Land Surface Temperature in Response to Land-Use/Cover Change. Geographical Research, 49:1, 23-36, doi: 10.1111/j.1745-5871.2010.00686.x.

Appendix

Group 1

Type and percentage of different land use class in the selected LST pixels for drawing LST time plots

Selected cells for plotting LST time plots, greenhouse farming

MODIS, land surface temperature, mod11a2 Tile: h18v03	MODIS FID	Longitude	Latitude	% greenhouse 2000	% greenhouse 2003	% greenhouse 2006	% greenhouse 2008	2003-2000	2006-2003	2008-2006
Cell (row, column): 956, 339	24813	4.59833	52.0292	19.882	19.686	69.752	69.656	-0.196	50.066	-0.096
Cell (row, column): 866, 366	14321	5.04914	52.7792	0.000	0.000	0.000	58.501	0.000	0.000	58.501
Cell (row, column): 866, 367	14322	5.06291	52.7792	0.000	0.000	0.000	59.496	0.000	0.000	59.496
Cell (row, column): 956, 310	24784	4.20554	52.0292	90.188	90.041	89.757	92.650	-0.147	-0.285	2.894
Cell (row, column): 957, 309	24951	4.19121	52.0208	90.913	92.027	90.633	92.129	1.114	-1.394	1.496
Cell (row, column): 958, 313	25121	4.24459	52.0125	88.565	85.919	84.153	81.582	-2.646	-1.766	-2.571
Cell (row, column): 959, 313	25287	4.2438	52.0042	86.192	83.840	83.495	87.805	-2.352	-0.345	4.310
Cell (row, column): 961, 306	25632	4.1475	51.9875	89.177	88.427	81.998	83.380	-0.749	-6.429	1.382

Selected cells for plotting LST time plots, recreation area

MODIS, land surface temperature, mod11a2 Tile: h18v03	MODIS FID	Longitude	Latitude	% recreation 2000	% recreation 2003	% recreation 2006	% recreation 008	2003-2000	2006-2003	2008-2006
Cell (row, column): 1003, 451	31664	6.06234	51.6375	0.000	0.000	59.225	59.188	0.000	59.225	-0.037
Cell (row, column): 936, 416	21685	5.66237	52.1958	84.735	84.931	85.028	85.028	0.196	0.098	0.000
Cell (row, column): 947, 319	23307	4.33471	52.1042	87.583	87.838	87.982	87.904	0.256	0.143	-0.078

Selected cells for plotting LST time plots, forest

MODIS, land surface temperature, mod11a2 Tile: h18v03	MODIS FID	Longitude	Latitude	%forest 2000	%forest 2003	%forest 2006	%forest 2008	2003-2000	2006-2003	2008-2006
Cell (row, column): 983, 438	29201	5.90953	51.8042	10	10	80.984	81.098	-88.865	80.304	0.114
Cell (row, column): 920, 472	6886	6.44304	52.3292	100.000	100.000	100.000	100.000	0.000	0.000	0.000
Cell (row, column): 922, 42	19572	5.84086	52.3125	100.000	100.000	100.000	100.000	0.000	0.000	0.000
Cell (row, column): 927, 427	20294	5.82175	52.2708	100.000	100.000	100.000	100.000	0.000	0.000	0.000
Cell (row, column): 938, 433	21994	5.89128	52.1792	100.000	100.000	100.000	100.000	0.000	0.000	0.000
Cell (row, column): 1041, 413	35852	5.5137	51.3208	100.000	100.000	100.000	100.000	0.000	0.000	0.000

Selected cells for plotting LST time plots, open agriculture

MODIS, land surface temperature, mod11a2 Tile: h18v03	MODIS FID	Longitude	Latitude	% Open agriculture 2000	% Open agriculture 2003	% Open agriculture 2006	% Open agriculture 2008	2003-2000	2006-2003	2008-2006
Cell (row, column): 819, 505	1833	7.0275	53.1708	93.629	92.679	3.938	3.938	-0.950	-88.740	0.000
Cell (row, column): 810, 356	11494	4.96477	53.2458	99.808	0.109	0.109	0.109	-99.699	0.000	0.000
Cell (row, column): 835, 519	3152	7.19977	53.0375	100.000	100.000	100.000	100.000	0.000	0.000	0.000
Cell (row, column): 1012, 415	8979	5.56976	51.5625	100.000	100.000	100.000	100.000	0.000	0.000	0.000
Cell (row, column): 958, 386	25191	5.23296	52.0125	100.000	100.000	100.000	100.000	0.000	0.000	0.000
Cell (row, column): 854, 414	38855	5.72358	52.8792	100.000	100.000	100.000	100.000	0.000	0.000	0.000
Cell (row, column): 785, 409	1	5.73081	53.4542	100.000	100.000	100.000	100.000	0.000	0.000	0.000

Selected cells for plotting LST time plots, build-up area

MODIS, land surface temperature, mod11a2 Tile: h18v03	GRID FID	Longitude	Latitude	%Build-up 2000	% Build-up 2003	% Build-up 2006	% Build-up 2008	2003-2000	2006-2003	2008-2006
Cell (row, column): 820, 508	1840	7.06783	53.1625	0.000	0.000	0.000	97.972	0.000	0.000	97.972
NO LST VALUE	18809	5.15053	52.3542	0.000	91.155	88.146	96.733	91.154	-3.009	8.587
Cell (row, column): 978, 342	28397	4.62004	51.8458	17.981	16.720	90.644	90.582	-1.261	73.923	-0.062
Cell (row, column): 1011, 379	8933	5.08811	51.5708	97.638	97.634	97.634	97.634	-0.004	0.000	0.000
Cell (row, column): 922, 508	19606	6.93133	52.3125	95.215	95.806	95.232	95.233	0.591	-0.574	0.001
Cell (row, column): 966, 303	26514	4.10308	51.9458	100.000	99.899	100.000	100.000	-0.101	0.101	0.000
Cell (row, column): 1021, 423	37032	5.66766	51.4875	97.019	96.940	96.873	96.873	-0.079	-0.067	0.000
Cell (row, column): 934, 437	40599	5.9501	52.2125	96.775	96.584	96.793	96.791	-0.191	0.210	-0.002

Selected cells for plotting LST time plots, inland water

MODIS, land surface temperature, mod11a2 Tile: h18v03	MODIS FID	Longitude	Latitude	%water2000	%water2003	%water2006	%water2008	2003-2000	2006-2003	2008-2006
Cell (row, column): 907, 387	17583	5.29696	52.4375	21.976	70.697	77.313	77.313	48.721	6.616	0.000
Cell (row, column): 817, 506	1542	7.04413	53.1875	0.000	0.000	77.932	77.932	0.000	77.932	0.000
Cell (row, column): 853, 420	13481	5.80754	52.8875	100.000	100.000	100.000	100.000	0.000	0.000	0.000
Cell (row, column): 875, 440	15193	6.05818	52.7042	100.000	100.000	100.000	100.000	0.000	0.000	0.000
Cell (row, column): 936, 342	21612	4.65633	52.1958	100.000	100.000	100.000	100.000	0.000	0.000	0.000
Cell (row, column): 887, 420	39526	5.7699	52.6042	100.000	100.000	100.000	100.000	0.000	0.000	0.000
Cell (row, column): 913, 414	40246	5.65962	52.3875	100.000	100.000	100.000	100.000	0.000	0.000	0.000

Land use types in the selected pixels with sharp land use changes to draw LST time plots

MODIS FID	Dominant land use 2000	Dominant land use 2003	Dominant land use 2006	Dominant land use 2008
24813	Open agriculture	Open agriculture	Greenhouse farming	Greenhouse farming
14321	Open agriculture	Open agriculture	Open agriculture	Greenhouse farming
14322	Open agriculture	Open agriculture	Open agriculture	Greenhouse farming
1833	Open agriculture	Open agriculture	Inland waterway and Offshore area	Inland waterway and Offshore area
11494	Open agriculture	Inland waterway and	Inland waterway and	Inland waterway and
29201	Open agriculture	Open agriculture	forest	forest
31664	Open agriculture	Open agriculture	Recreational area	Recreational area
17583	Open agriculture	Inland waterway and Offshore area	Inland waterway and Offshore area	Inland waterway and Offshore area
1542	Open agriculture	Open agriculture	Inland waterway and Offshore area	Inland waterway and Offshore area
1840	Open agriculture	Open agriculture	Open agriculture	Build-up area
28397	Open agriculture	Open agriculture	Build-up area	Build-up area

Group 2

LST time plots for selected pixels with land use changes.

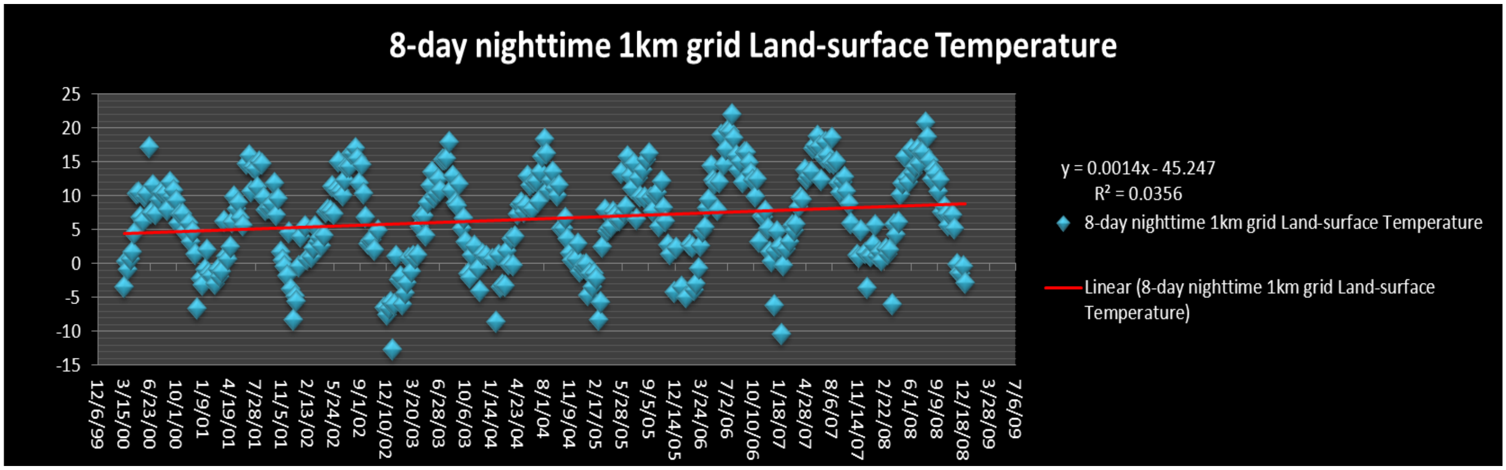

Latitude: 53.1875 Longitude: 7.04413 MODIS: mod11a2 Tile: h18v03 Year: 2000 Cell (row, column): 817, 506

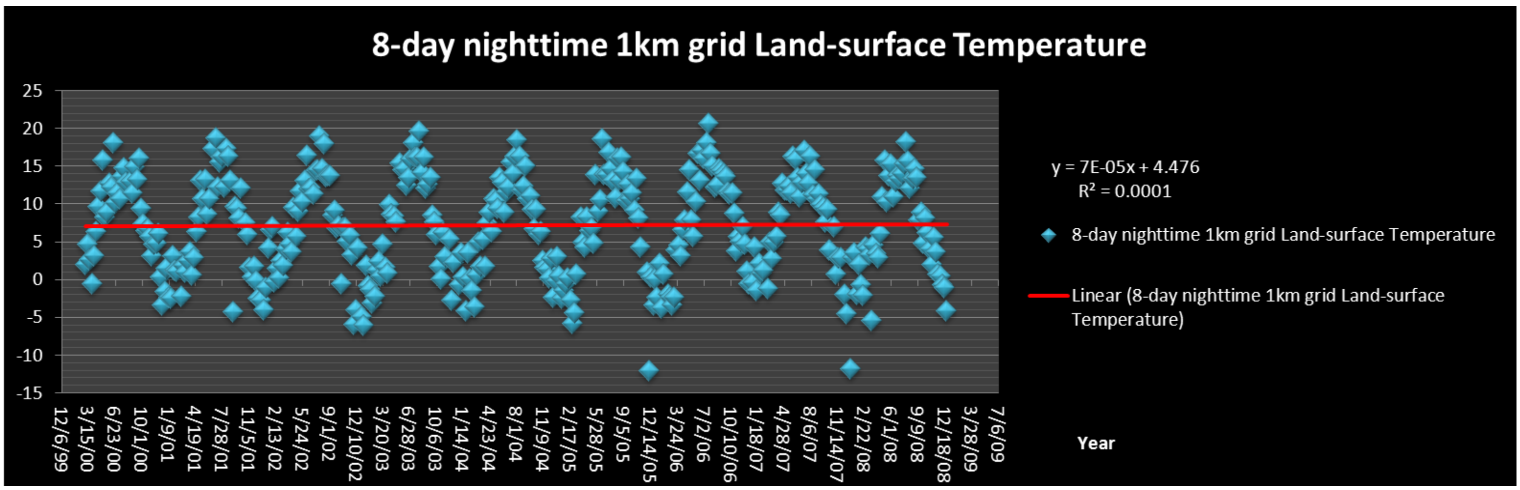

Latitude: 51.8458 Longitude: 4.62004 MODIS: mod11a2 Tile: h18v03 Year: 2000 Cell (row, column): 978, 342

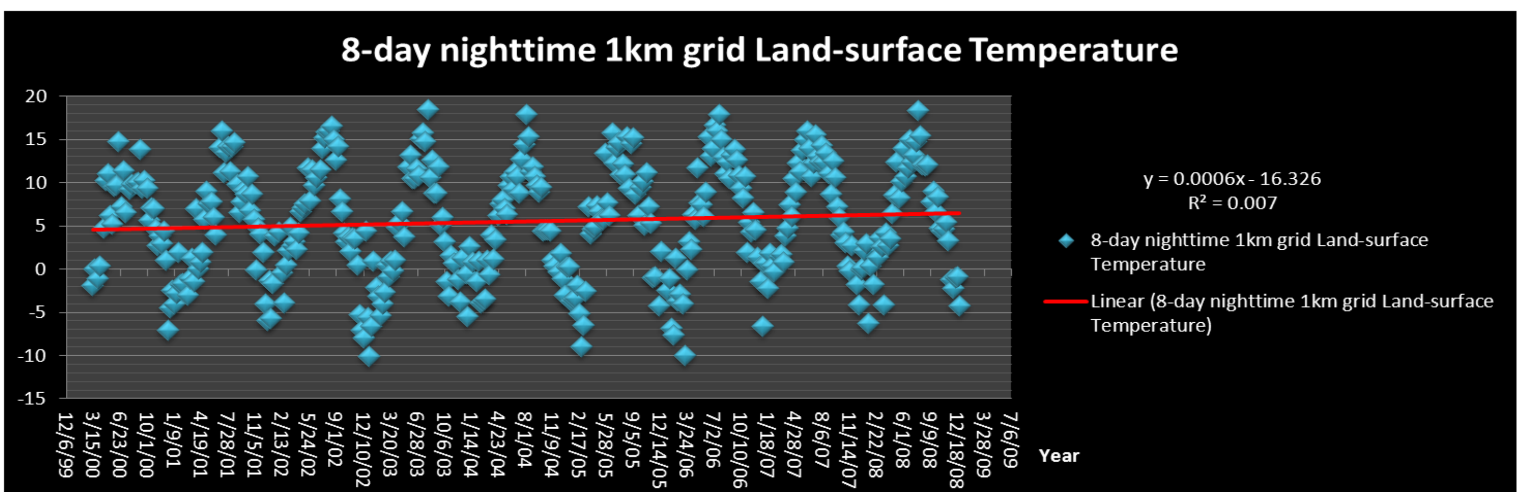

Latitude: 53.1625 Longitude: 7.06783 MODIS: mod11a2 Tile: h18v03 Year: 2000 Cell (row, column): 820, 508

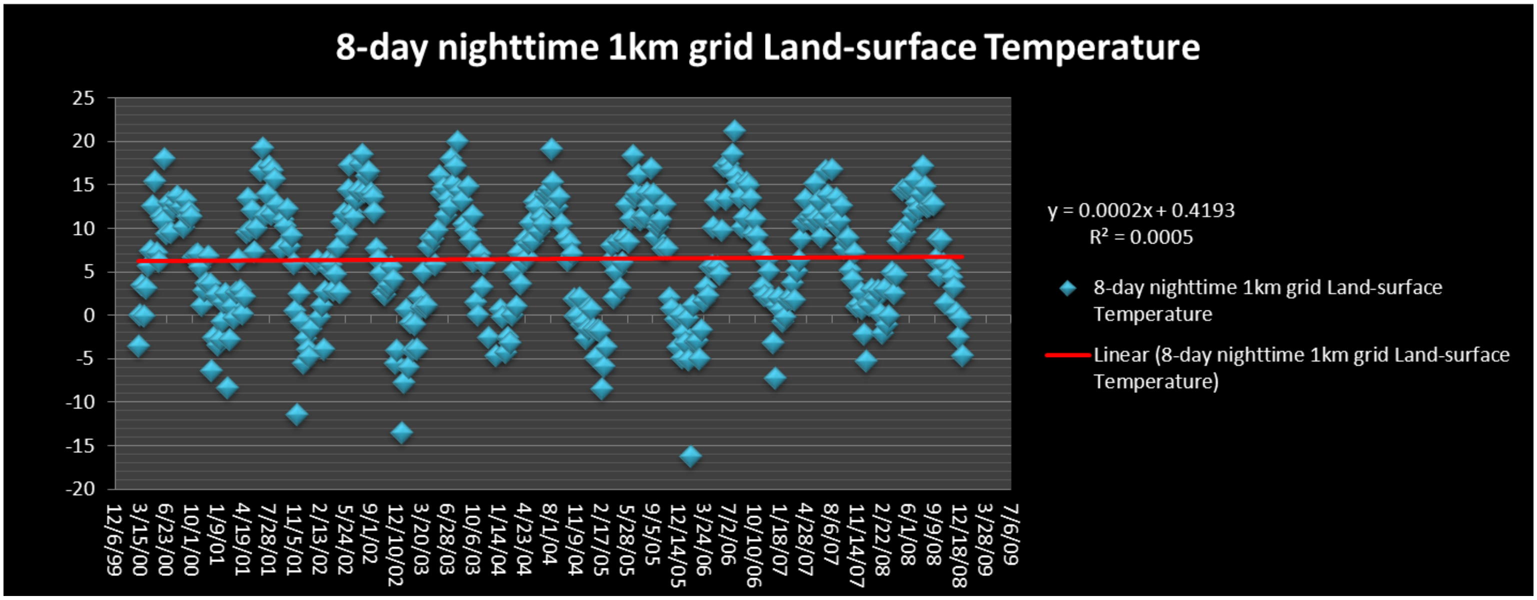

Latitude: 51.8042 Longitude: 5.90953 MODIS: mod11a2 Tile: h18v03 Year: 2000 Cell (row, column): 983, 438

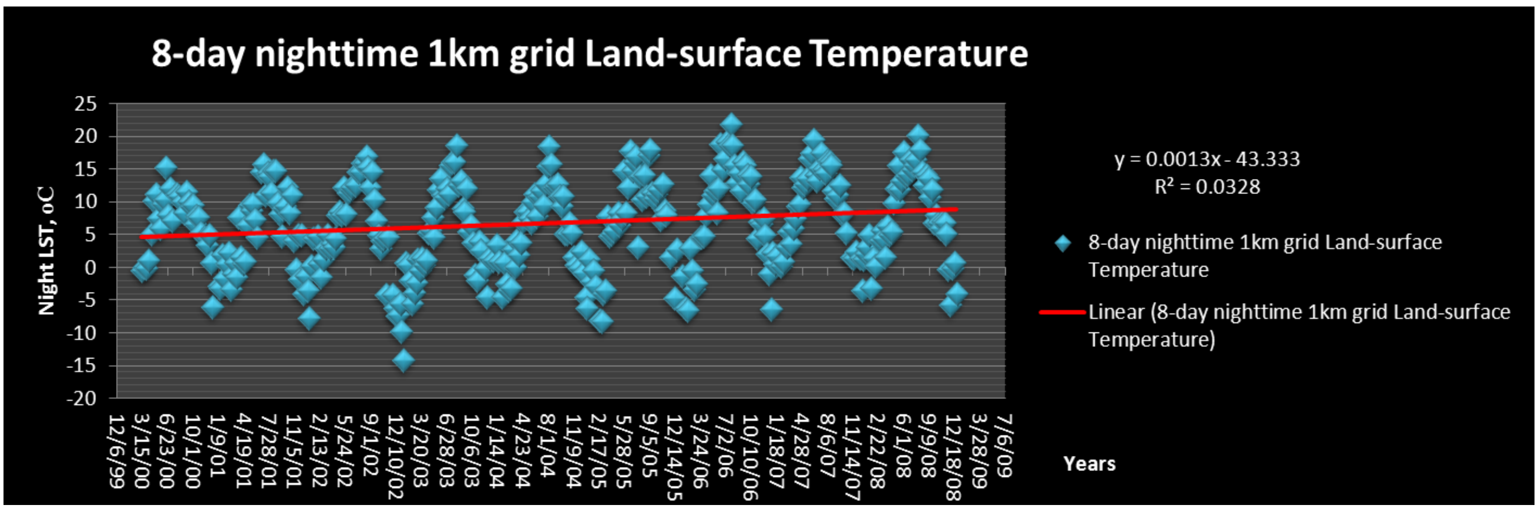

Latitude: 53.1708 Longitude: 7.0275 MODIS: mod11a2 Tile: h18v03 Year: 2000 Cell (row, column): 819, 505

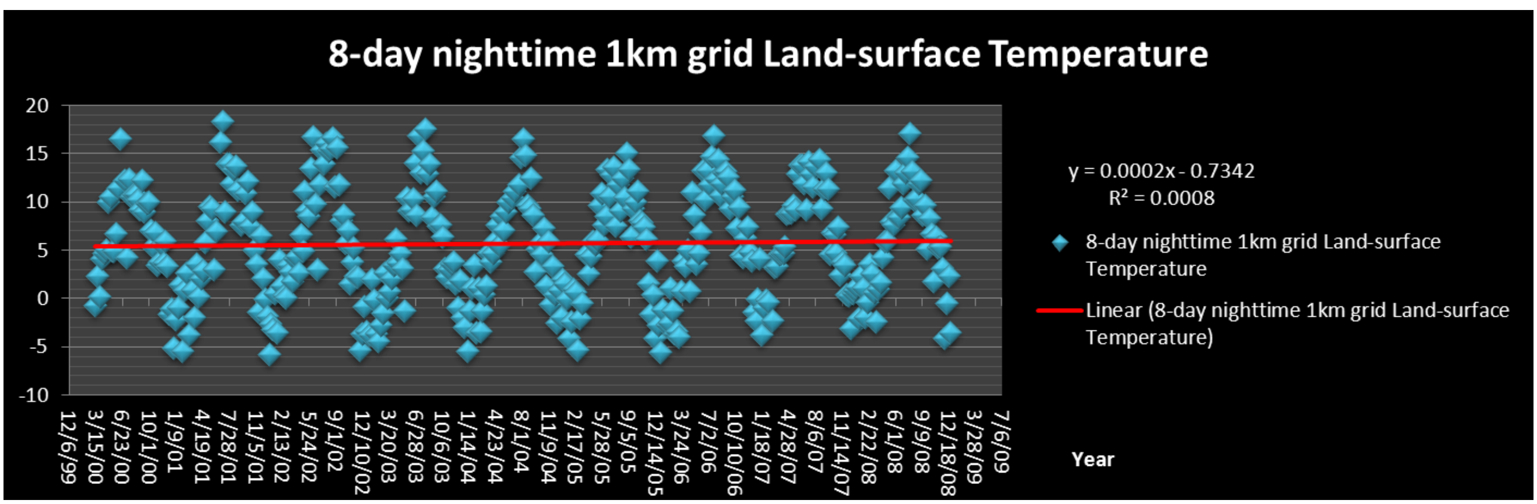

Latitude: 53.2458 Longitude: 4.96477 MODIS: mod11a2 Tile: h18v03 Year: 2000 Cell (row, column): 810, 356

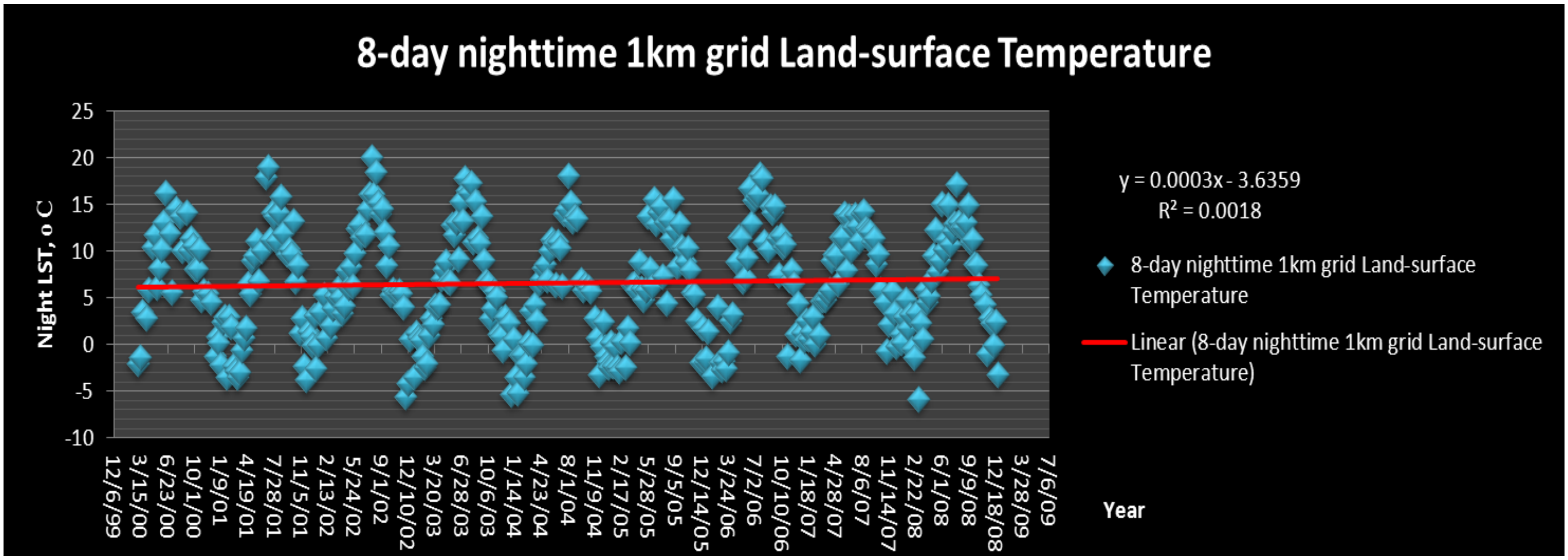

Latitude: 51.6375 Longitude: 6.06234 MODIS: mod11a2 Tile: h18v03 Year: 2000 Cell (row, column): 1003, 451

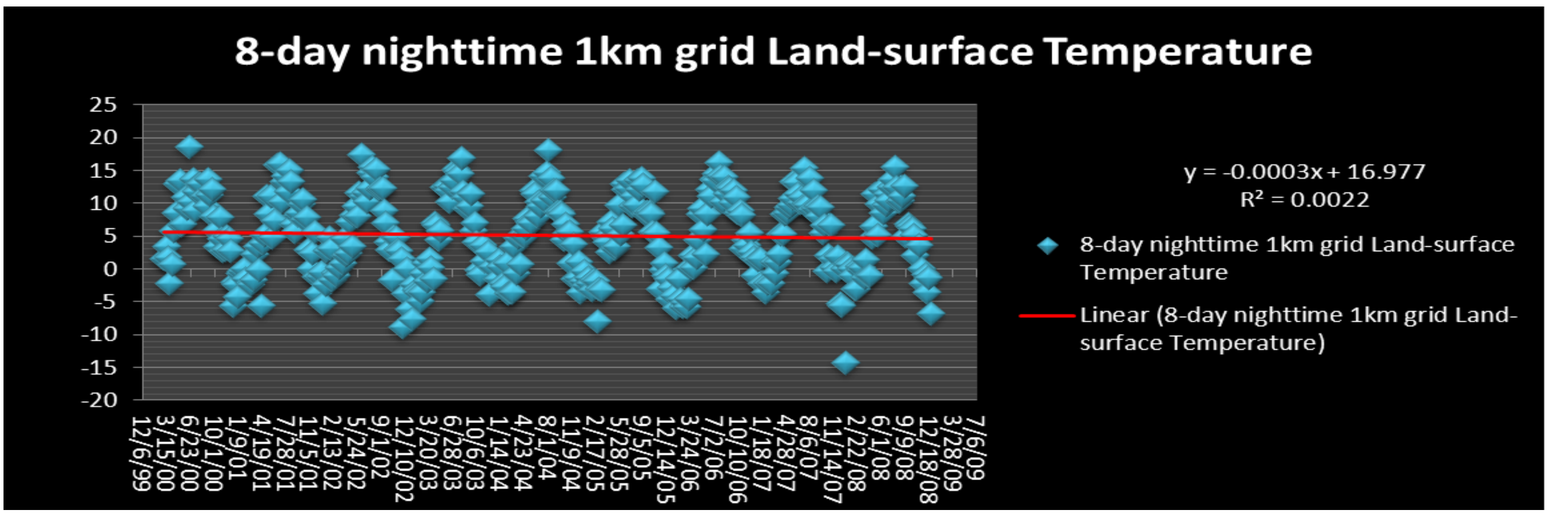

Attitude: 52.0292 Longitude: 4.59833 MODIS: mod11a2 Tile: h18v03 Year: 2000 Cell (row, column): 956, 339

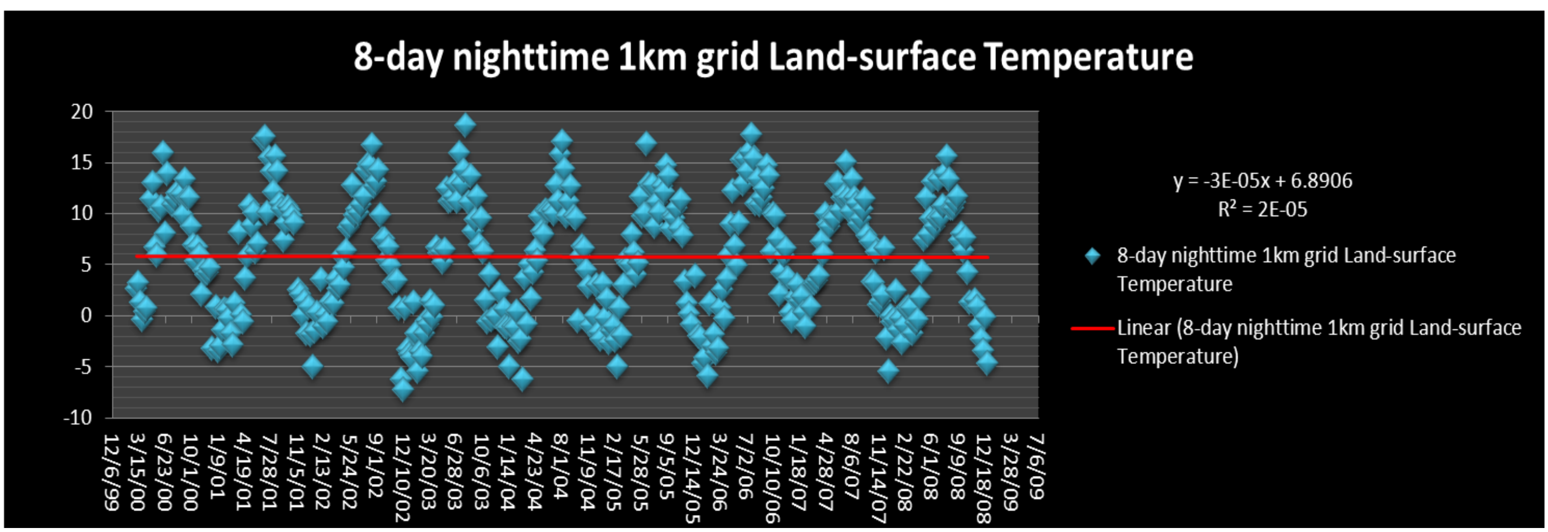

Latitude: 52.7792 Longitude: 5.04914 MODIS: mod11a2 Tile: h18v03 Year: 2000 Cell (row, column): 866, 366

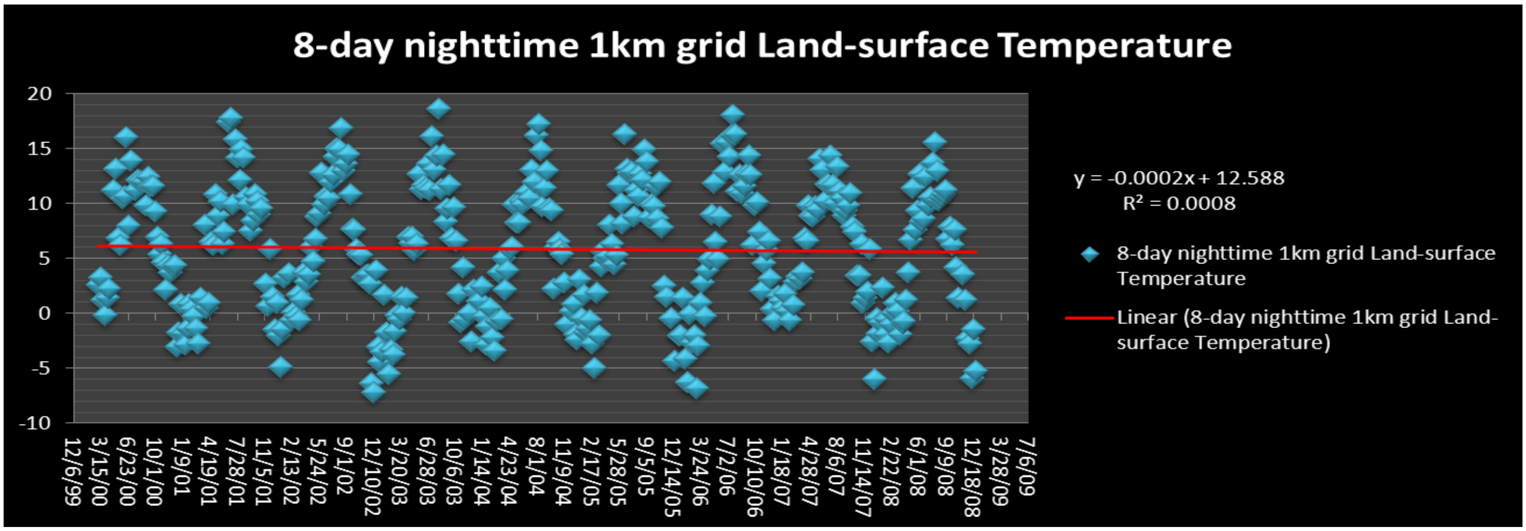

Latitude: 52.7792 Longitude: 5.06291 MODIS: mod11a2 Tile: h18v03 Year: 2000 Cell (row, column): 866, 367

Group 3

LST time plots for fixed land use pixels.

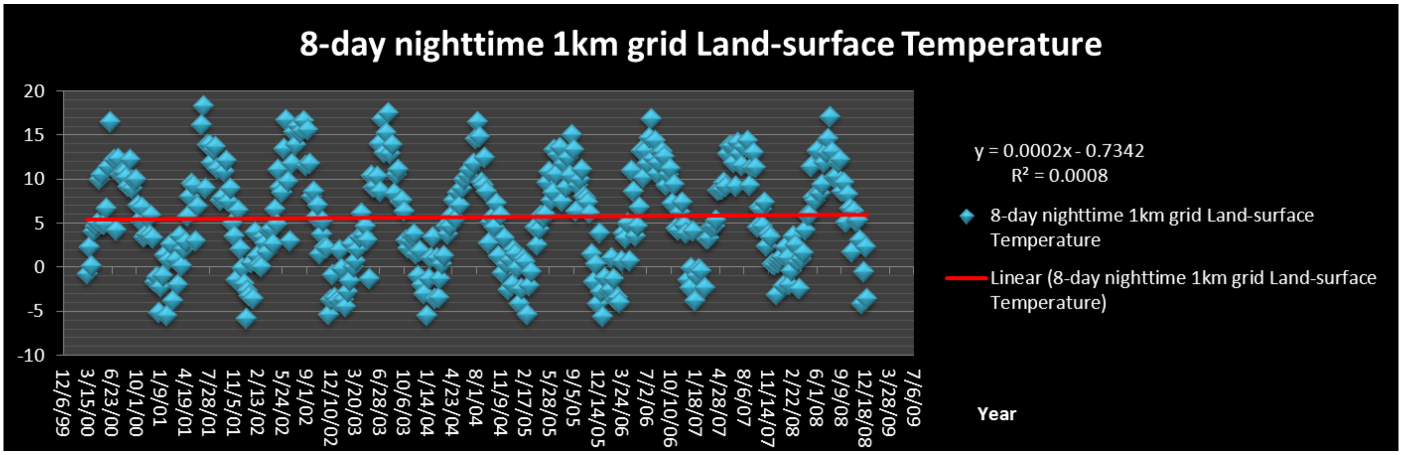

Longitude: 5.73081 MODIS: mod11a2 Tile: h18v03 Cell (row, column): 785, 409

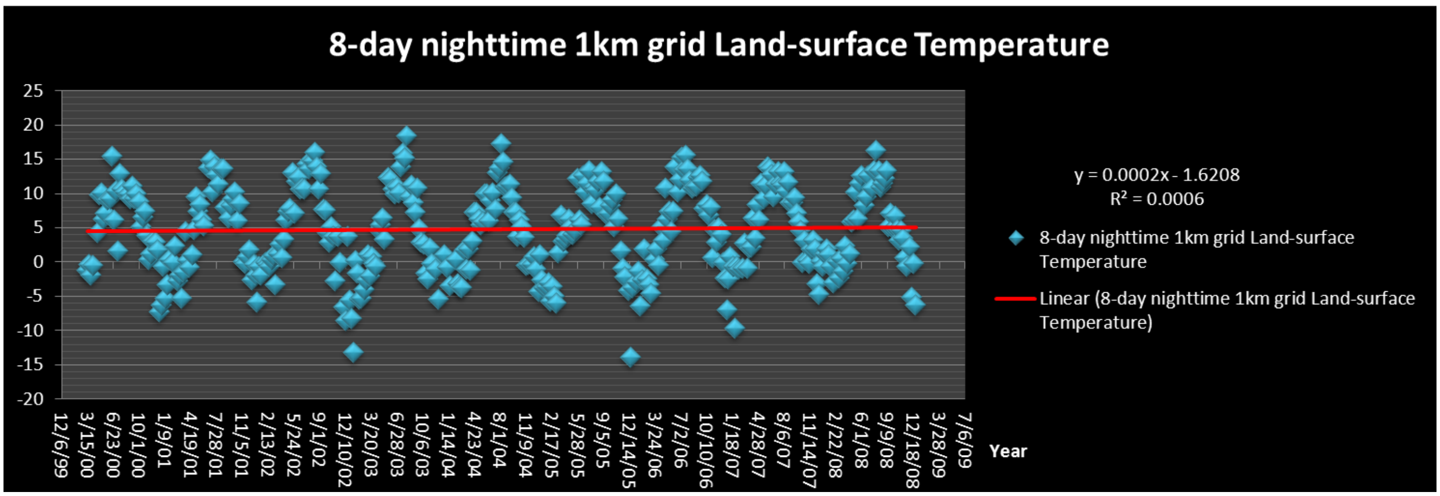

Latitude: 53.0375 Longitude: 7.19977000000 MODIS: mod11a2 Tile: h18v03 Cell (row, column): 835, 519 100

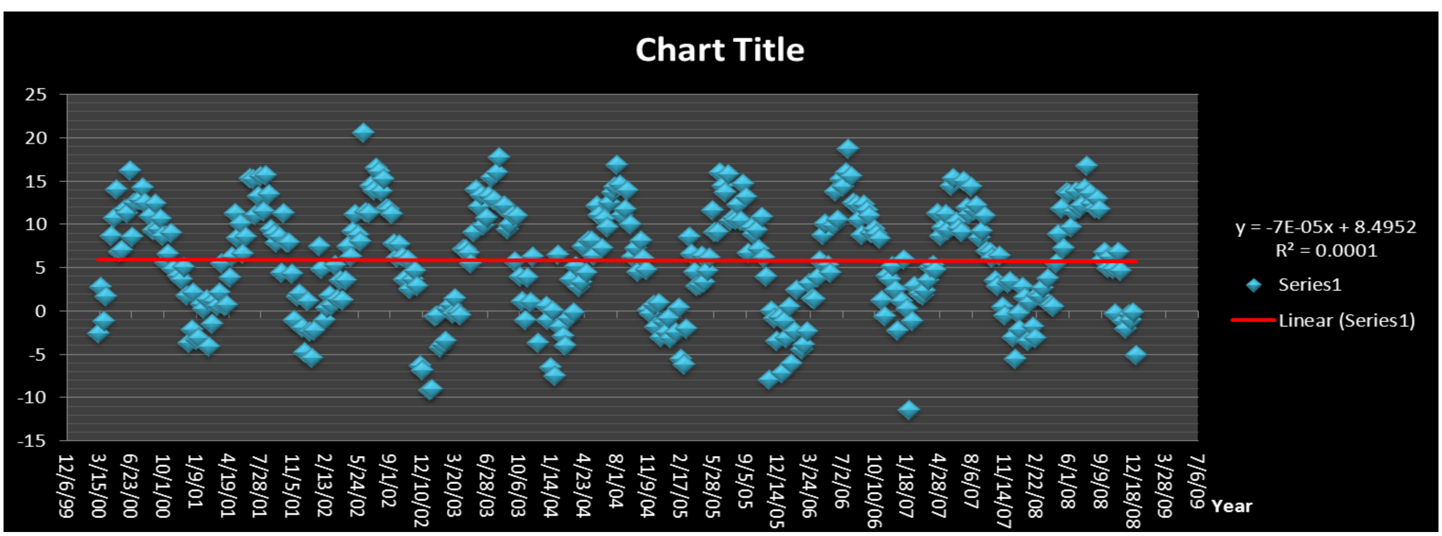

Latitude: 51.5625 Longitude: 5.56976 MODIS: mod11a2 Tile: h18v03 Cell (row, column): 1012, 415

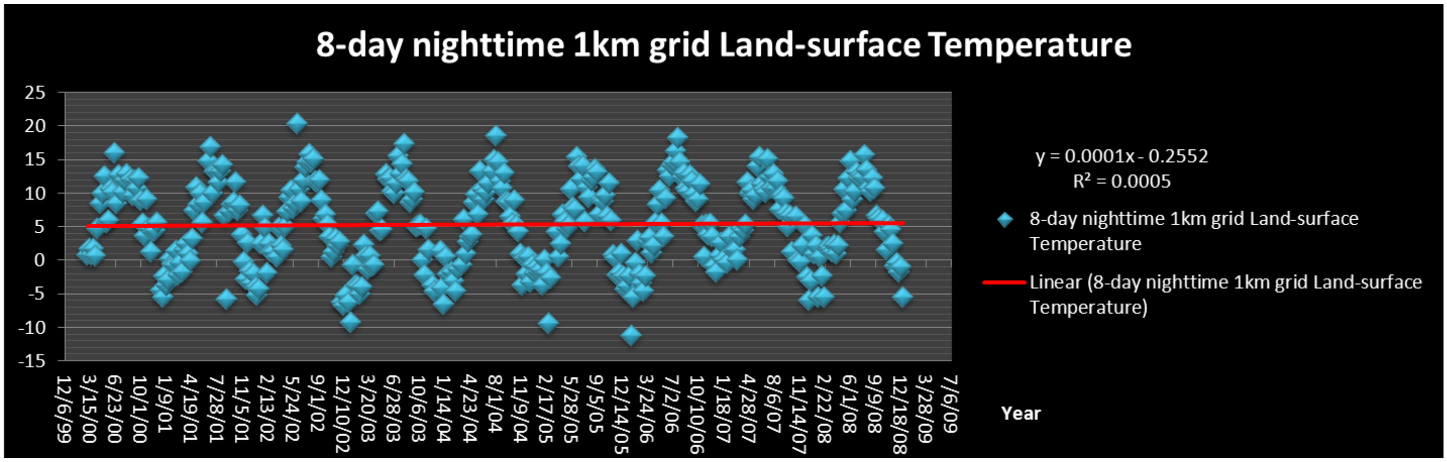

Latitude: 52.0125 Longitude: 5.23296 MODIS: mod11a2 Tile: h18v03 Cell (row, column): 958, 386

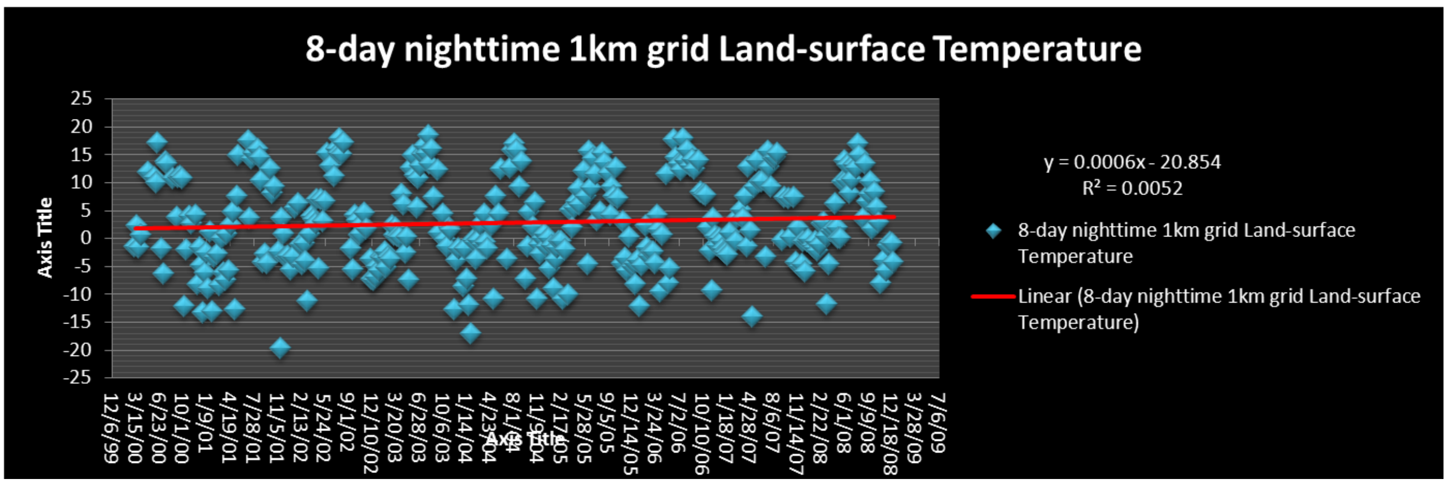

Latitude: 52.8792 Longitude: 5.72358 MODIS: mod11a2 Tile: h18v03 Cell (row, column): 854, 414

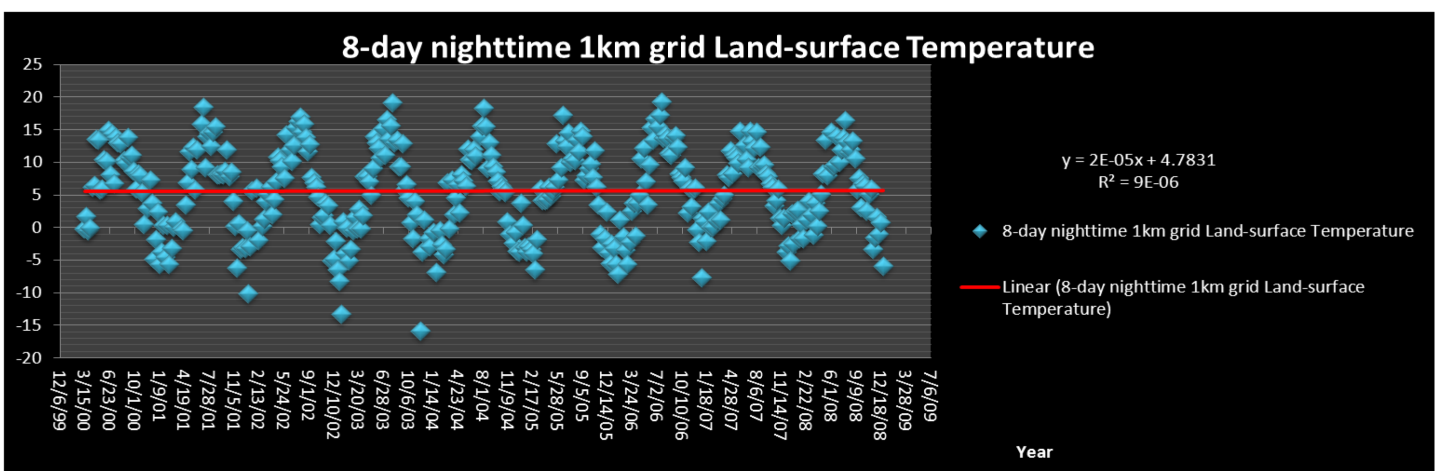

Latitude: 52.3292 Longitude: 6.44304 MODIS: mod11a2 Tile: h18v03 Cell (row, column): 920, 472

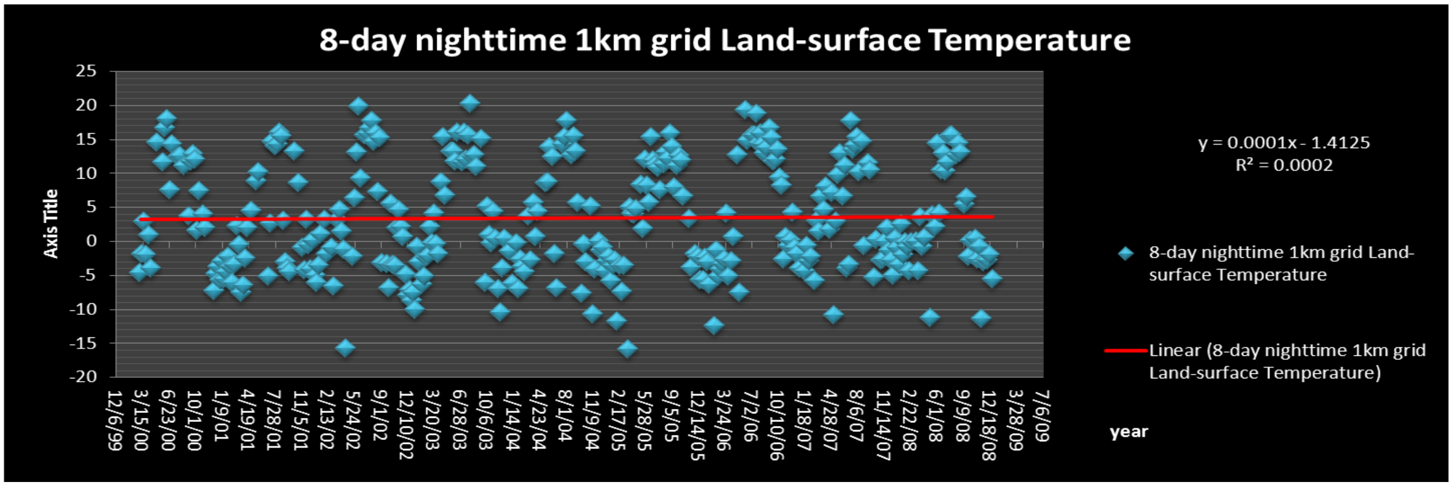

Latitude: 52.3125 Longitude: 5.84086 MODIS: mod11a2 Tile: h18v03 Cell (row, column): 922, 428

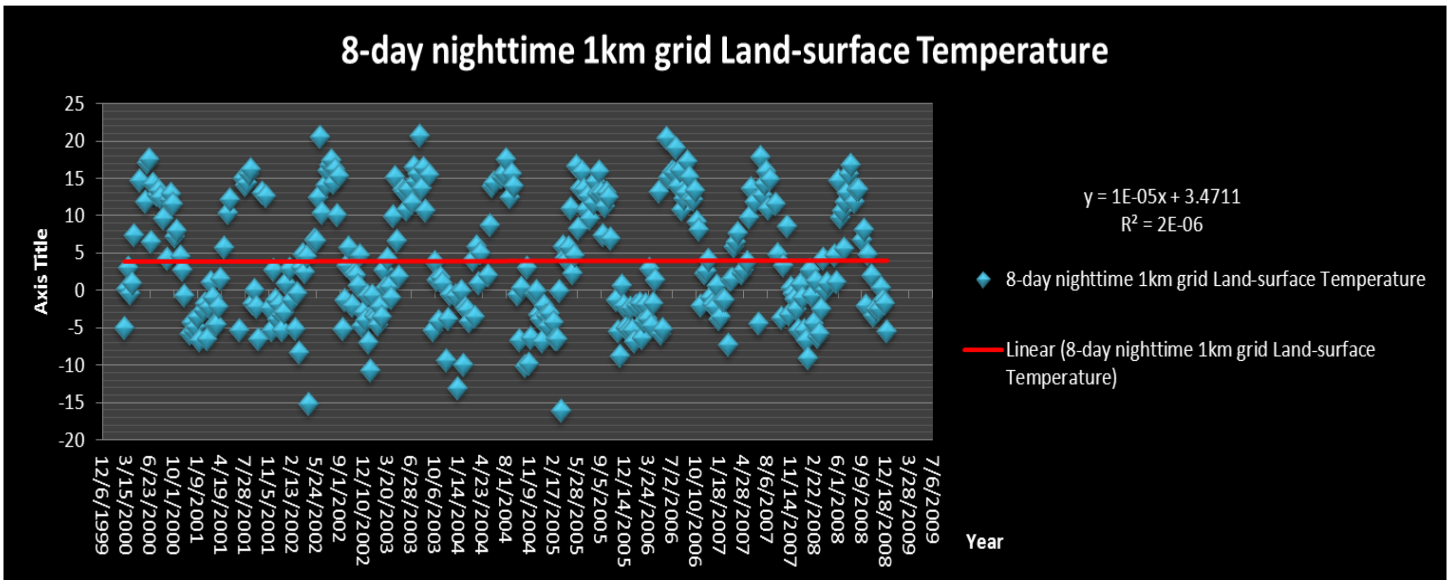

Latitude: 52.2708 Longitude: 5.82175 MODIS: mod11a2 Tile: h18v03 Cell (row, column): 927, 427

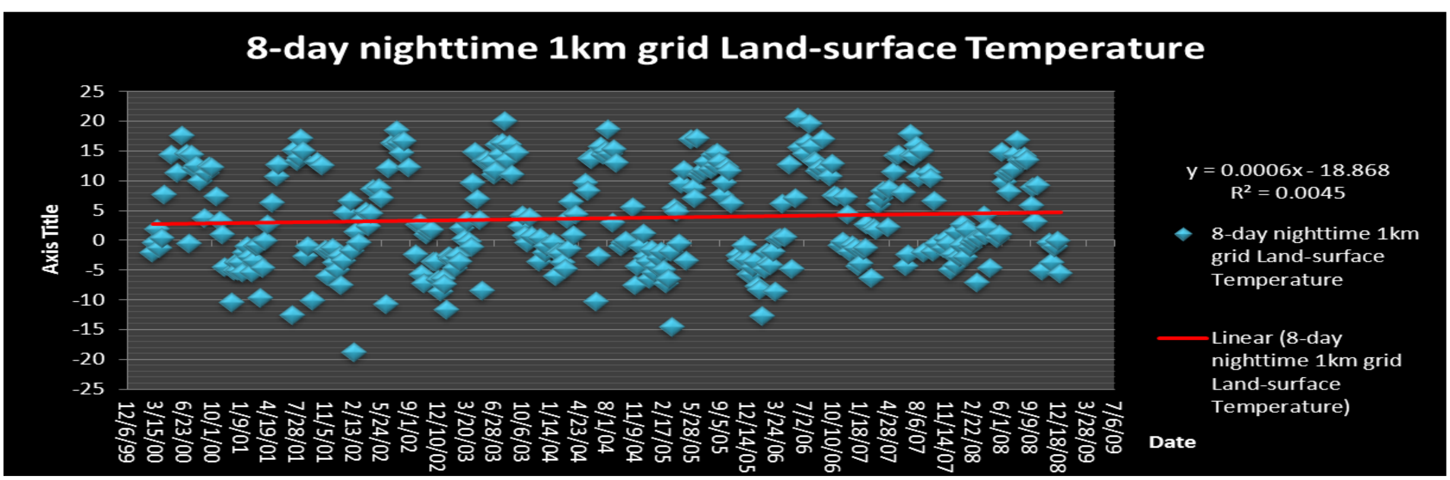

Latitude: 52.1792 Longitude: 5.89128 MODIS: mod11a2 Tile: h18v03 Cell (row, column): 938, 433

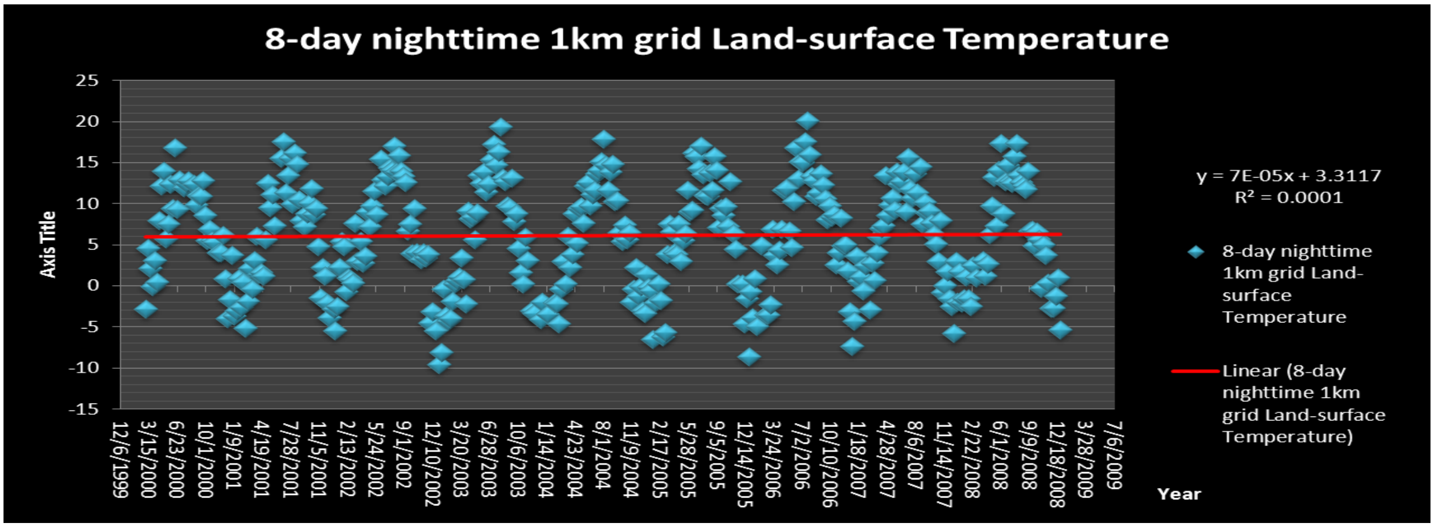

Latitude: 51.3208 Longitude: 5.5137 MODIS mod11a2 Tile: h18v03 Cell (row, column): 1041, 413

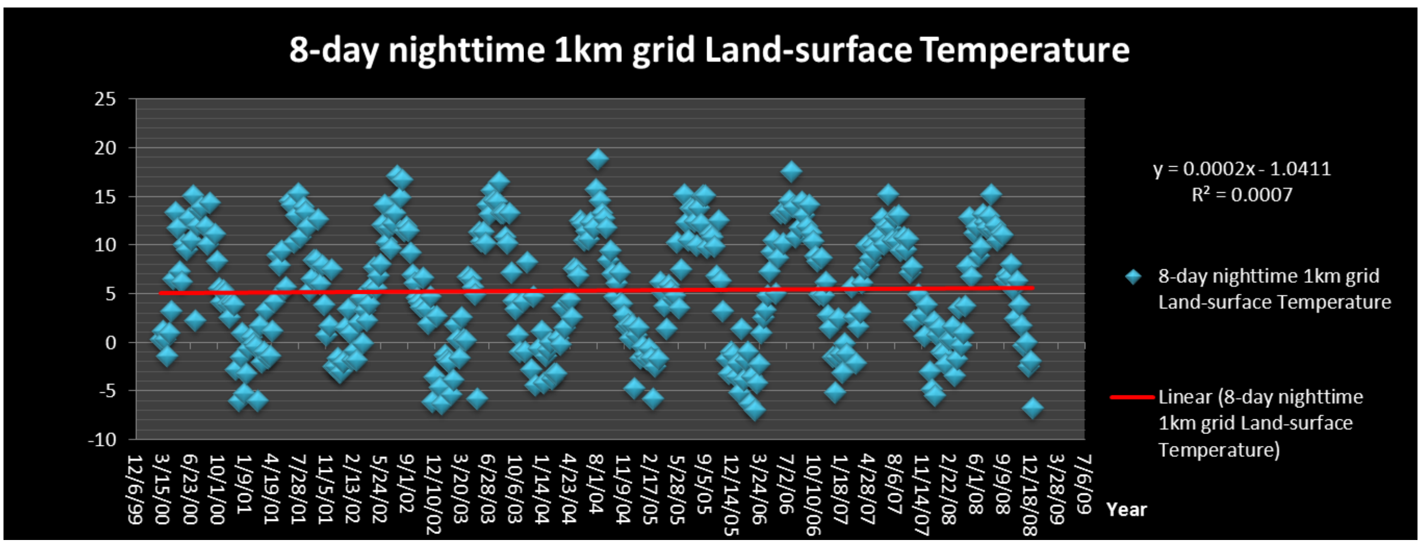

Latitude: 52.0292 Longitude: 4.20554 MODIS: mod11a2 Tile: h18v03 Cell (row, column): 956, 310

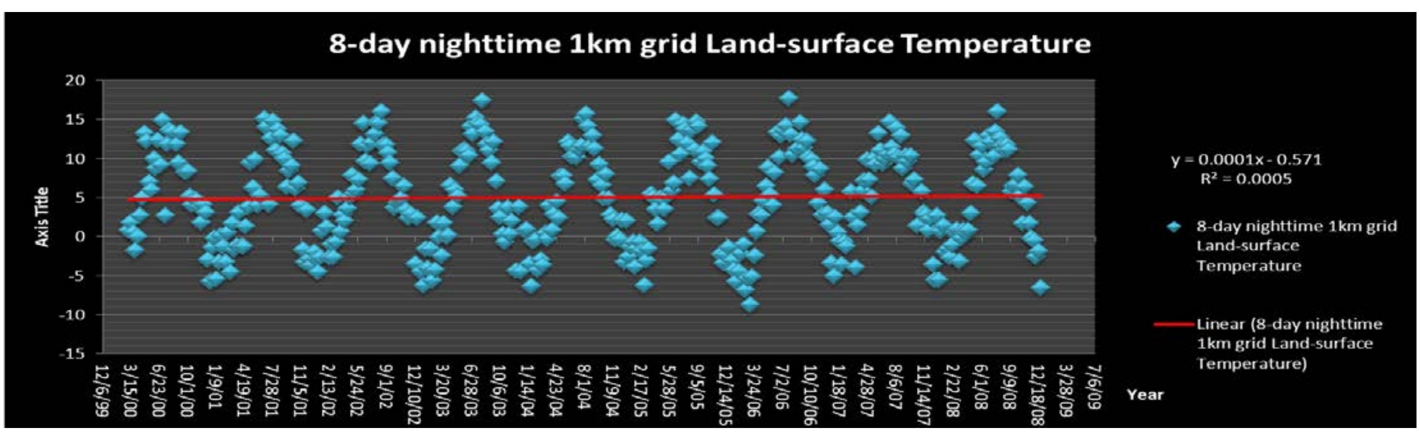

Latitude: 52.0208 Longitude: 4.19121 MODIS: mod11a2 Tile: h18v03 Cell (row, column): 957, 309

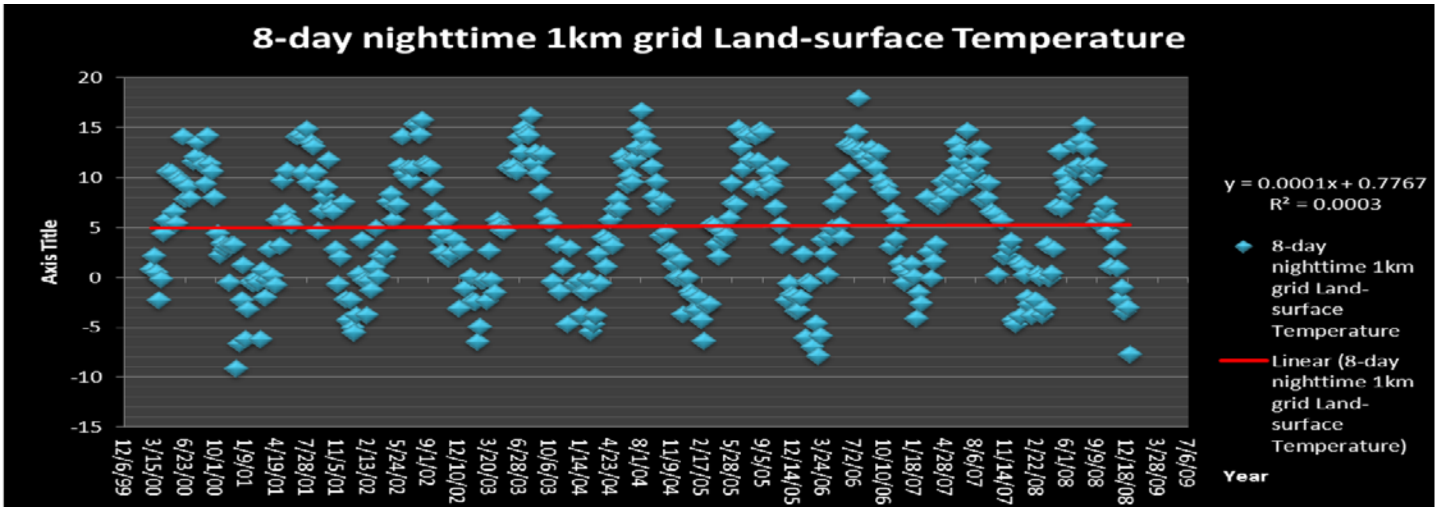

Latitude: 52.0125 Longitude: 4.24459 MODIS: mod11a2 Tile: h18v03 Cell (row, column): 958, 313

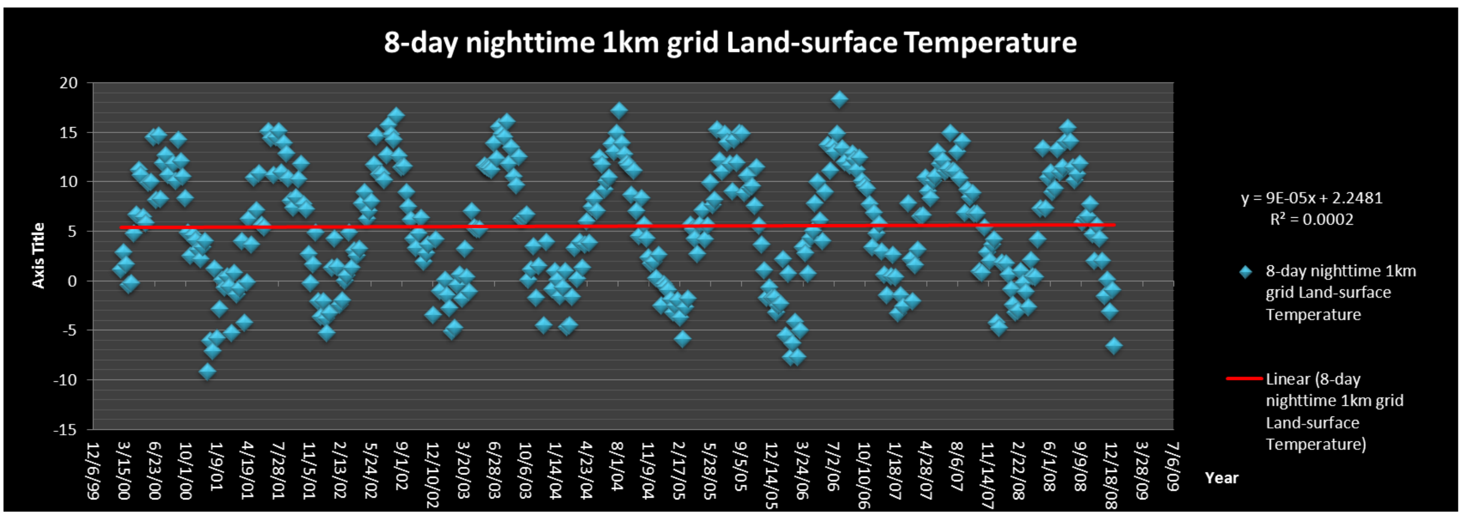

Latitude: 52.0042 Longitude: 4.2438 MODIS: mod11a2 Tile: h18v03 Cell (row, column): 959, 313

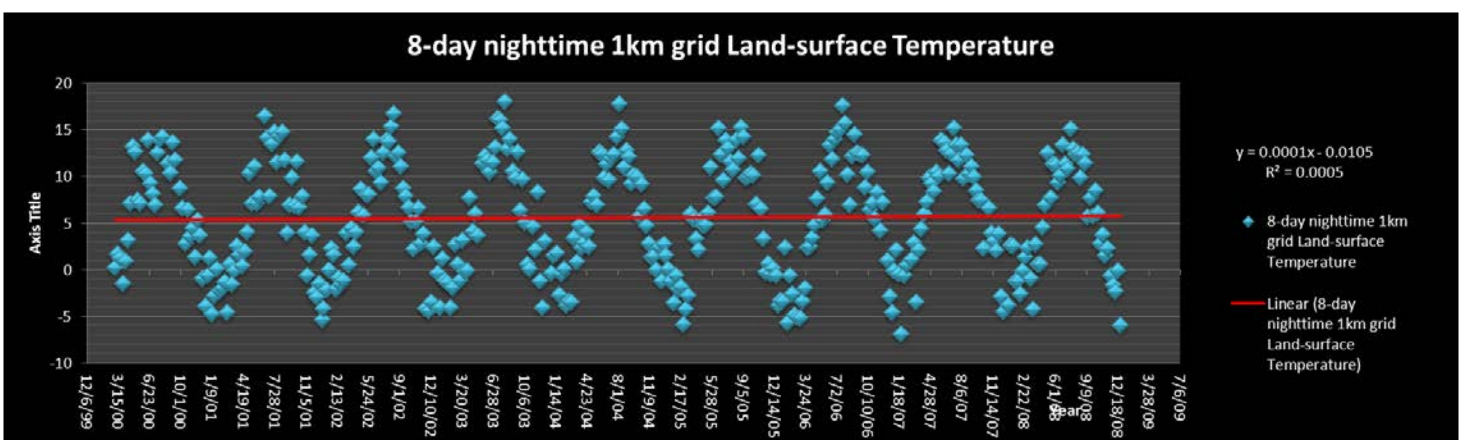

Latitude: 51.9875 Longitude: 4.1475 MODIS: mod11a2 Tile: h18v03 Cell (row, column): 961, 306

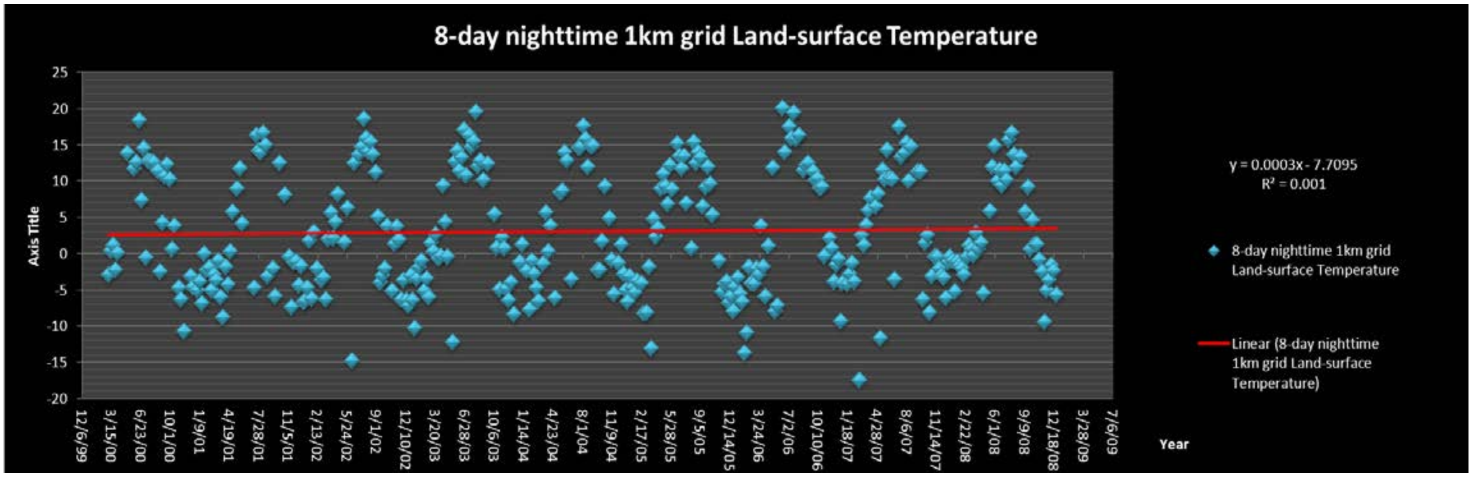

Latitude: 52.195800 Longitude: 5.66237 MODIS mod11a2 Tile: h18v03 Cell (row, column): 936, 416

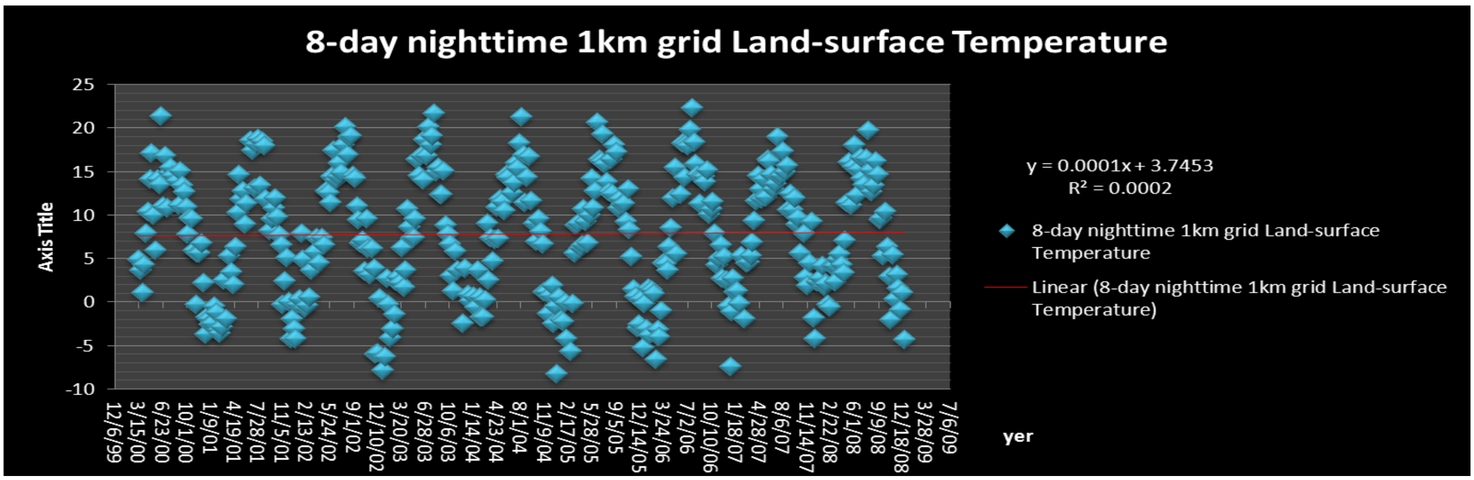

Latitude: 52.1042 Longitude: 4.33471 MODIS: mod11a2 Tile: h18v03 Year, Cell 947, 319

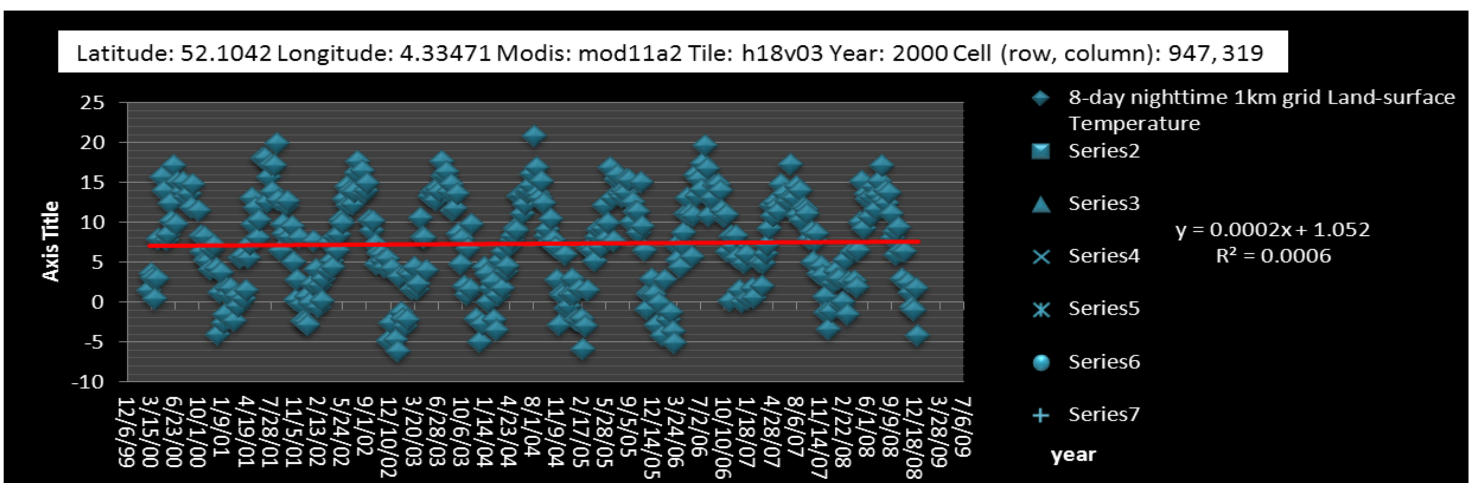

Latitude: 51.5708 Longitude: 5.08811 MODIS: mod11a2 Tile: h18v03 Cell (row, column): 1011, 379

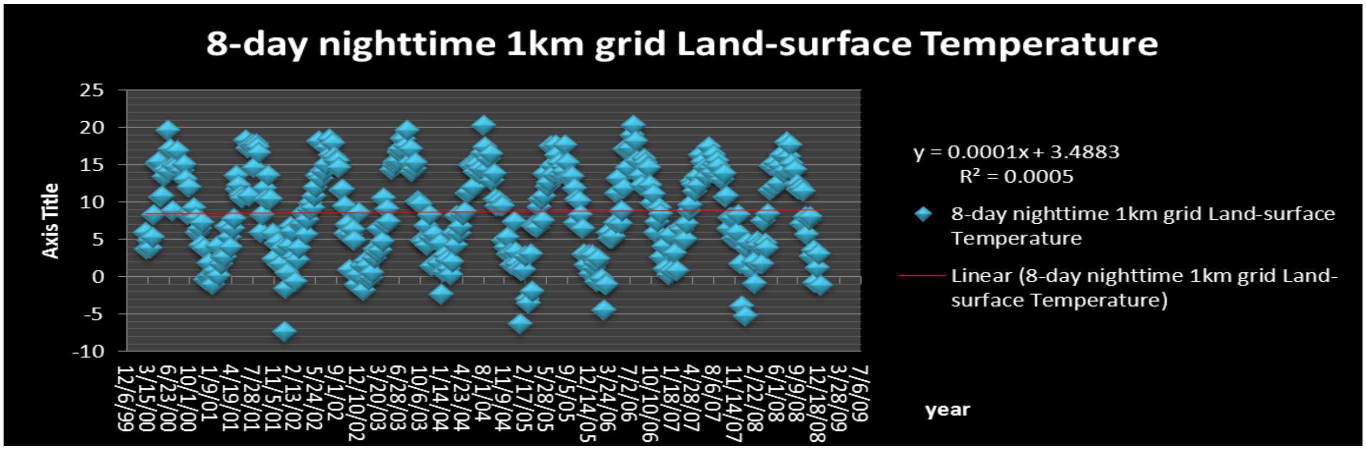

Latitude: 52.3125 Longitude: 6.93133 MODIS: mod11a2 Tile: h18v03 Year: 2000 Cell (row, column): 922, 508

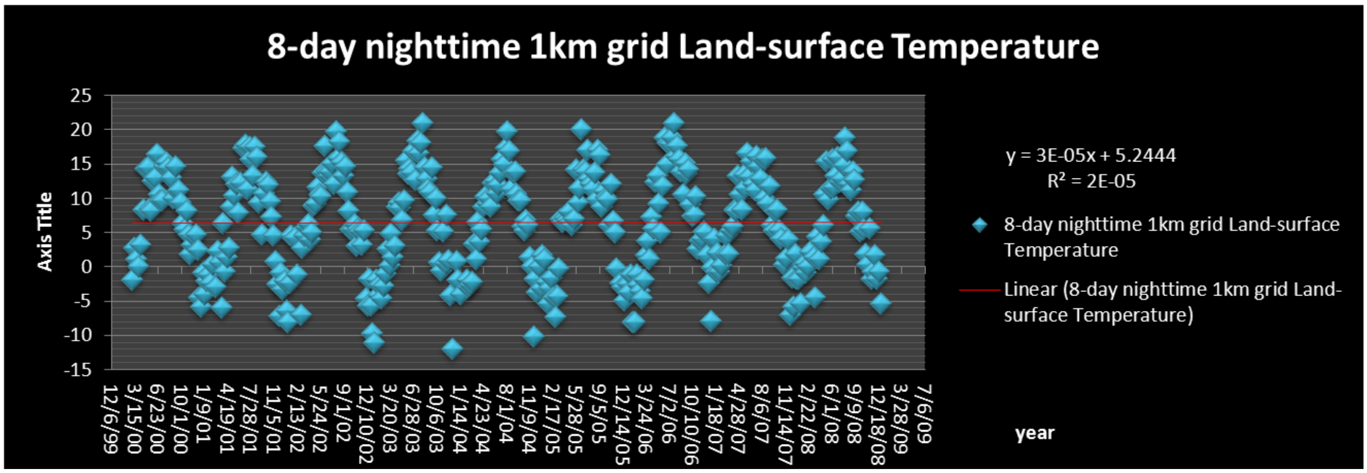

Latitude: 51.9458 Longitude: 4.10308 MODIS: mod11a2 Tile: h18v03 Year: 2000 Cell (row, column): 966, 303

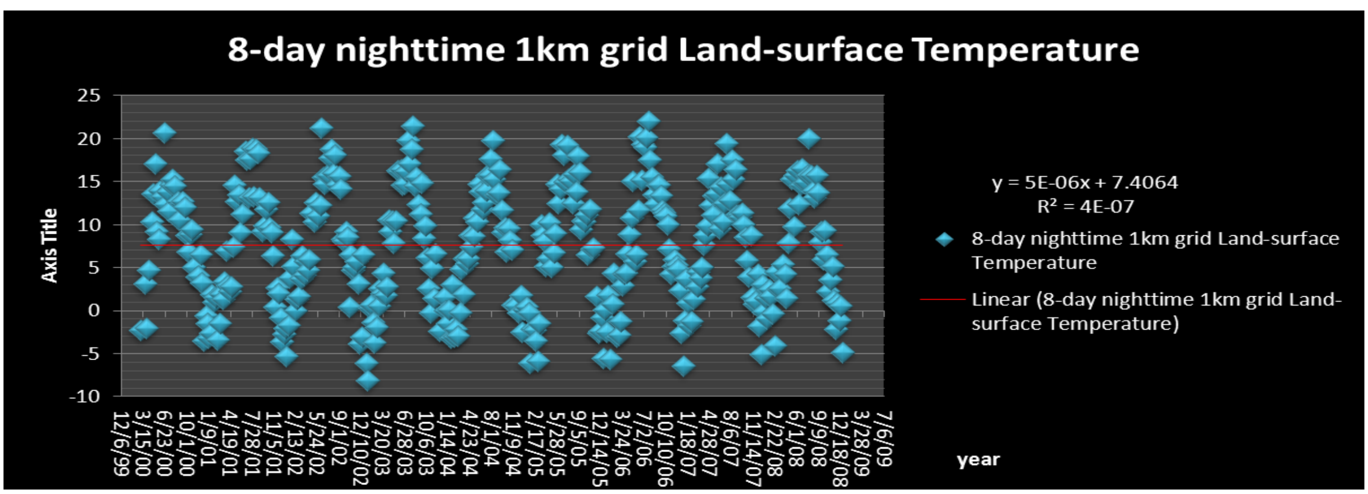

Latitude: 51.4875 Longitude: 5.66766 MODIS: mod11a2 Tile: h18v03 Year: 2000 Cell (row, column): 1021, 423

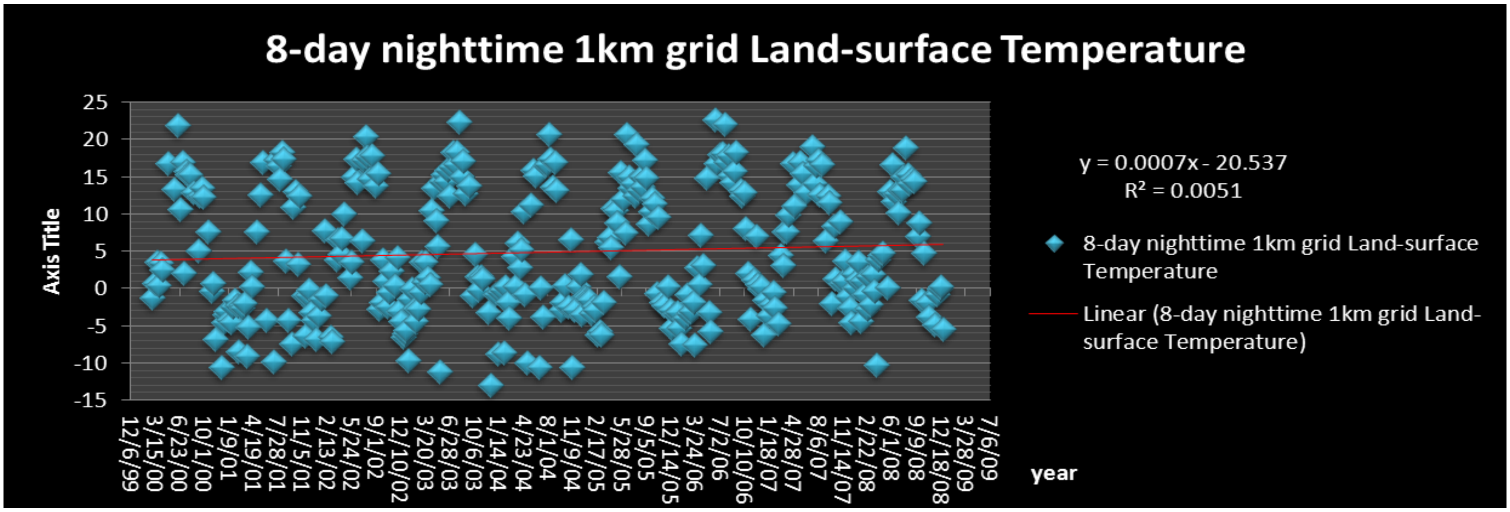

Latitude: 52.2125 Longitude: 5.9501 MODIS: mod11a2 Tile: h18v03 Year: 2000 Cell (row, column): 934, 437

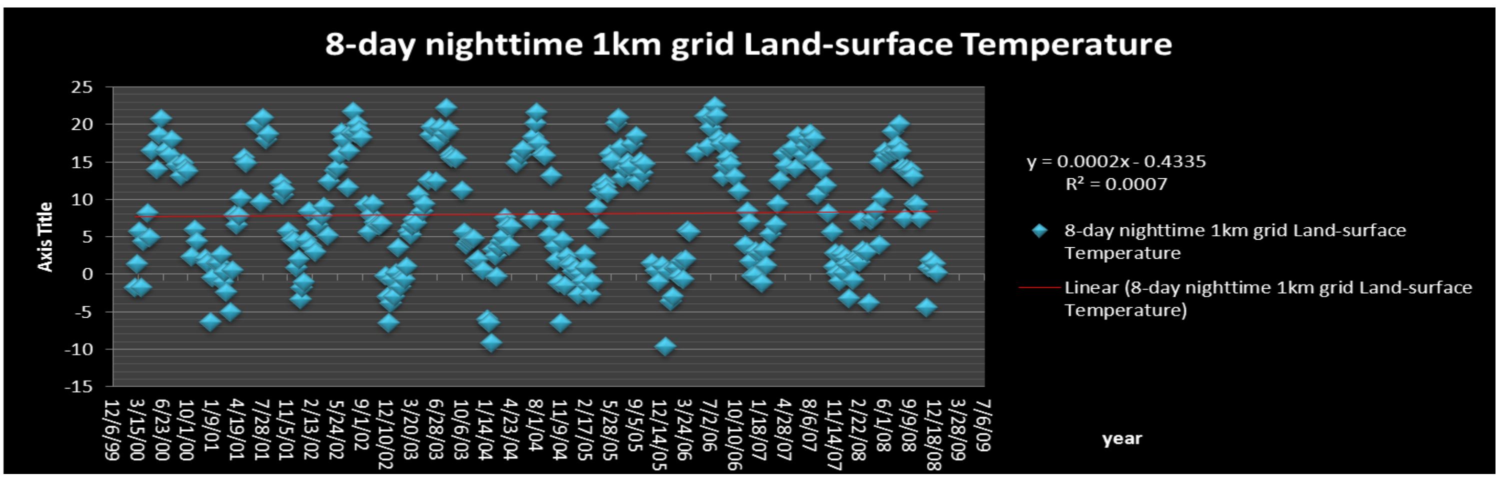

Latitude: 52.8875 Longitude: 5.80754 MODIS: mod11a2 Tile: h18v03 Year: 2000 Cell (row, column): 853, 420

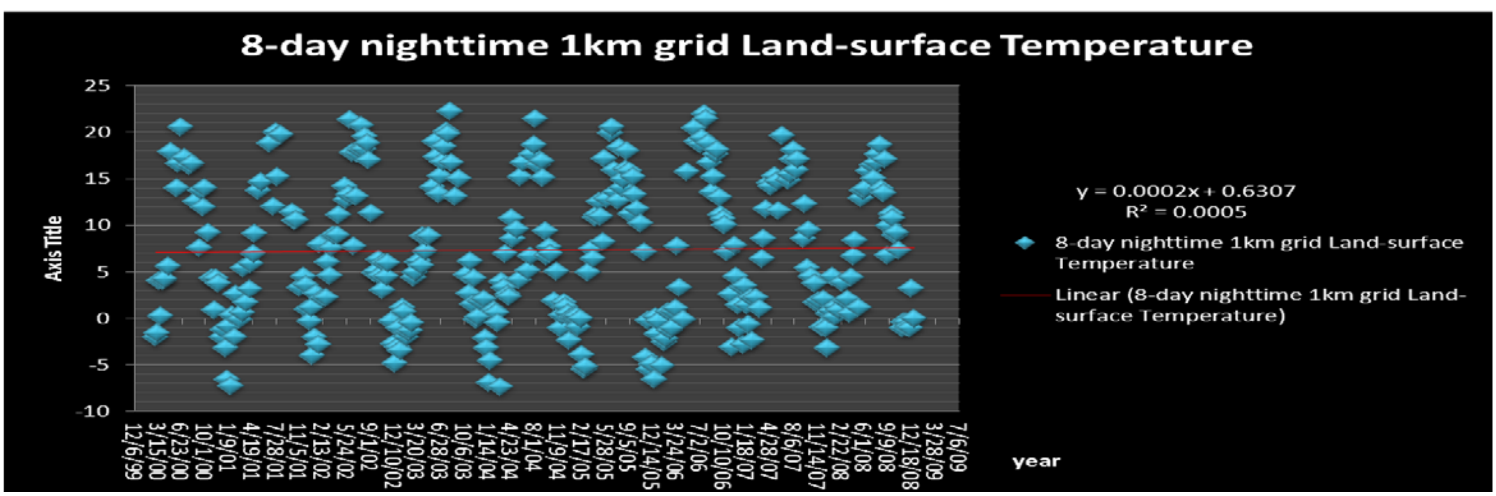

Latitude: 52.704200 Longitude: 6.05818 MODIS: mod11a2 Tile: h18v03 Year: 2000 Cell (row, column): 875, 440

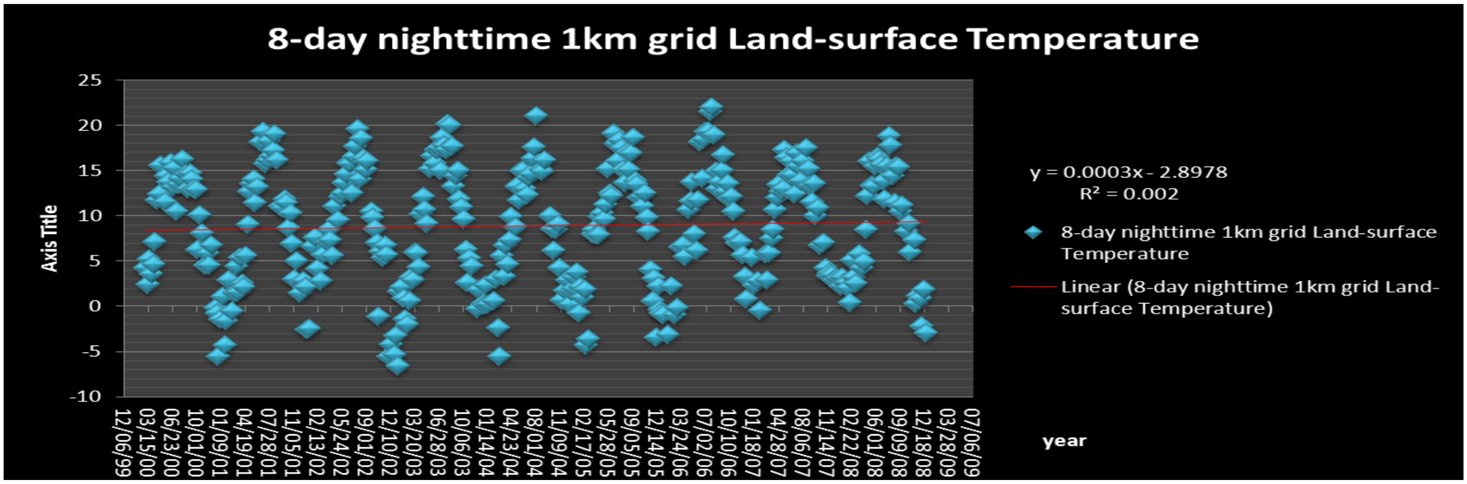

Latitude: 52.1958 Longitude: 4.65633 MODIS: mod11a2 Tile: h18v03 Year: 2000 Cell (row, column): 936, 342

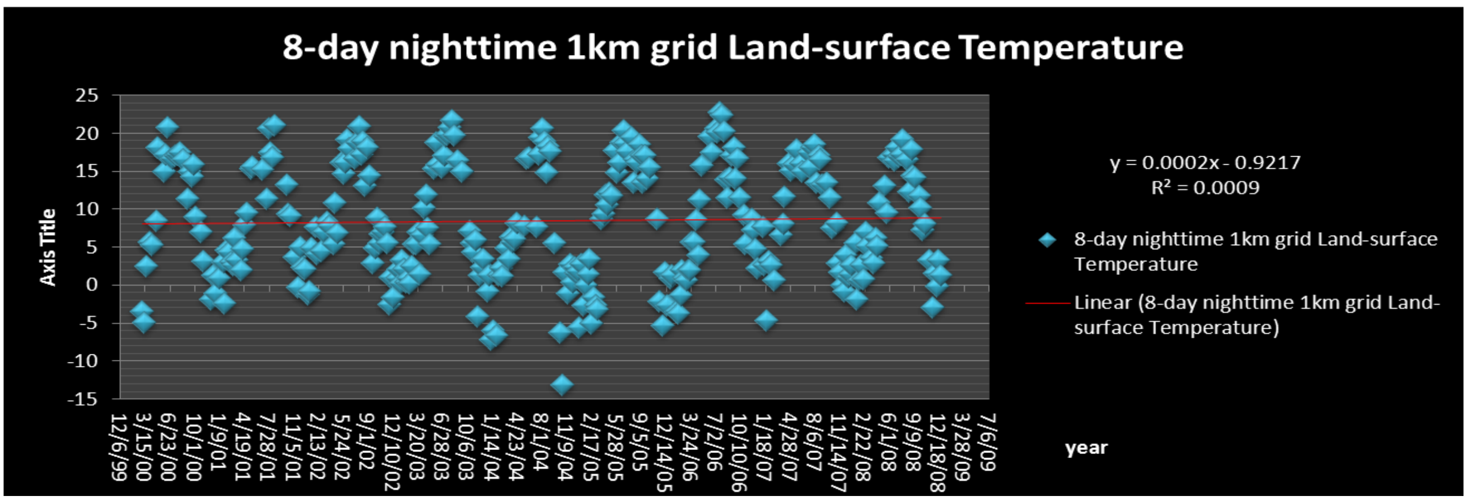

Latitude: 52.6042 Longitude: 5.7699 MODIS: mod11a2 Tile: h18v03 Year: 2000 Cell (row, column): 887, 420

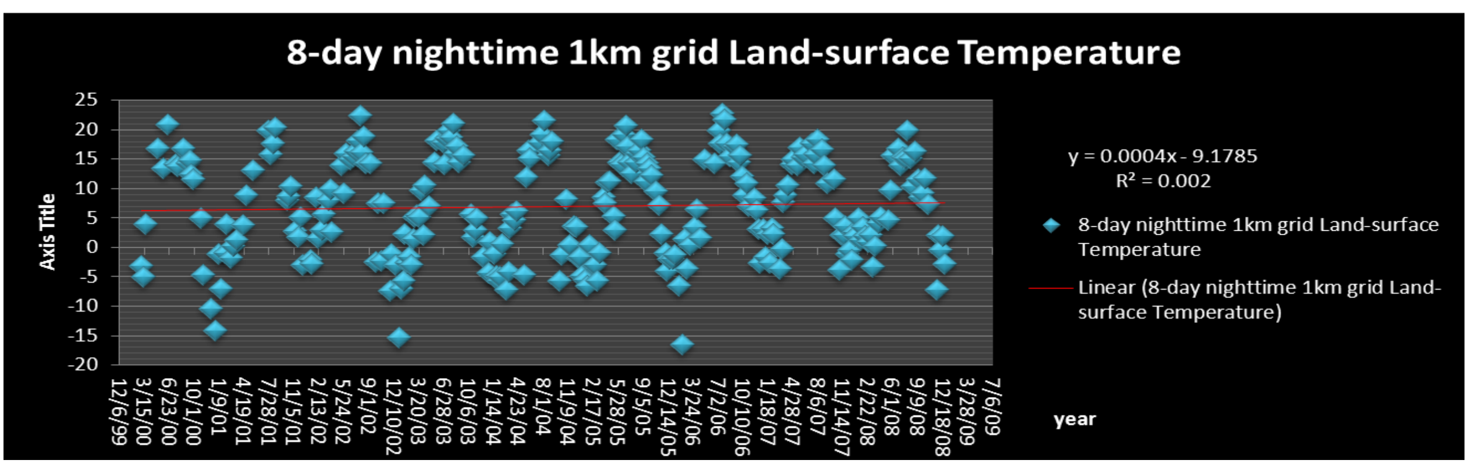

Latitude: 52.3875 Longitude: 5.65962 MODIS: mod11a2 Tile: h18v03 Year: 2000 Cell (row, column): 913, 414

Group 4

Land use change maps

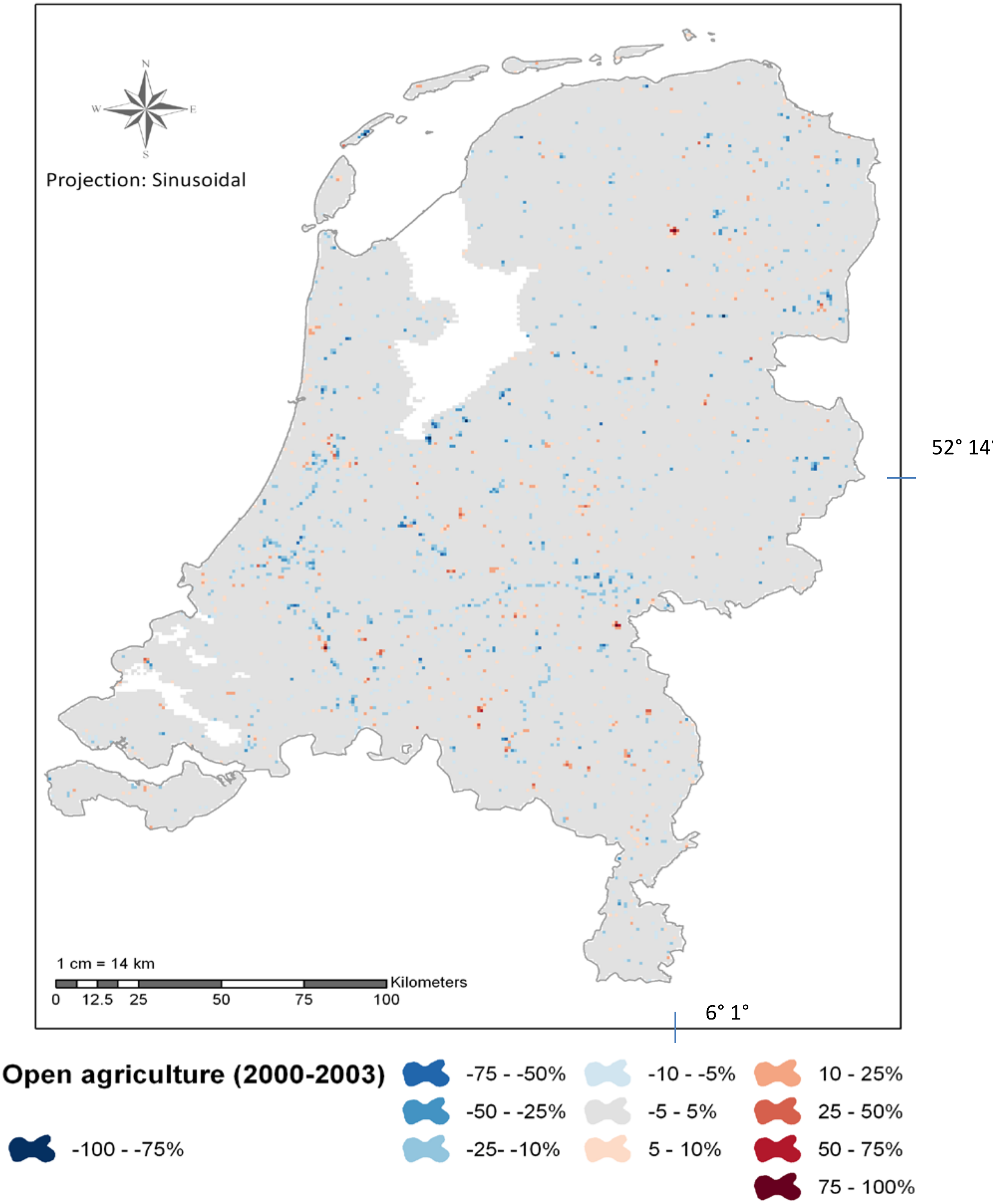

Figure 1 - Open agriculture change map from 2000 to 2003.

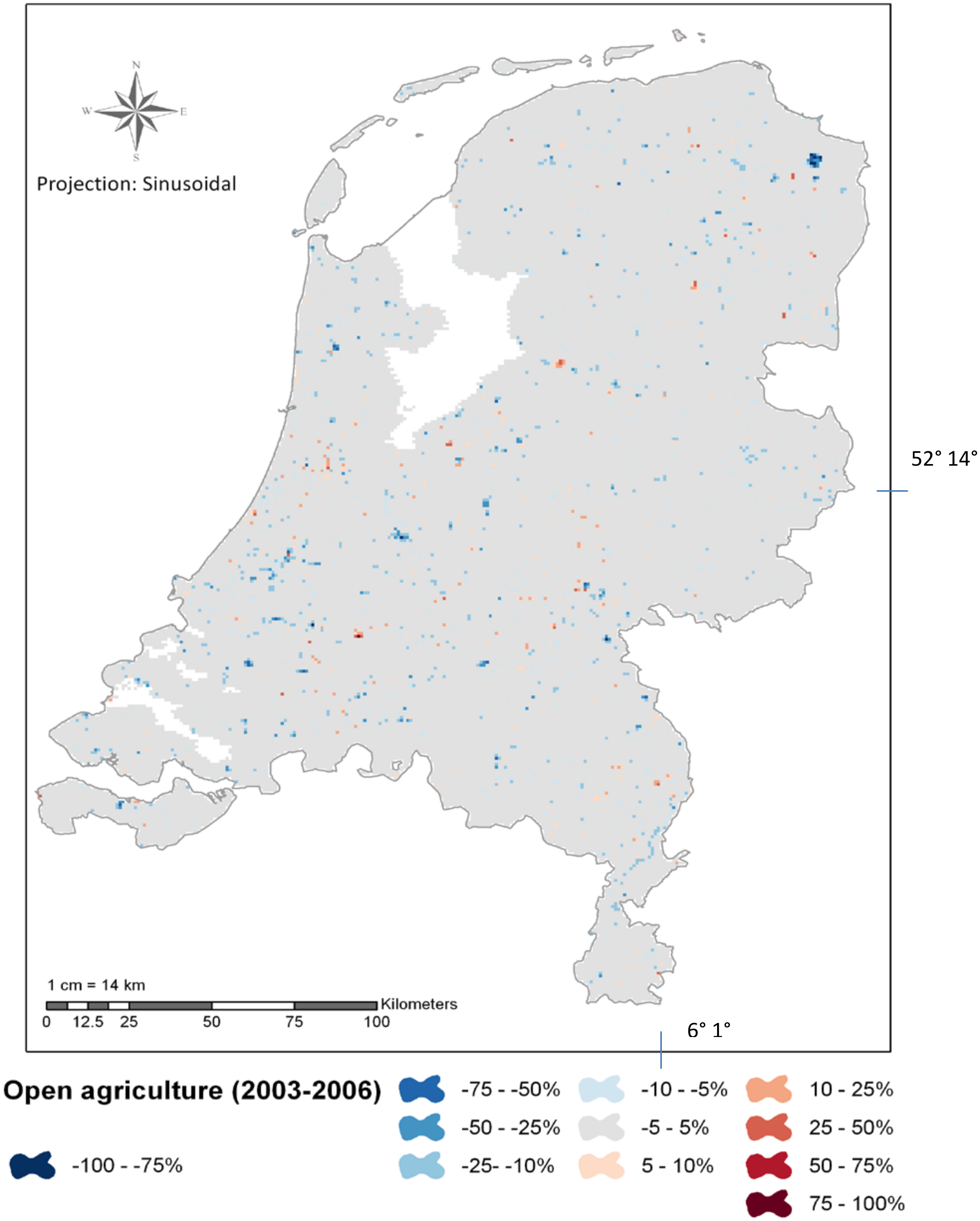

Figure 2 - Open agriculture change map from 2003 to 2006.

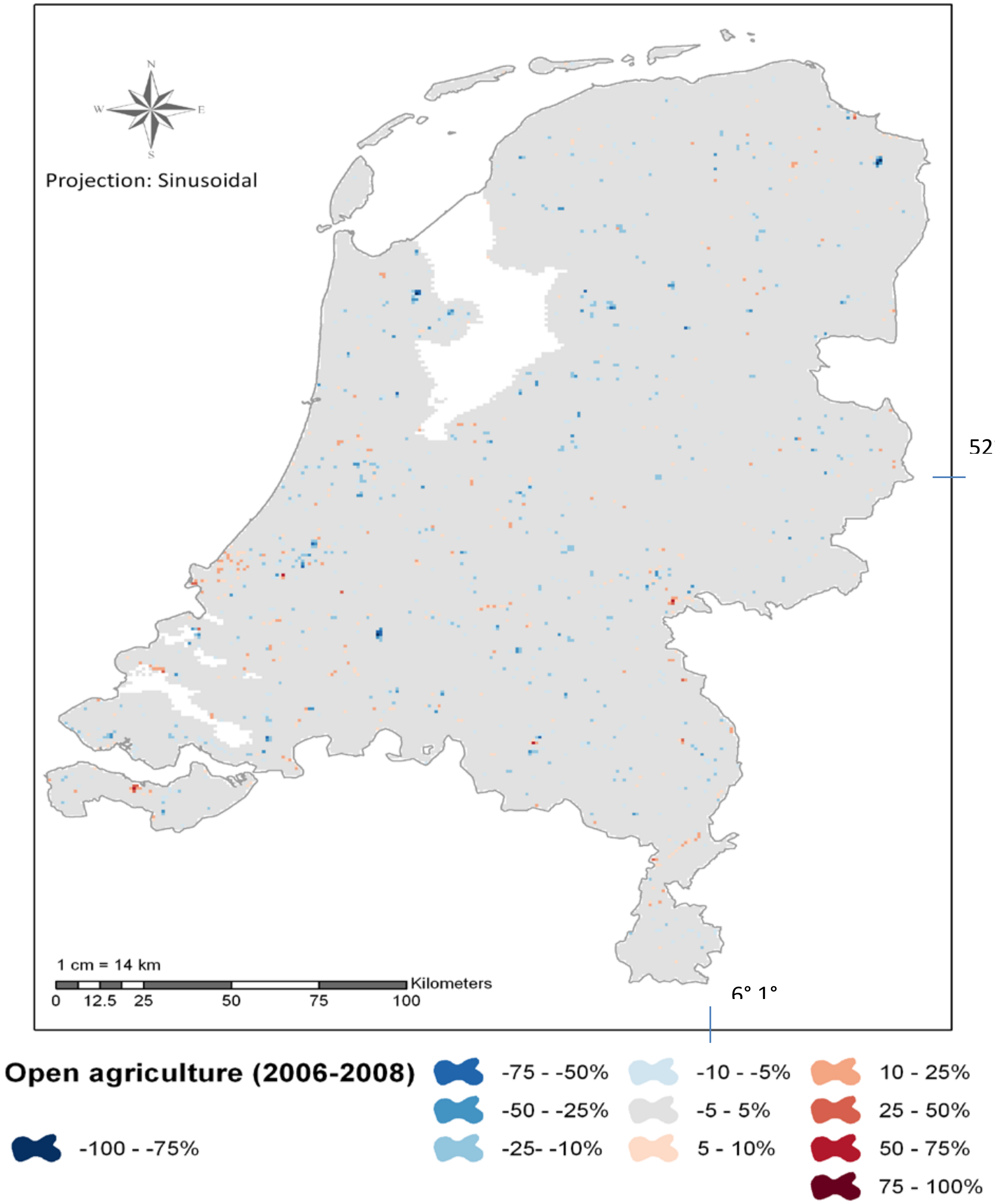

Figure 3 - Open agriculture change map from 2006 to 2008.

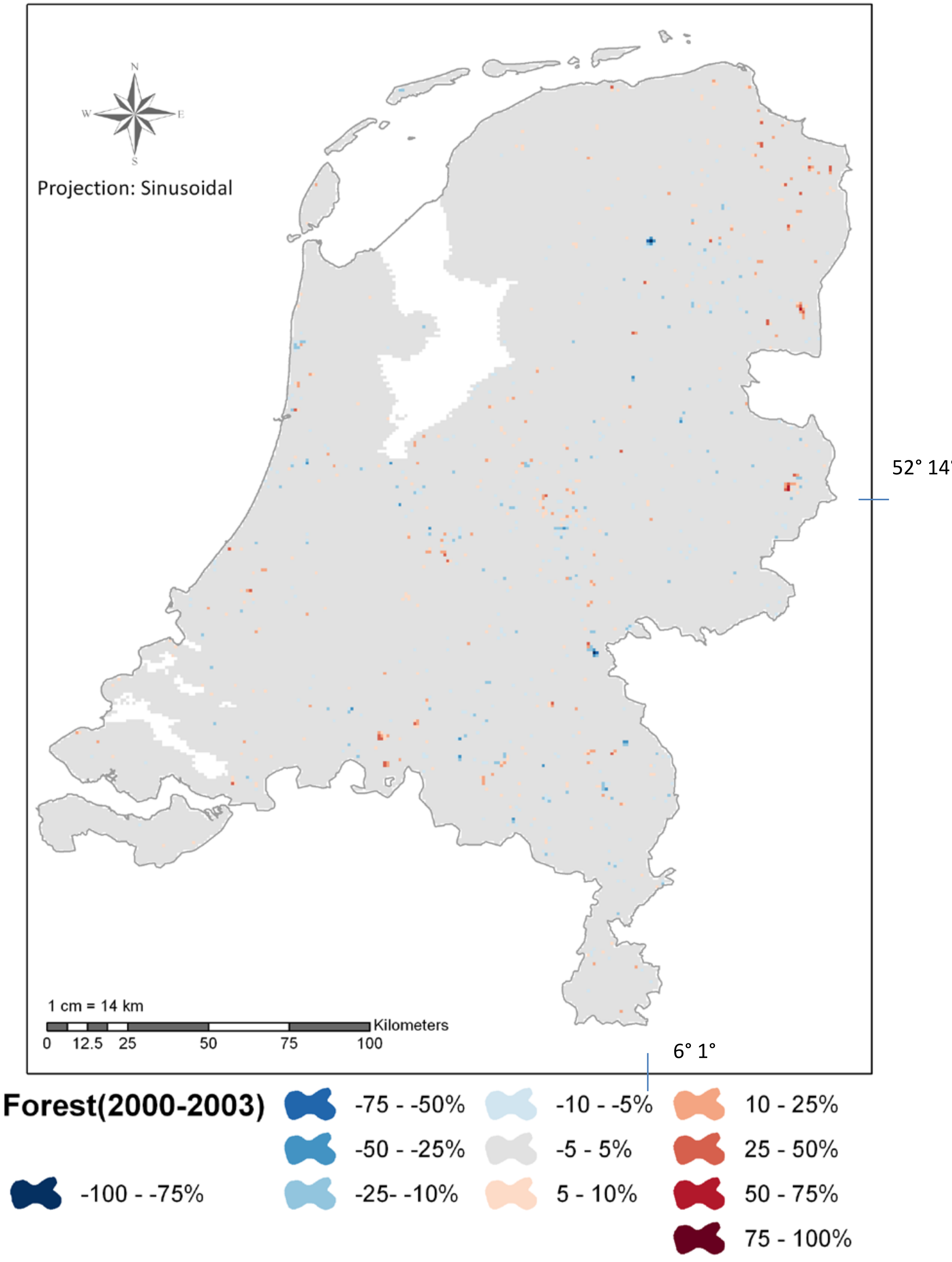

Figure 4 - Forest change map from 2000 to 2003.

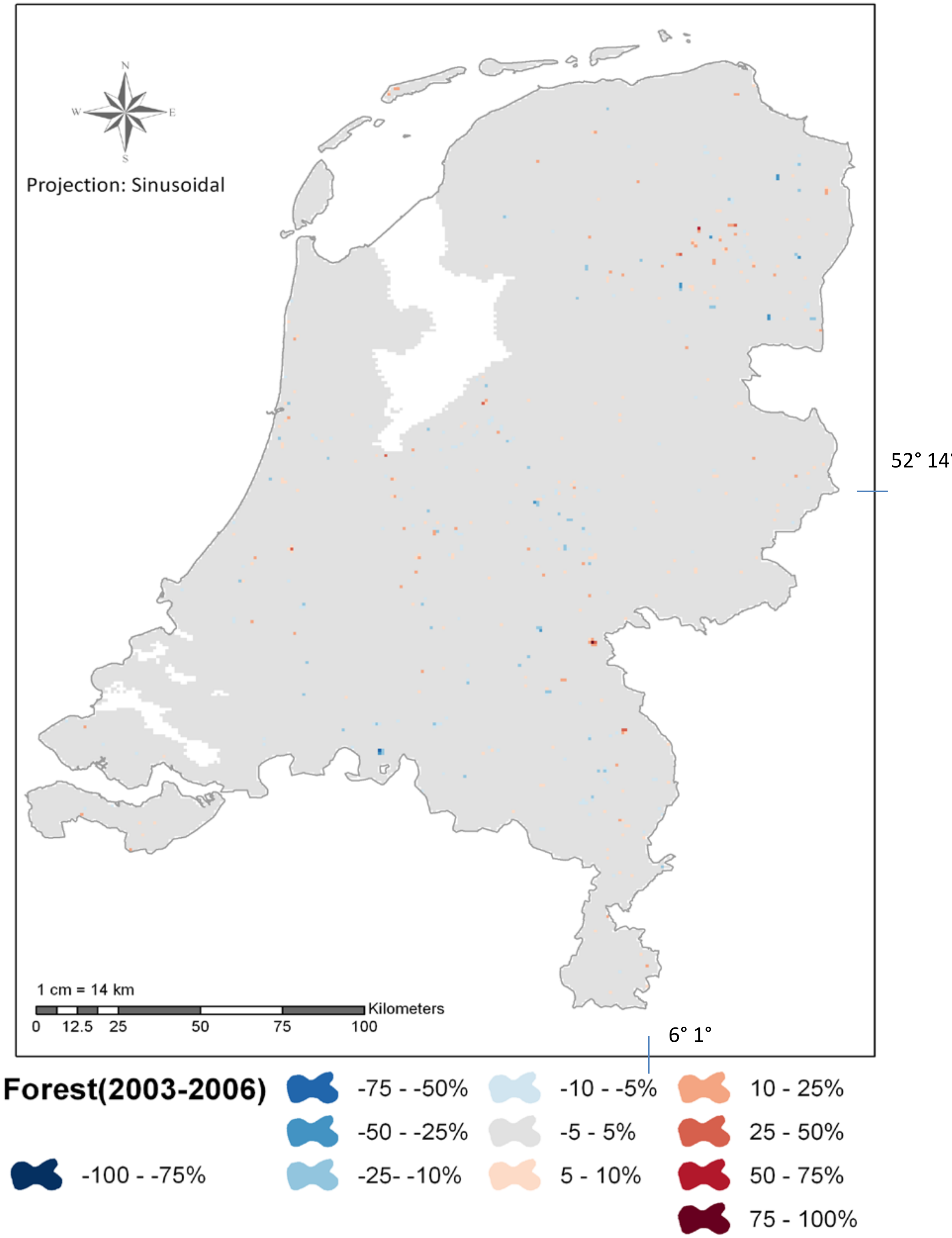

Figure 5 - Forest change map from 2003 to 2006.

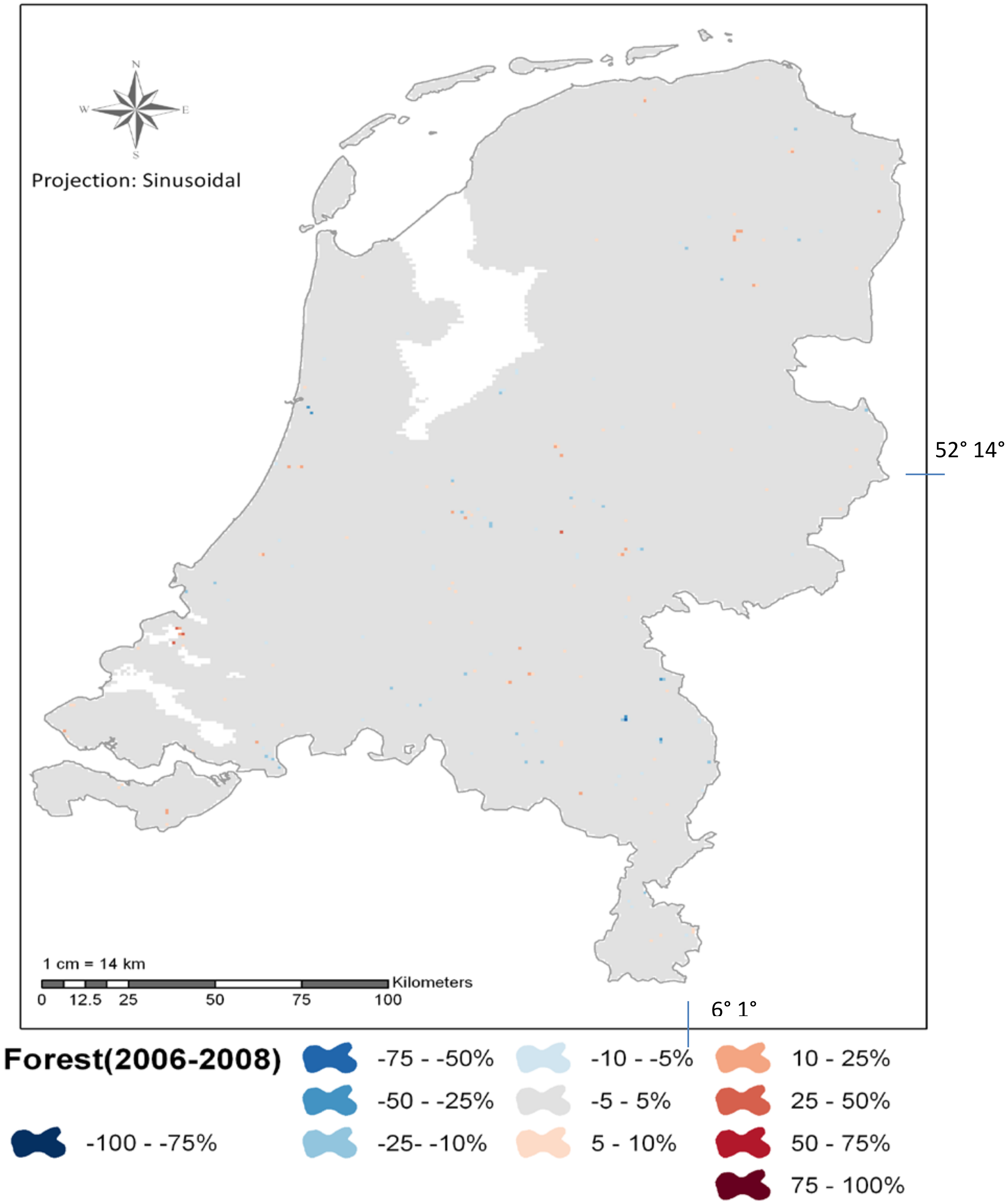

Figure 6 - Forest change map from 2006 to 2008.

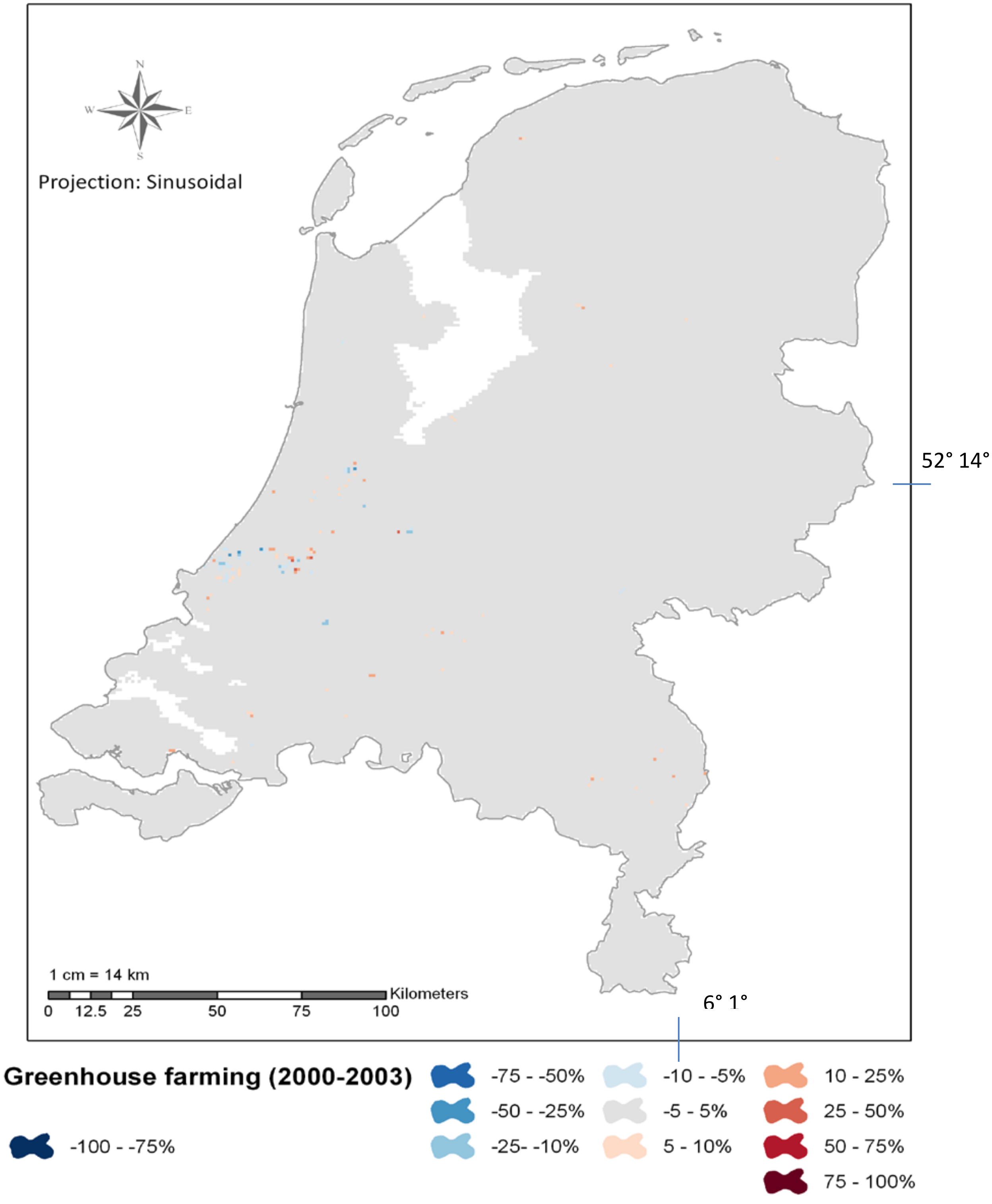

Figure 7 - Greenhouse farming change map from 2000 to 2003.

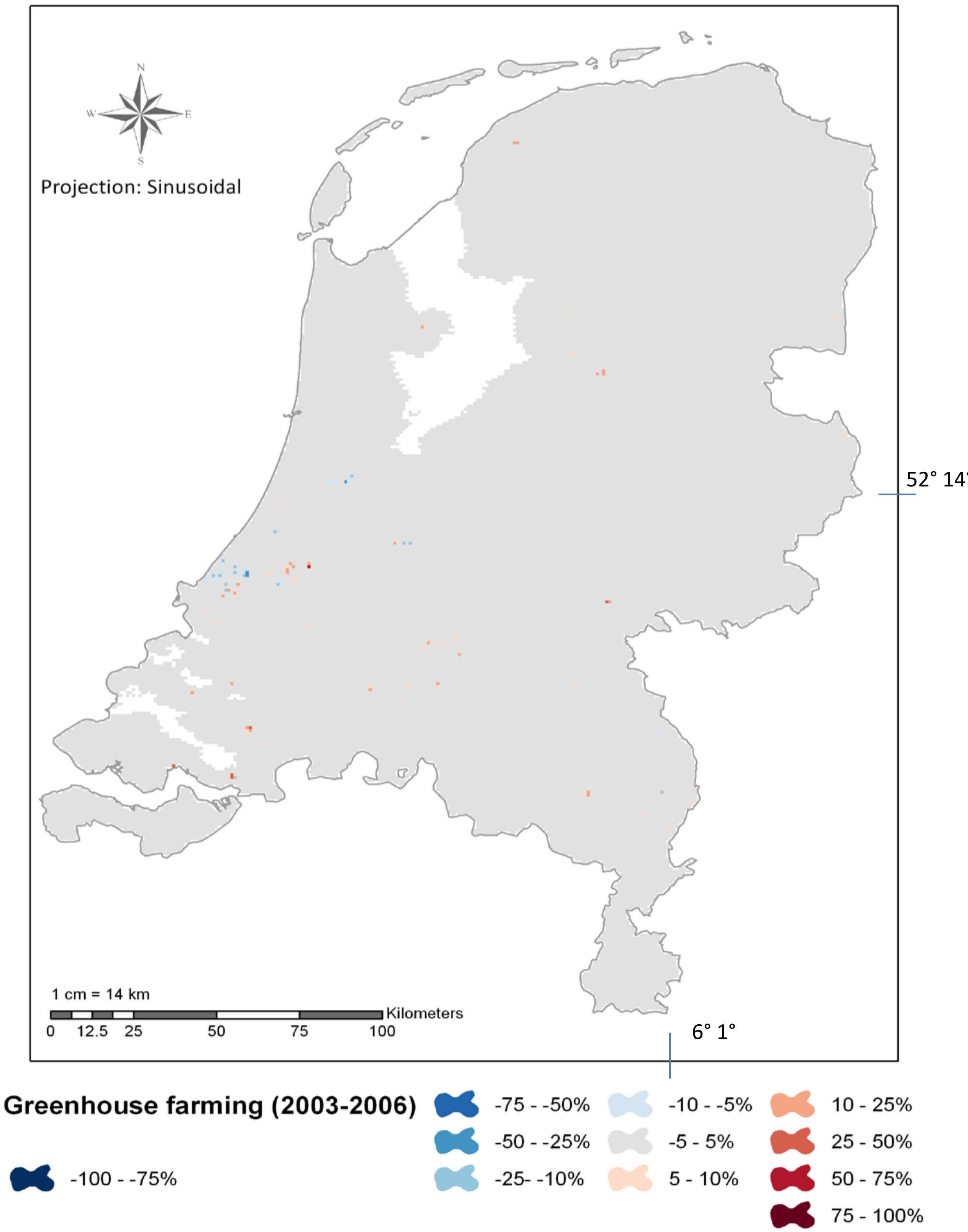

Figure 8 - Greenhouse farming change map from 2003 to 2006.

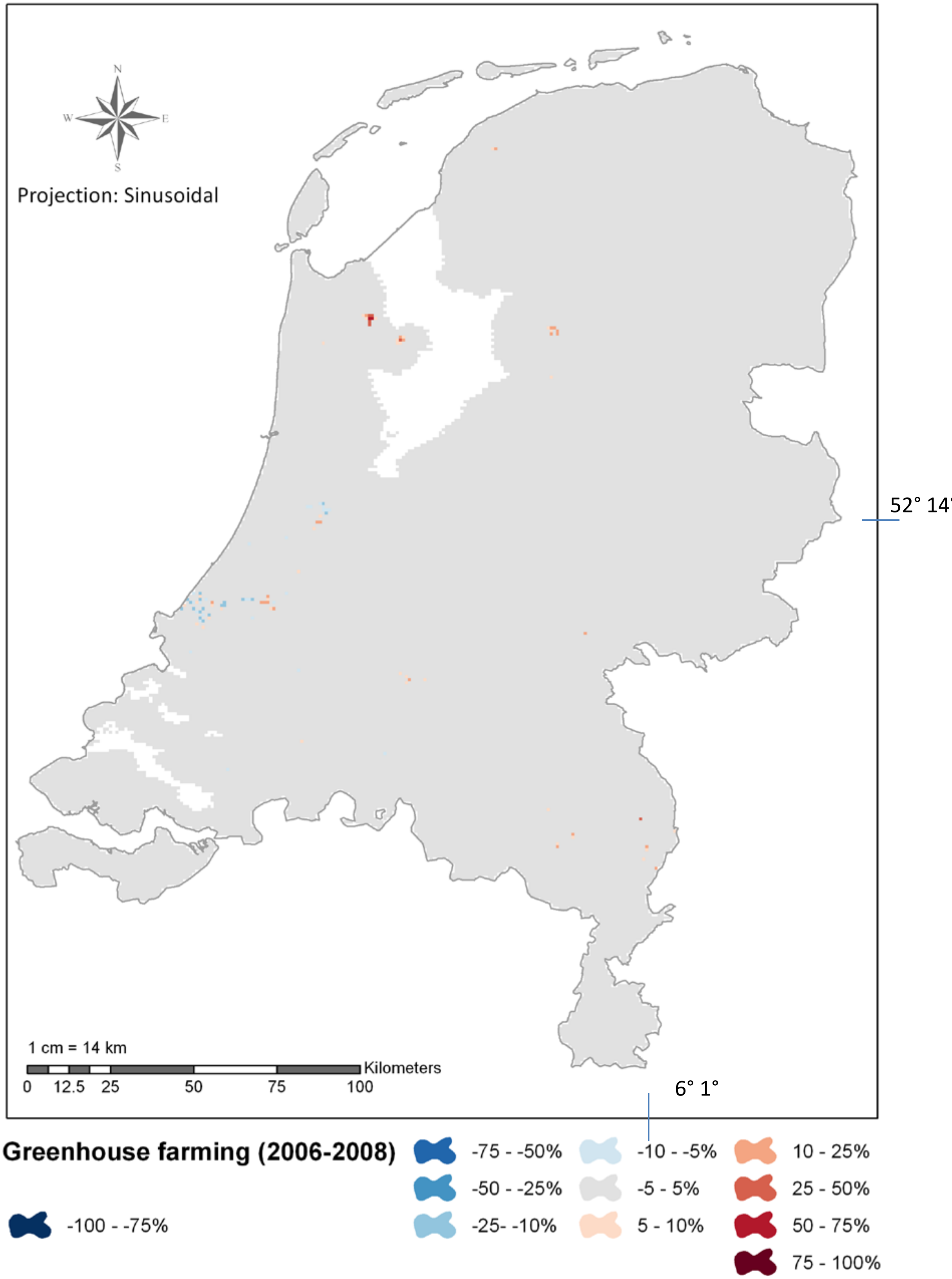

Figure 9 - Greenhouse farming change map from 2006 to 2008.

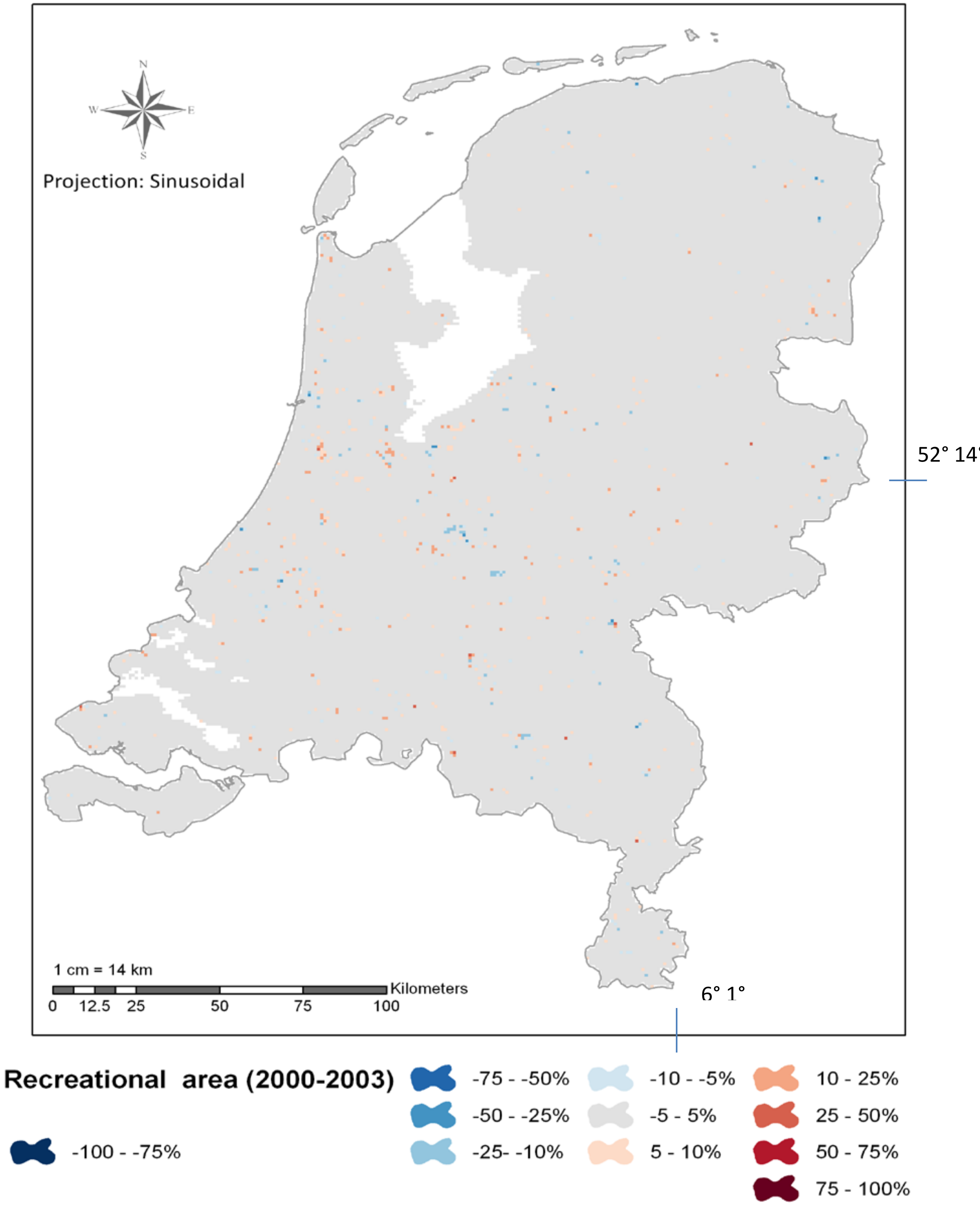

Figure 10 - Recreation area change map from 2000 to 2003.

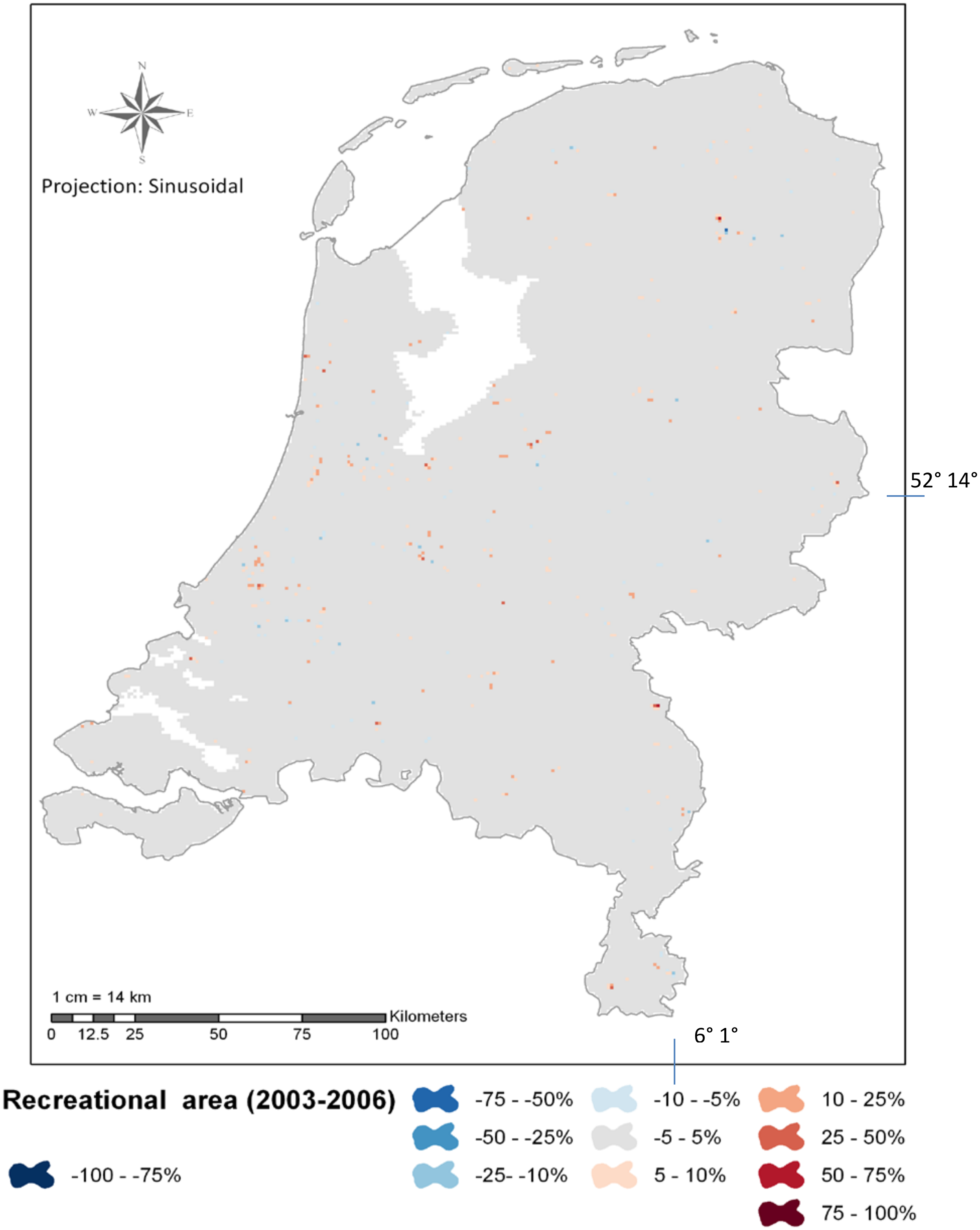

Figure 11 - Recreation area change map from 2003 to 2006.

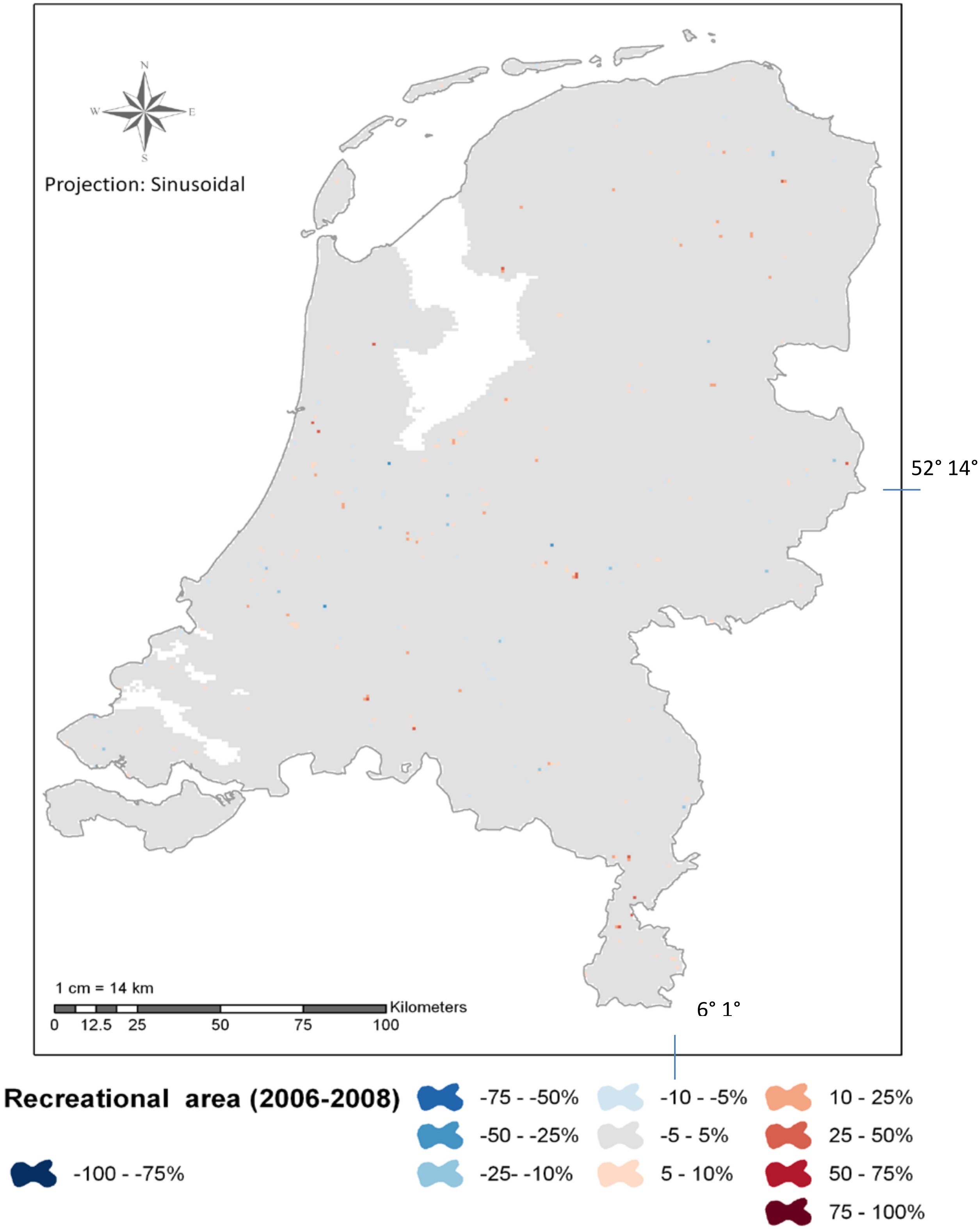

Figure 12 - Recreation area change map from 2006 to 2008.

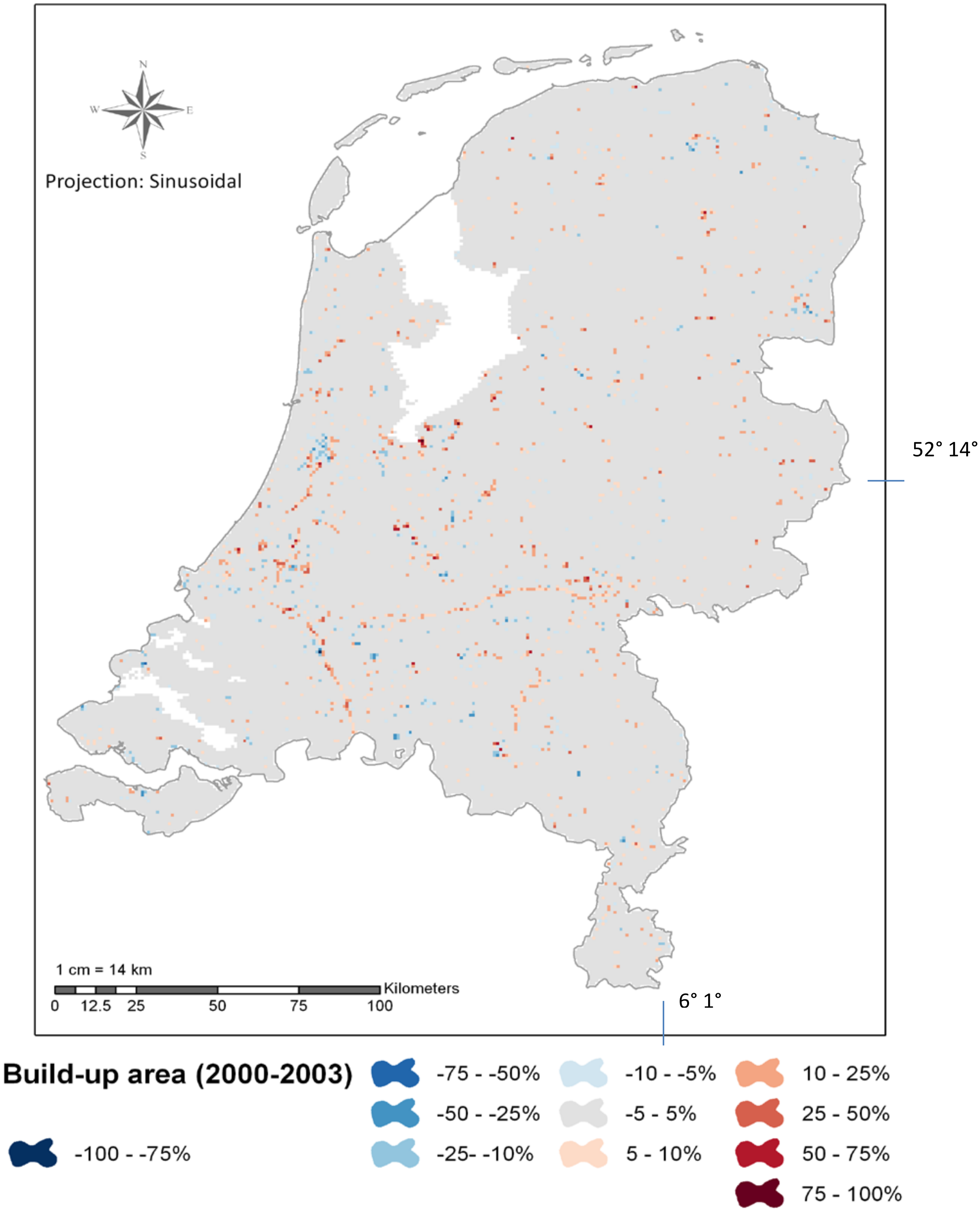

Figure 13 - Build-up area change map from 2000 to 2003.

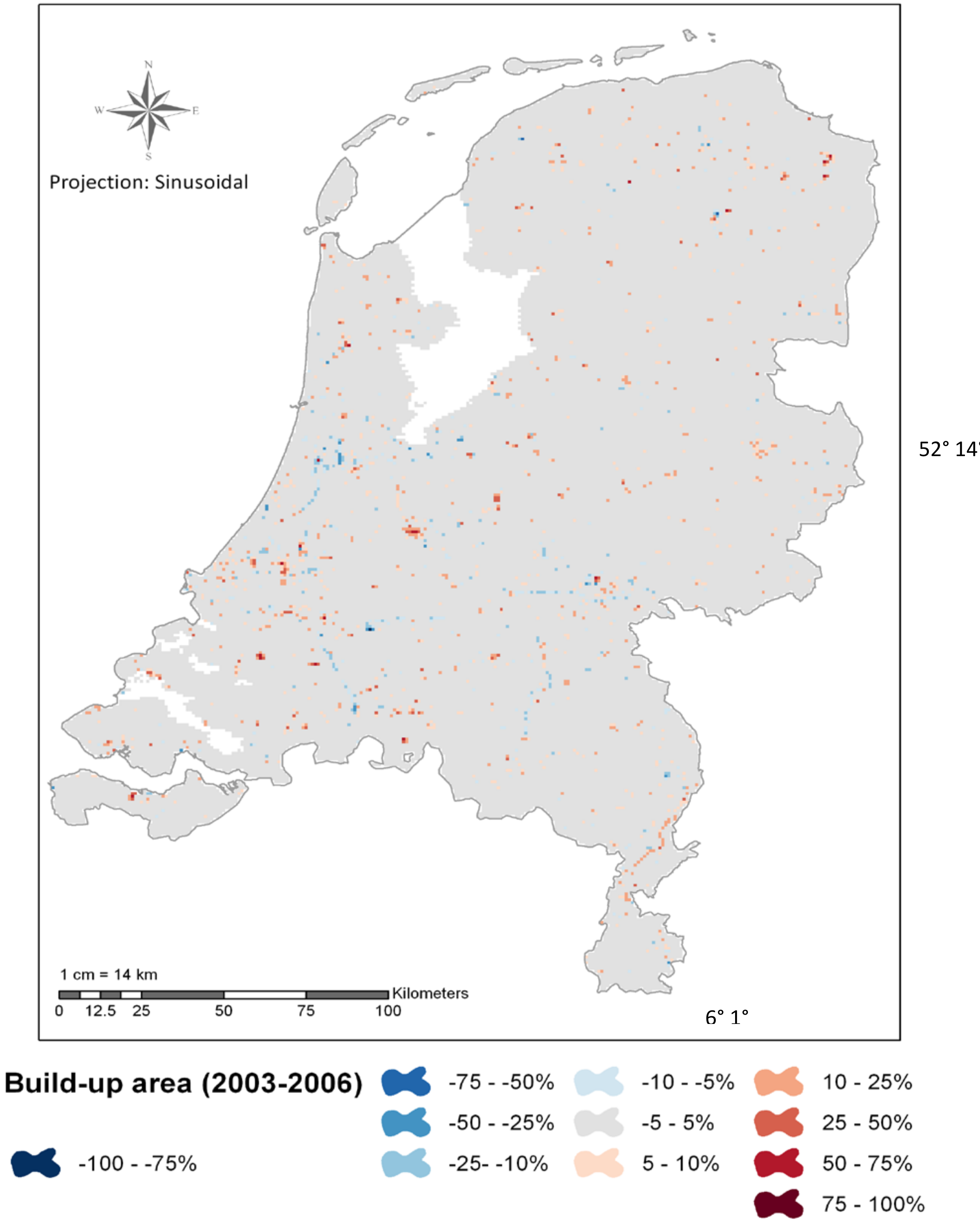

Figure 14 - Build-up area change map from 2003 to 2006.

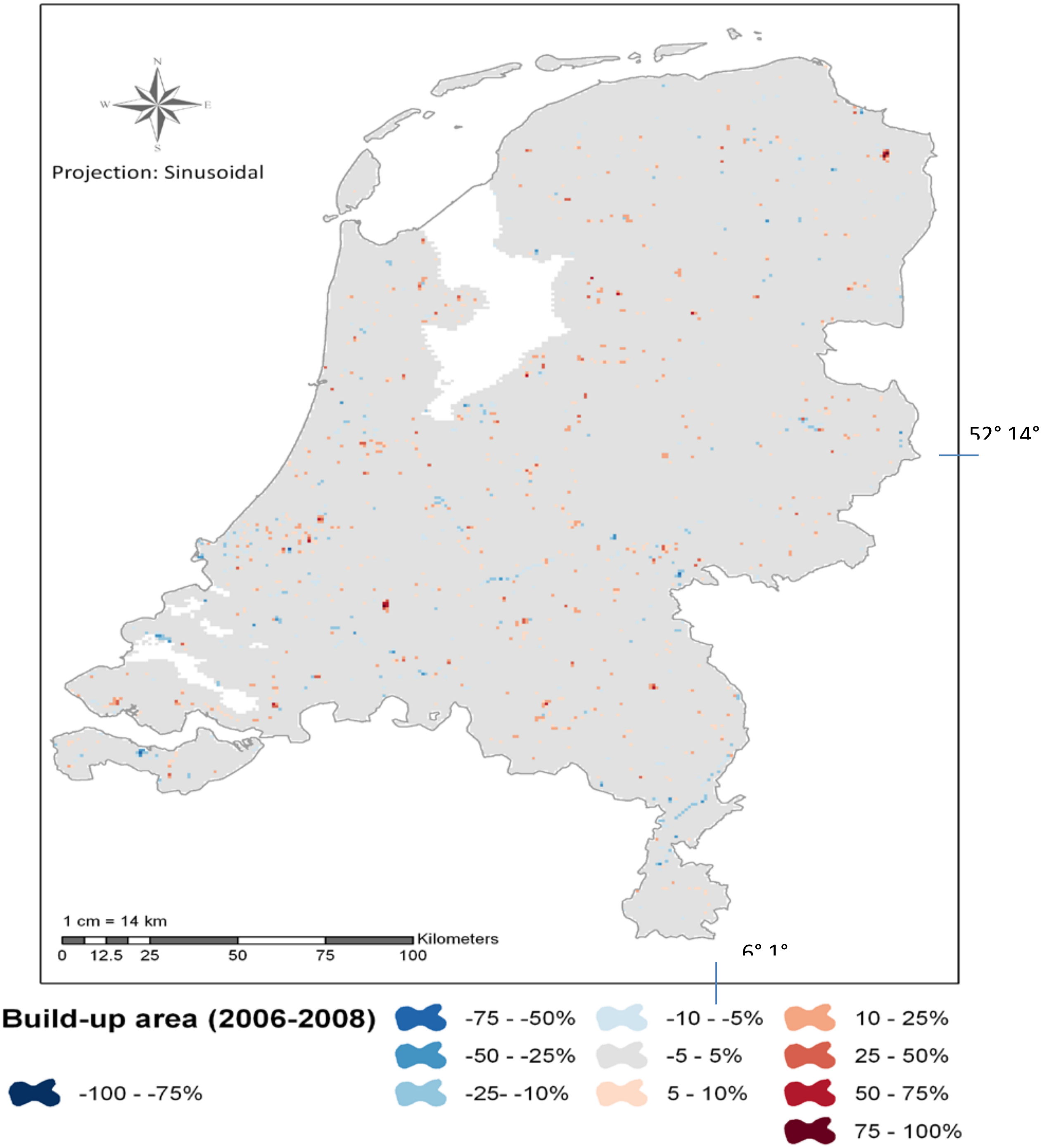

Figure 15 - Build-up area change map from 2006 to 2008.

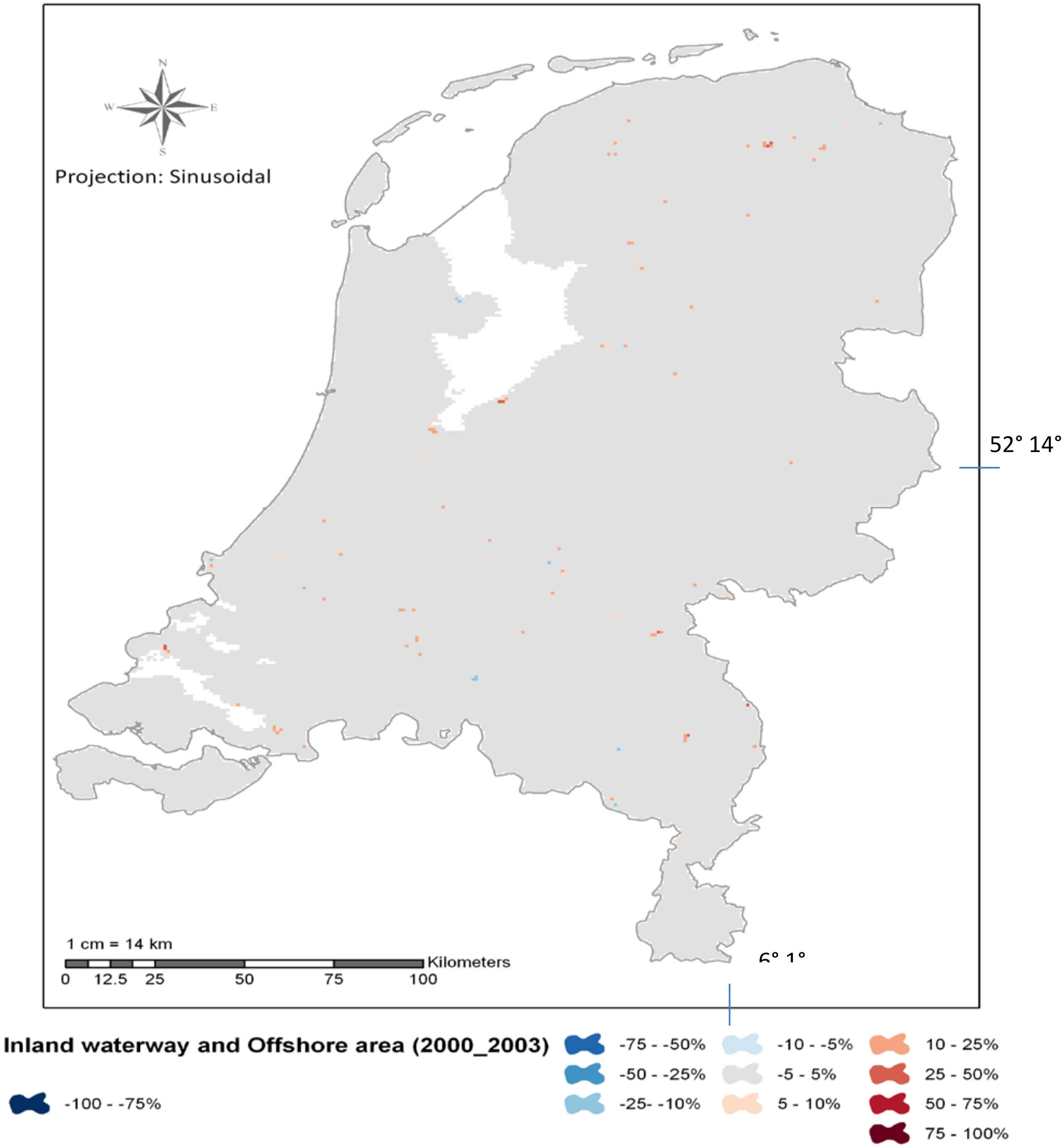

Figure 16 - Inland waterway and offshore area change map from 2000 to 2003.

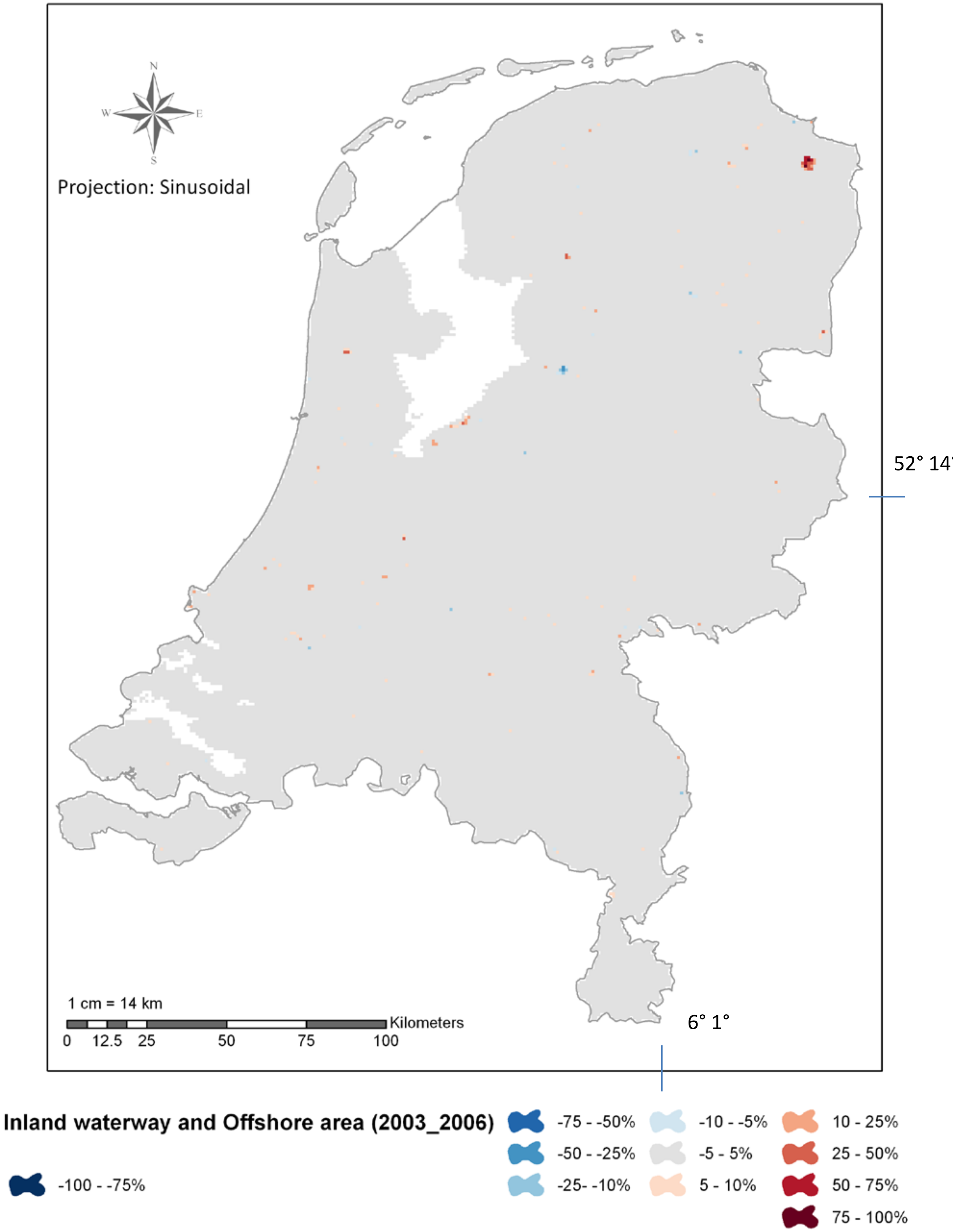

Figure 17 - Inland waterway and offshore area change map from 2003 to 2006.

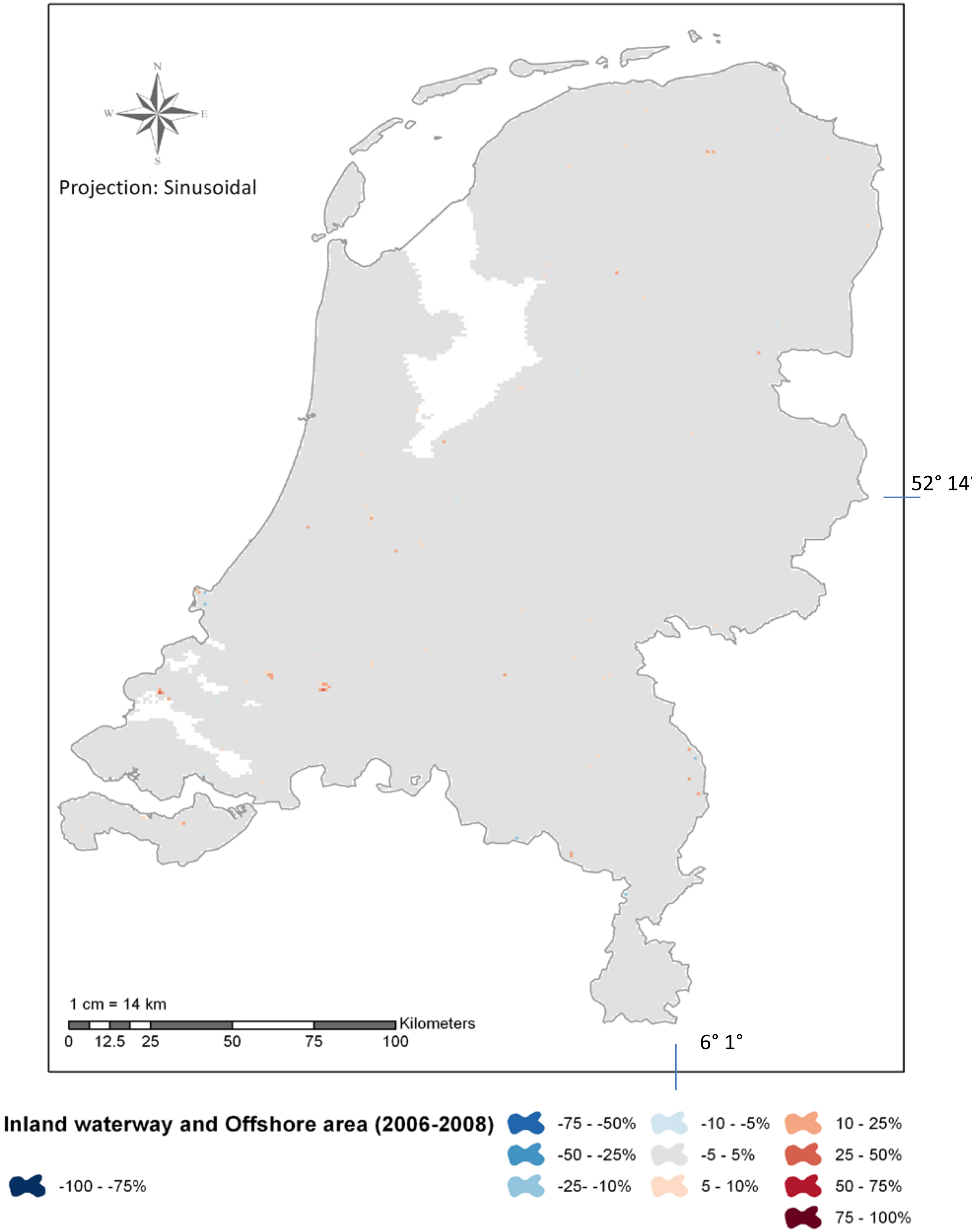

Figure 18 - Inland waterway and offshore area change map from 2006 to 2008.

Group 5

LST Aggregation analyses, spatial mean

Province scale, years 2003, 2008

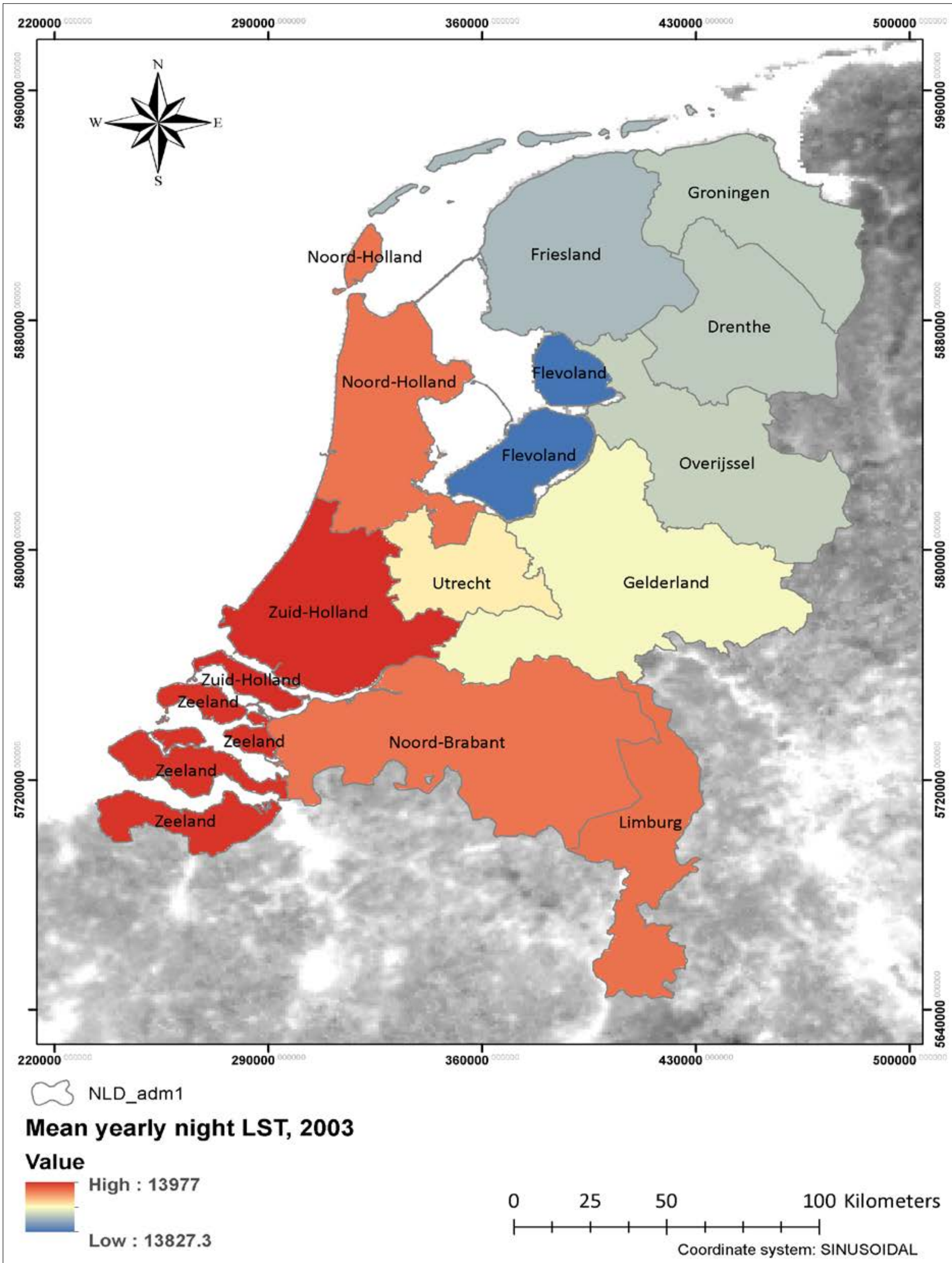

The up-scaled mean yearly night LST mean to Dutch province scale, 2003

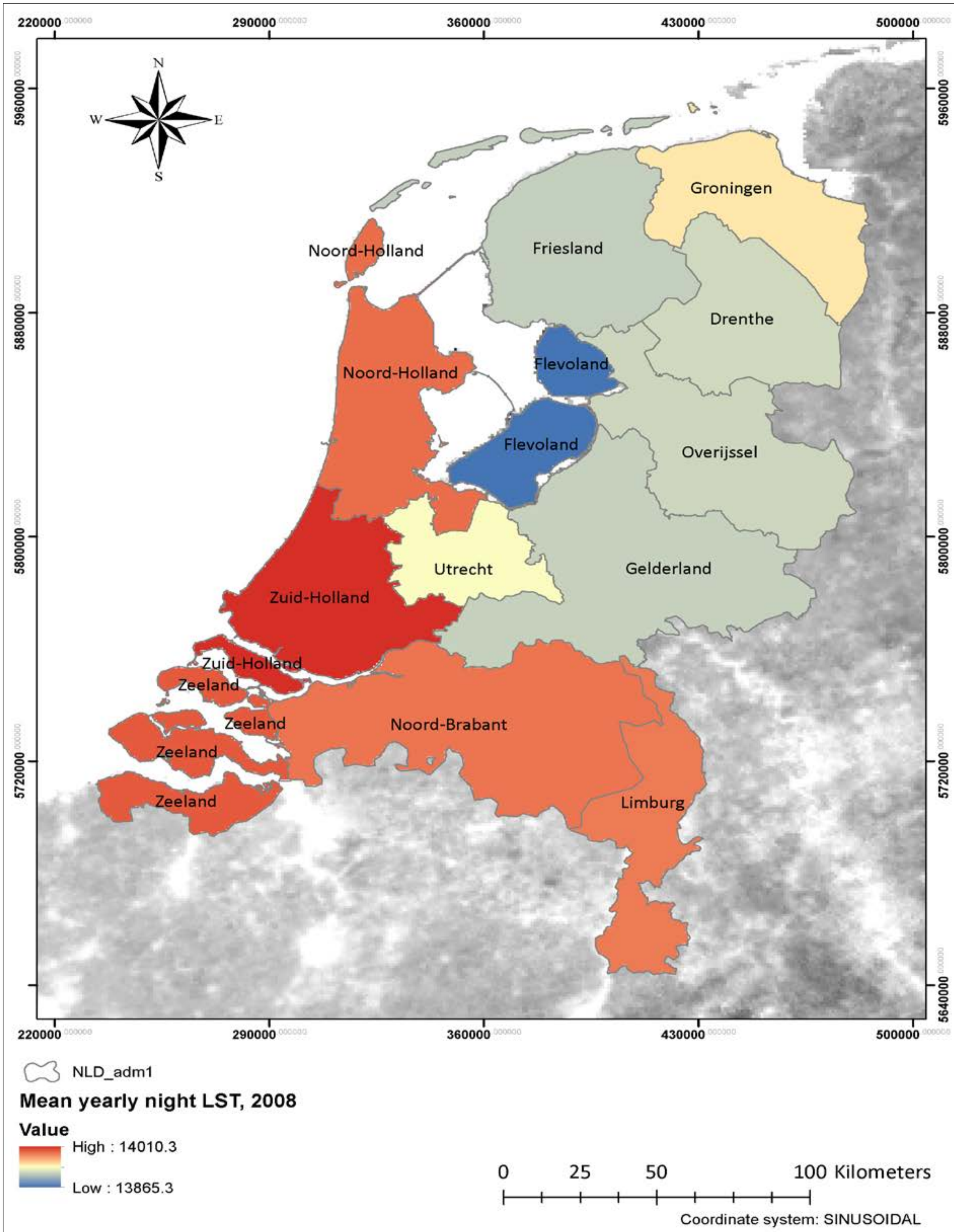

The up-scaled mean yearly night LST mean to Dutch province scale, 2008

Department of Physical Geography and Ecosystem Science, Lund University

Lund University GEM thesis series are a series of master theses of students of the international master program on Geo-information Science and Earth Observation for Environmental Modelling and Management (GEM). The program is a cooperation of EU universities in Iceland, the Netherlands, Poland, Sweden and UK, as well a partner university in Australia. In this series only master thesis are included of students that did their project at Lund University. Other theses of this program can be found at the ITC, the Netherlands (www.gem-msc.org or www.itc.nl).

The student thesis reports are available at the Geo-Library, Department of Physical Geography and Ecosystem Science, University of Lund, Sölvegatan 12, S-223 62 Lund, Sweden. Report series started 2013. The complete list and electronic versions are also electronic available at the LUP student papers (www.nateko.lu.se/masterthesis) and through the Geo-library (www.geobib.lu.se).